SYNTHESIS AND CHARACTERIZATION OF

CHIRAL GERMANIUM COMPOUNDS FOR

ASYMMETRIC HYDROGERMYLATION OF

ORGANIC COMPOUNDS

By

MIGUEL ANGEL LEAL JUNIOR

Bachelor of Science in Chemistry
University of Texas Rio Grande Valley
Brownsville, Texas
2016

Submitted to the Faculty of the
Graduate College of the
Oklahoma State University
in partial fulfillment of
the requirements for
the Degree of
DOCTOR OF PHILOSOPHY
July 2021

SYNTHESIS AND CHARACTERIZATION OF

CHIRAL GERMANIUM COMPOUNDS FOR

ASYMMETRIC HYDROGERMYLATION OF

ORGANIC COMPOUNDS

Dissertation Approved:

Dr. Charles S. Weinert

Dissertation Adviser

Dr. Allen W. Apblett

Dr. Richard A. Bunce

Dr. Christopher J. Fennell

Dr. Tracy Quan

ii

ACKNOWLEDGEMENTS

I would like to first acknowledge and sincerely thank my advisor, Dr. Charles Scott Weinert, for all the years of constant support, patience, and mentorship he has provided. Dr. Weinert has produced an environment where I can have the freedom to test myself and learn from every possible successful or failed experiment. His unwavering determination and work ethic is something to admire and has shaped me into the chemist I am today. I feel truly fortunate to have had the opportunity of working with him. I would also like to express my gratitude my committee members Dr. Apblett, Dr. Bunce, Dr. Fennell, and Dr. Quan for their valuable insight, advice, and for the knowledge they have imparted on me in the classroom.

I would also like to deeply thank my wonderful lab mates Sangeetha Komanduri, Alex Shumaker, and Ardalan Hayatifar for their unrelenting positivity and encouragement throughout these hard years. They have shown me firsthand the level of mental fortitude one must have in graduate school and have also been the most supportive and loving lab mates I could ask for. Additionally, I would also like to thank my colleagues Michael Harris, Kwame Glinton, Jennifer Minnick, Habeeb Al-Mashala, Erik Lantz, Colton Calvert, and Eric Butson for the many years of friendship and laughs. I would also like to thank Martha Halihan for allowing me to be her teaching assistant. She has helped me grow tremendously as a teacher and has always offered her support and guidance when I needed it the most.

I would like to thank my family and friends from back home. My father and mother Miguel and Martha, my brothers Erik and Joel, and my sister Cindy for their love and encouragement throughout my academic studies. I also would like to thank my coaches Manny and Martha for their faith, guidance, and reassurance in me. Without the support of my family and friends this journey would have never been possible. This degree is a direct result of their unconditional love and belongs to them as much as it does to me.

Lastly, I would like to sincerely express my gratitude to my undergraduate research advisors, Dr. Tarek M. Trad and Dr. Mohammed J. Uddin, for allowing me to work in their labs as an undergraduate. It was through their support and mentorship that catalyzed my journey to pursue a graduate degree.

Name: MIGUEL ANGEL LEAL JUNIOR

Date of Degree: JULY 2021

Title of Study: SYNTHESIS AND CHARACTERIZATION OF CHIRAL
GERMANIUM COMPOUNDS FOR ASYMMETRIC
HYDROGERMYLATION OF ORGANIC COMPOUNDS

Major Field: CHEMISTRY

Abstract: Oligogermanes have long been studied and analyzed due to their innate ability to undergo σ-delocalization along the Ge-Ge backbone. Due to this property, oligogermanes can exhibit unique optical and electrical properties, along with a tunable band gap that is dependent on their size, structure, and substituents. The focus of this dissertation will be around the synthesis of a new class of trigermanes and tetragermanes.

The trigermanes $Bu^tMe_2GeGePh_2GeMe_2Bu^t$ and $PhMe_2GeGePh_2GeMe_2Ph$ and the tetragermanes $Et_3Ge(GePh_2)_2GeEt_3$ and $Bu^n_3Ge(GePh_2)_2GeBu^n_3$ were synthesized via the hydrogermolysis reaction. These species were characterized by UV/visible spectroscopy, cyclic voltammetry, and differential pulse voltammetry. The properties of the two trigermanes were also compared with those of $Bu^n_3GeGePh_2GeBu^n_3$, and the UV/visible absorption maxima of these three trigermanes fall in the narrow range of 246 - 249 nm while their oxidation potentials differ by 233 mV. Both $Bu^tMe_2GeGePh_2GeMe_2Bu^t$ and $Bu^n_3GeGePh_2GeBu^n_3$ exhibit two irreversible oxidation waves in their CVs and DPVs. Similarly, the absorption maxima for the two tetragermanes are similar and their oxidation potentials differ by only 58 mV. The CV and DPV of $Et_3Ge(GePh_2)_2GeEt_3$ exhibits three irreversible oxidation waves while that of $Bu^n_3Ge(GePh_2)_2GeBu^n_3$ contains only one. This dissertation will focus on gaining an understanding of the electronic properties, stability, and decomposition of these oligogermane catenates when oxidized using cyclic and differential pulse voltammetry studies.

This dissertation will also focus on synthesizing and characterizing germanium aryloxide compounds for hydrogermylation applications. Through the use of chiral auxiliaries and polyfunctional phenols, a germanium (II) and germanium (IV) species can be readily synthesized. The addition of a halide and an organic substituent can be added via an oxidative addition to the germanium (II) center, followed by a reduction to form a germanium hydride species. For the germanium (IV) center, a C_2-symmetric chiral germanium halide species can be formed readily, followed by a reduction to form a chiral germanium hydride for hydrogenation of other compounds. Further functionality studies on the chiral germanium (IV) species have been performed as this compound readily undergoes the formation of a chiral germylium species when introduced to $AlCl_3$. Such germylium species are rare, and with the use of a chiral auxiliary ligand, this compound to the best of our knowledge has yet to be reported.

TABLE OF CONTENTS

LIST OF TABLES

LIST OF FIGURES

LIST OF SCHEMES

CHAPTER I

INTRODUCTION

In 1886 a report of the new element germanium was published by Clemens Winkler after its isolation from the mineral argyrodite.[1,2] Germanium mirrored properties similar to the predicted element ekasilicon, which meant it lies in group 14 between silicon and tin, as was initially predicted by Dmitri Mendeleev in his report *The Periodic Law of the Chemical Elements* published 17 years earlier in 1869.[3] Argyrodite was mined in Himmelfurst Fundgrube, Freiburg, Germany and was originally thought to contain an amalgam of silver and mercury. In his report, Winkler reported that the correct chemical composition of argyrodite is Ag_8GeS_6.[4] In the present day, germanium is mainly found in ores of sphalerite and can also be isolated from ores of other elements such as lead, copper, and silver. With unique optical and electronic properties, germanium is used mainly in transistors, fiber optic systems, infrared imaging, and solar cell applications.[5] Germanium compounds having organic substituents have also been used in semiconductor materials such as $NOBF_4$, $FeCl_3$, and SbF_5.[6]

Germanium has five naturally occurring isotopes ^{70}Ge, ^{72}Ge, ^{73}Ge, ^{74}Ge, and ^{76}Ge with the most abundant isotope being ^{74}Ge having a natural abundance of 36%.[7] In 1887 Clemens Winkler synthesized the first organogermanium compound tetraethylgermane by reacting diethylzinc with germanium tetrachloride giving further insight to the unique metalloid properties of germanium.[8] While the main group elements such as silicon, germanium, and tin can form catenates and other organometallic compounds, germanium has not been as extensively studied as the other two elements. Catenated germanium compounds are of importance due to their distinctive optical and electrical properties. The optical and electrical properties of germanium catenates stem from the delocalization of their bonding electrons across the element-element backbone via overlap of their sp^3 hybridized molecular orbitals which is a phenomenon known as σ-delocalization. While germanium catenates structurally resemble saturated hydrocarbons, physically they resemble conjugated unsaturated hydrocarbons. The σ-delocalization that occurs in germanium catenates is maximized when the element-to-element backbone arrangement is in a *trans*-coplanar conformation as shown in Figure 1.1.[7,9,10]
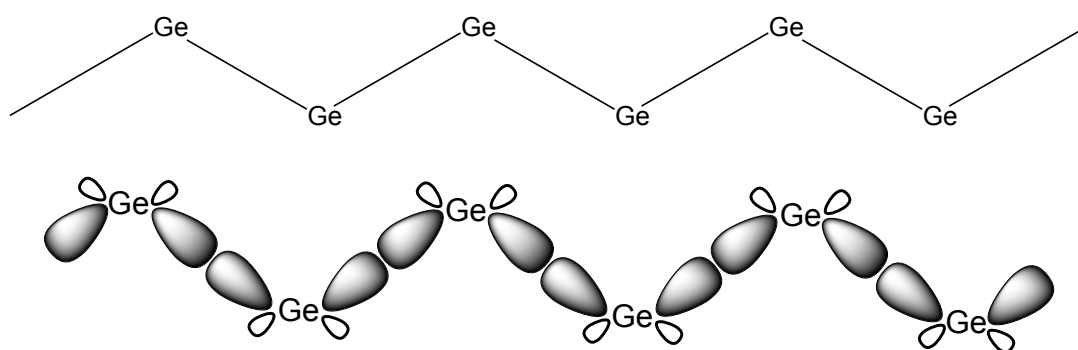
Figure 1.1: *Trans*-coplanar conformation of germanium catenates sp^3 orbital overlap allowing for σ-delocalization to occur.

Among the heavier group 14 catenates studies on the synthesis, properties, and overall chemistry of silicon-silicon and tin-tin catenates are well developed.[11–20] Studies of the synthesis, physical properties, and overall chemistry on germanium however, are much less explored. Compounds containing silicon-silicon and tin-tin bonds can be readily synthesized with rational synthetic procedures; however, synthesizing germanium-germanium compounds is not as facile. This is in part due to the formation of inseparable compound mixtures as well as low reaction yields. Therefore, a means of creating a logical synthetic approach for germanium catenates can be considered an area of high interest. Further detailed analysis of the physical and structural properties of oligogermanes can be carried out as well through the development of new synthetic methods. This chapter will focus on a brief history of germanium compounds, past and current synthetic methods for the production of oligogermanes and give a brief insight on Chapters II–IV.

As mentioned previously, the first organometallic germanium compound synthesized was Et_4Ge. It wasn't until 1925 that the first oligogermane compound hexaphenyldigermane ($Ph_3GeGePh_3$) was synthesized.[21] Currently there exists a multitude of different synthetic methods for the production of germanium-germanium bonds. There is the Wurtz-type coupling reaction, the demercuration of germyl mercury compounds, nucleophilic substitution of organogermanium halide compounds with organogermanium anions, and reactions of Grignard reagents with germanium (IV) halides[22–25] The synthesis of $Ph_3GeGePh_3$ was done through the reaction of Ph_3GeCl in the presence of sodium metal, as seen in Scheme 1.1.[26]

$$Ph_3GeCl \ + \ 2 \ Na \ \xrightarrow[\substack{Reflux, \ 1h \\ - \ 2 \ NaCl}]{C_6H_6} \ Ph_3Ge-GePh_3$$
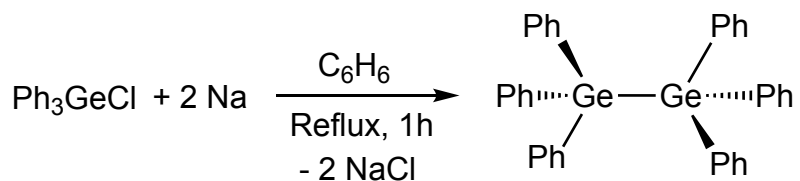
Scheme 1.1: Wurtz coupling of Ph_3GeCl with sodium.[26]

This eventually led to similar types of oligogermanes with varying substituents to be synthesized through Wurtz-type coupling reactions.[15,27–30] The first alkyl substituted digermane to be synthesized was $Et_3GeGeEt_3$ by reacting Et_3GeBr and sodium metal, then subsequently the methyl digermane derivative $Me_3GeGeMe_3$ was synthesized in a similar fashion but by using potassium instead. Wurtz coupling reactions have been shown to be useful in the preparation of small oligogermanes, especially digermanes, however, it is limited in its potential due to its inability to prepare higher oligoermanes, as well as low yields, and the formation of product mixtures.

A different synthetic method that was used to synthesize digermanes and also some longer oligogermanes is the reaction of germanium halides with Grignard reagents.[31–33] This method results in the formation of a series of di-, tri-, and tetragermanes with the ability to vary reaction conditions to change the product distribution as seen in Scheme 1.2. A caveat on the use of Grignard reactions, however, is the uncontrolled nucleophilic attack of the Grignard reagents on germanium halides that leads to low yields. It was also established that solvent choice plays a role in the reaction in that when diethyl ether or toluene is used as the solvent, larger amounts of tri- and tetragermanes to be formed.[34] Although this method can allow for some higher oligermanes to be produced, it cannot be used to prepare specific oligogermanes.[35]
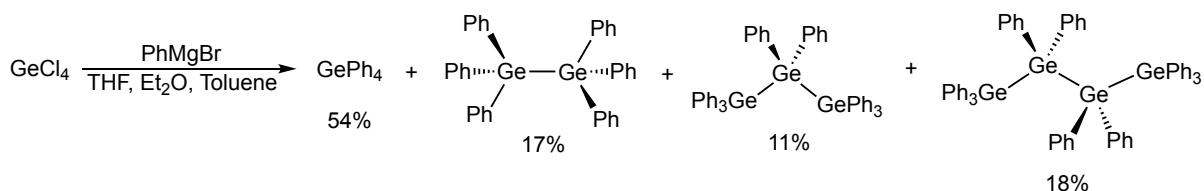
Scheme 1.2: PhMgBr is employed to do a series of nucleophilic attacks on $GeCl_4$ to produce a series of oligogermanes.[10]

It was not until 2005 that a significant improvement in oligogermane synthesis was reported by Mochida and co-workers where samarium(II) iodide was used as a reducing agent

to form germanium catenates. The use of samarium(II) iodide produced yields of up to 94% with high purity, as seen in Scheme 1.3 and Table 1.1, and was a vast improvement over previous synthetic methods.[36–39]

$$2 \ R_3GeCl + R'_2GeCl_2 \ \xrightarrow[\text{HMPA/THF}]{\text{10 eq. SmI}_2} \ R_3Ge \underset{}{\overset{}{\diagup}} \overset{\displaystyle R' \ \ \ R'}{\underset{}{Ge}} \diagdown GeR_3$$
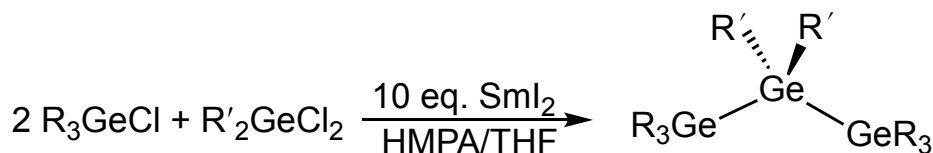
Scheme 1.3. Schematic for the synthesis of a trigermane using germanium halides and samarium (II) iodide.[38]

Table 1.1 Substituents used in the coupling of germanium halides with Sm (II) Iodide.[38]

R_3 = Et, R`$_2$ = Ph, 94%	R_3 = ^{i}Pr, R`$_2$ = Ph, 30%
R_3 = Me, R`$_2$ = Ph, 87%	R_3 = Et, R`$_2$ = PhMe, 70%
R_3 = ^{n}Bu, R`$_2$ = Ph, 87%	

The typical samarium(II) iodide reduction reactions are carried out in a mixture of THF and hexamethylphosphoric triamide (HMPA). It was found that HMPA plays a key role in the reaction by increasing the rate of product formation. The variation of the halide bonded to the germanium also has an effect on the reaction rate as well as yield. This trend can be seen in Table 1.2. It was also noted that the high efficiency of using samarium(II) iodide versus other group 1 metals lies in its mild reduction potential, making it a more practical option as a single-electron reductant than other species such as sodium or potassium.[40]

Table 1.2 Reaction time and yields for various organogermanium halide coupling reactions.[38]

Germanium Compound	Product	Elapsed Time (hours)	Yield (%)
Et$_3$GeCl	Et$_3$GeGeEt$_3$	24	69
Et$_3$GeBr	Et$_3$GeGeEt$_3$	15	73

Bu₃GeCl	Bu₃GeGeBu₃	24	62
Bu₃GeBr	Bu₃GeGeBu₃	15	66
^{i}Pr₃GeCl	(^{i}Pr₆Ge₂)	24	39
^{i}Pr₃GeCl	(^{i}Pr₆Ge₂)	15	45
Ph₂MeGeCl	Ph₂MeGeGeMePh₂	12	95
Ph₂MeGeBr	Ph₂MeGeGeMePh₂	1	98

The hydrostannolysis reaction used to couple tin atoms together has proven to be a useful method for synthesizing oligostannanes.[17,41,42] However, this method did not proceed as well with germanium analogues. It was surmised that in order for this reaction to proceed, highly electron withdrawing groups on the germanium atom in a germane were needed to "activate" the germanium-hydrogen bond and allow the hydrogermolysis reaction to proceed.[43] The hydrogermolysis reaction could then be used to form germanium-germanium bonds in hexane at 100°C for one to two hours to form oligogermanes as seen in Scheme 1.4.
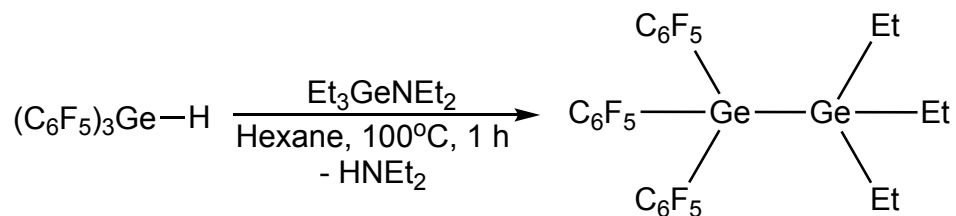
Scheme 1.4. The use of an "activated" Ge–H reacting with a germyl amine to produce a digermane.[43,44]

This method of synthesizing oligogermanes was used sparingly due to the necessity of the electron withdrawing groups to "activate" the hydrogen, which limited the potential to synthesize oligogermanes with varying substituents on the germanium atoms. A list of known

products that have been produced using the "activated" hydrogermolysis reaction are listed in Table 1.3.[43–45]

Table 1.3 Oligogermanes synthesized using the "activated" hydrogermolysis reaction.[43,44]

Germanium Hydrogen	Germyl Amine	Oligogermane	Yield (%)
$(C_6F_5)_3GeH$	$(p\text{-Tol})_3GeNMe_2$	$(p\text{-Tol})_3GeGe(C_6F_5)_3$	66
$(C_6F_5)_2GeH_2$	$(p\text{-Tol})_3GeNMe_2$	$((p\text{-Tol})_3Ge)_2Ge(C_6F_5)_2$	51
$(C_6F_5)_3GeH$	Ph_3GeNMe_2	$Ph_3GeGe(C_6F_5)_3$	86
$(C_6F_5)_3GeH$	Et_3GeNEt_2	$Et_3GeGe(C_6F_5)_3$	91
$(C_6F_5)_2GeH_2$	Et_3GeNEt_2	$(Et_3Ge)_2Ge(C_6F_5)_2$	66

In 2006, Weinert and co-workers reported the successful use of the hydrogermolysis reaction to synthesize a series of oligogermanes in high purity with yields of 80 – 85%.[46] Similar to the hydrostannolysis reaction, it employed the use of a germyl amine and a germanium hydride to form the germanium-germanium bond as seen in Scheme 1.5. The reaction was originally attempted in benzene at room temperature and in refluxing benzene or toluene but failed to produce a germanium-germanium bond as would typically occur successfully in the hydrostannolysis reaction. It was only when the reaction was carried out in refluxing acetonitrile (CH_3CN) that the oligogermane could be formed after a 48-hour reaction time.
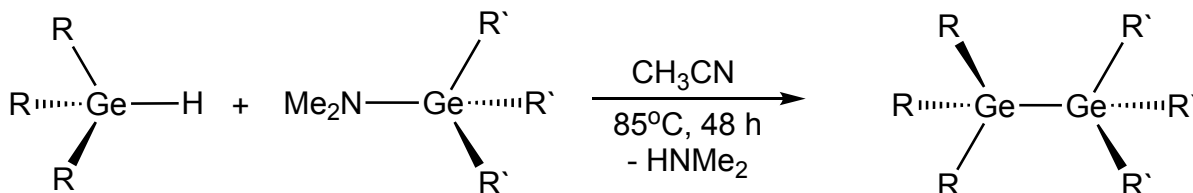
Scheme 1.5. The hydrogermolysis reaction used for the synthesis of oligogermanes.[46]

Unlike the hydrogermolysis reaction that used the "activated" germanium bonded hydrogen, this reaction proceeded with both alkyl, aryl, or a combination of both types of substituents as long as the solvent used was CH_3CN. The question as to why the reaction only proceeded when done in CH_3CN was later understood when the reaction was done in deuterated acetonitrile (CD_3CN) and analyzed via ^{1}H NMR spectroscopy. It was discovered that the reaction proceeds through the formation of an intermediate α-germyl nitrile species. Further studies and reactions were carried out in order to synthesize the α-germyl nitrile species independently and confirm this theory. This was achieved by reacting a germanium halide compound with (cyanomethyl)lithium ($LiCH_2CN$) that is generated from the reaction of lithium diisopropylamide and CH_3CN as shown in Scheme 1.6.[47]
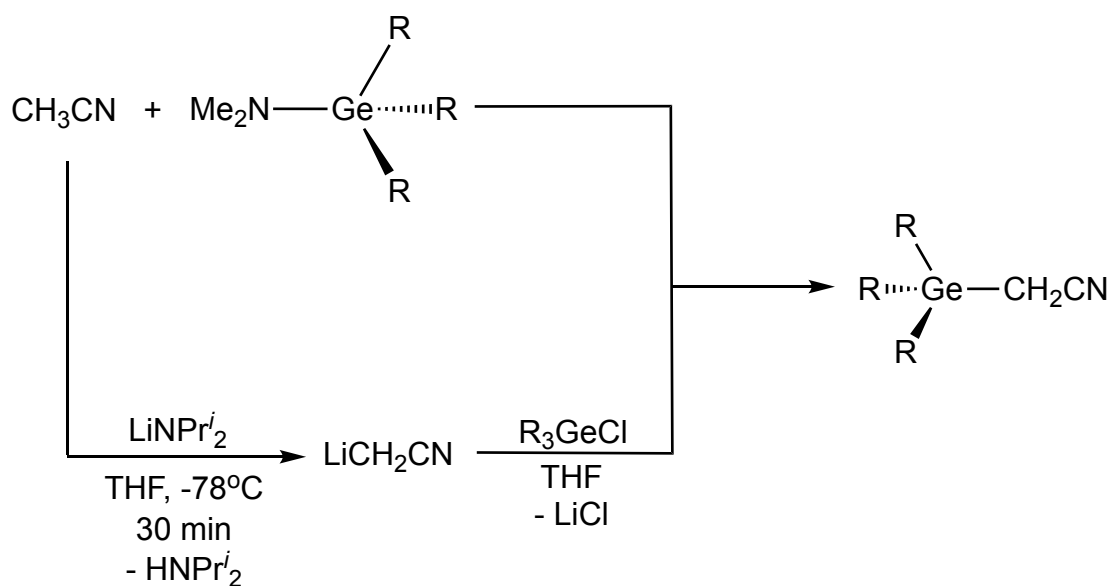
Scheme 1.6. Synthesis of the α-germyl nitrile species intermediate through a nucleophilic attack on a germanium halide.[47]

Three separate α-germyl nitrile species bearing phenyl, *tert*-butyl, and isopropyl groups were synthesized. In these reactions, the formation of the α-germyl nitrile occurred in 6 hours *in situ* in CD_3CN compared to the typical 48-hour reaction time for the hydrogermolysis reaction to

completely form the digermane. This detail lead to the proposal that the formation of the α-germyl nitrile is the fast step in the synthesis of the digermane.[47] Table 1.4 shows the full list of digermanes synthesized by Weinert and co-workers via the hydrogermolysis reaction.

Table 1.4 Synthesis of digermanes using the hydrogermolysis reaction as reported.[46–49]

Reactants	Product	Yield (%)	λ_{max} (nm)
$Bu_3GeNMe_2 + Ph_3GeH$	$Bu_3GeGePh_3$	83	232
$Et_3GeNMe_2 + Ph_3GeH$	$Et_3GeGePh_3$	84	231
$Bu_3GeNMe_2 + Me_3GeH$	$Bu_3GeGeMe_3$	86	-
$Pr^i_3GeNMe_2 + Ph_3GeH$	$Pr^i_3GeGePh_3$	91	234
$Bu^s_3GeNMe_2 + Ph_3GeH$	$Bu^s_3GeGePh_3$	81	244
$Me_2PhGeNMe_2 + Ph_3GeH$	$Me_2PhGeGePh_3$	76	244
$Bu^i_3GeNMe_2 + Ph_3GeH$	$Bu^i_3GeGePh_3$	79	232
$Hex^n_3GeNMe_2 + Ph_3GeH$	$Hex^n_3GeGePh_3$	43	241
$(C_{18}H_{37})_3GeNMe_2 + Ph_3GeH$	$(C_{18}H_{37})_3GeGePh_3$	50	236
$Bu^tMe_2GeNMe_2 + Ph_3GeH$	$Bu^tMe_2GeGePh_3$	89	238

The use of the hydrogermolysis reaction has been used for the synthesis of longer oligogermanes,[50,51] and branched germanes[52–55] as well with moderate to high yields, therefore, making it a useful method for oligogermane synthesis. To date the longest fully characterized oligogermane has been synthesized by reacting $HPh_2Ge(GePh_2)_2GePh_2H$ with two equivalents of $Pr_3^iGeNMe_2$ via the hydrogermolysis reaction to produce the hexagermane $Pr_3^iGe(GePh_2)_4GePr_3^i$ with a yield of 53%.[50] The continued utility of the hydrogermolysis

reaction for synthesizing longer discrete branched and linear oligogermanes has made it a highly useful tool for germanium-germanium bond synthesis.

An underlying goal of our research efforts is to further understand how the σ-delocalization that occurs along the germanium-germanium backbone in oligogermanes leads to their unique optical and electrical properties. Chapter II will focus on the synthesis and characterizion of a new series of trigermanes along with exploring their unique absorption maxima and electrochemistry. Chapter III will focus on the synthesis of polyfunctional phenols to be reacted with germanium(II) and germanium(IV) compounds to yield germanium aryloxides. Through a series of reactions, the primary goal is to form aryloxide germanium hydrides to be used as potential hydrogenating agents. Chapter IV will build upon the studies described in Chapter III but will describe the use of chiral auxiliaries to synthesize chiral germanium compounds. The reactivity and functionality studies done in Chapter IV should lead to new methods of synthesizing chiral germanium species and chiral germylium ions where their potential properties will be discussed in further detail.

CHAPTER II

PREPARATION, ABSORPTION SPECTRA, AND ELECTROCHEMISTRY OF THE

TRIGERMANES $R_3GeGePh_2GeR_3$ (R_3 = Bu^tMe_2, $PhMe_2$, Bu^n_3) AND

TETRAGERMANES $R_3Ge(GePh_2)_2GeR_3$ (R_3 = Et_3, Bu^n_3)

2.1 Introduction

Catenated silanes, germanes, and stannanes have shown to possess inherent σ-delocalization. This property among the group 14 elements involves electrons in the σ-bonding orbital being delocalized across the entirety, or a significant part of, the element-element backbone as opposed to being localized between two atoms as is commonly found in more organic systems.[56–60] It is this direct phenomenon of σ-delocalization that leads to intriguing properties found in group 14 catenated systems. Their absorption is mainly in the ultraviolet (UV) region occurring through an electronic transition from the $\sigma \rightarrow \sigma^*$ molecular orbital, and it is likely that their emissive properties stem from the relaxation of electrons from the $\sigma^* \rightarrow \sigma$ molecular orbital. The aforementioned electronic properties suggest that compounds with σ-delocalization have potential to be used as tunable emissive materials or as single molecule conductors.[61]

Oligogermanes are a class of compounds that attribute their physical properties to σ-delocalization. As such, oligogermanes display absorption, and emission in the UV or visible region, and are electronically active in that they can also be oxidized using either cyclic or differential pulse voltammetry (CV and DPV). Oligogermanes characteristically exhibit one or more irreversible oxidation waves in their CVs and DPVs. Furthermore, the emission spectra in both solution and the solid phase of oligogermanes normally have maxima in the visible regions.[7,10,62–66]

Studies performed on oligogermanes have indicated that both the oxidation potentials, as well as the position of their absorption and emission maxima, largely depend on both the length of the germanium-germanium backbone and the intrinsic properties of the organic substituents that are attached to the germanium-germanium backbone. Whether the organic substituents are electron withdrawing or donating play a role in the physical properties of the oligogermane. However, the variation of the chain length has been shown to have a more significant effect on the spectral and electrochemical properties over the variation of substituents.

As mentioned previously, discrete oligogermanes have been known for nearly a century, with the first reported compound being $Ph_3GeGePh_3$ in 1925.[67] The various synthetic methods of preparing oligogermanes include Wurtz-type coupling,[68,69] the nucleophilic attack of germyllithium reagents on germyl halides,[70] demurcuration of germylmercury compounds,[71] the use of germyl Grignard reagents,[72,73] reductive coupling using SmI_2,[74,75] and the main synthetic technique used in this project, bond formation via the hydrogermolysis reaction occurring between a germyl amine and a germane as shown in Schemes 2.1.[46,55,76–79]

$$\underset{\underset{R}{\overset{R}{\diagup}}}{\overset{R}{\diagdown}}Ge{-}H \ + \ R`_3Ge{-}NMe_2 \quad \xrightarrow[\substack{85°C,\ 48\ h \\ -\ HNMe_2}]{CH_3CN} \quad R_3Ge{-}GeR`_3$$
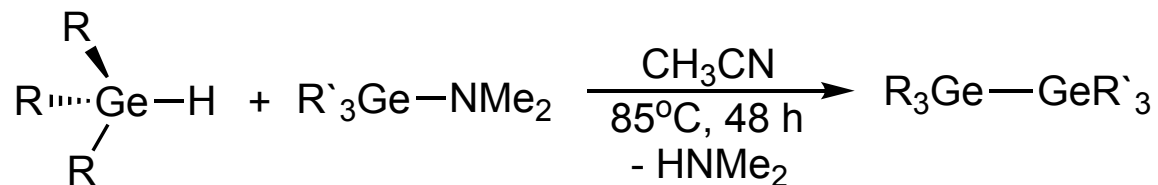
Scheme 2.1: The reaction between a germyl amine and a germane in acetonitrile to form a digermane known as the hydrogermolysis reaction.[46]

The hydrogermolysis reaction has been employed for the synthesis of a wide variety of linear, branched, and cyclic oligogermanes. Included in this chapter is the synthesis and investigation of the structure/property relationships in the linear trigermanes $R_3GeGePh_2GeR_3$ (R_3 = Bu^tMe_2, $PhMe_2$, and nBu^n_3) and the tetragermanes $R_3Ge(GePh_2)_2GeR_3$ (R_3 = Et_3 and Bu^n_3), including the analysis of their electrochemistry and absorption spectra. The variation of the oxidation potentials and UV/Visible absorption maxima with respect to the inductive electron donating ability of the attached organic substituents are a focus of these studies.

2.2 Results and Discussion

Commercially available alkyl and aryl substituted germanium chlorides were used as the starting materials for synthesizing the germyl amine and germanium hydride building blocks in the hydrogermolysis reaction. The reagents R_3GeCl (R = Et_3, Bu^n_3, Me_2Ph, Bu^tMe_2) were all treated with 1.5 equivalents of lithium dimethyl amide to yield the germyl amine that was then purified through a short path distillation. As for the hydrides, diphenyl germanium dihydride (Ph_2GeH_2) was purchased from Gelest and was used without further purification.

The trigermanes $Bu^tMe_2GeGePh_2GeMe_2Bu^t$ (**1**) and $PhMe_2GeGePh_2GeMe_2Ph$ (**2**) were synthesized via the hydrogermolysis reaction. The reactions leading to the final

products (**1**) and (**2**) were sluggish, and the overall reaction was found to not be complete after the typical reaction time of 48 hours.[10,46,47] A potential cause of this could be the volatile nature of the germyl amines $Bu^tMe_2GeNMe_2$ and $PhMe_2GeNMe_2$. Due to the high temperature reaction conditions, the germyl amines could be in the gas phase throughout the reaction therefore prolonging the desired α-nitrile species from forming via the reaction with CH_3CN. Even when there was a slight excess of the germyl amine present, the reaction mixture still contained unreacted germanium hydride. After 48 hours, a ^{1}H NMR spectrum indicated that there were two separate resonances present in the solution mixture, one being identified to belong to Ph_2GeH_2, and the other being unknown. The position of this latter resonance was however indicative of a germanium hydride being present. In the preparation of (**1**), a singlet at δ 5.29 ppm was observed in the ^{1}H NMR spectrum of the reaction mixture. This resonance was assigned to the hydride of the digermane derivative $Bu^tMe_2GeGePh_2H$ that was forming during the hydrogermolysis reaction. Similarly, in the formation of (**2**) a hydride resonance was also noted after 48 hours. This resonance appeared at δ 5.34 ppm in the ^{1}H NMR spectrum and was assigned to the digermane derivative $PhMe_2GeGePh_2H$. The spectra indicating the two digermane derivative resonances of (**1**) and (**2**) are shown in Figure 2.1.

14
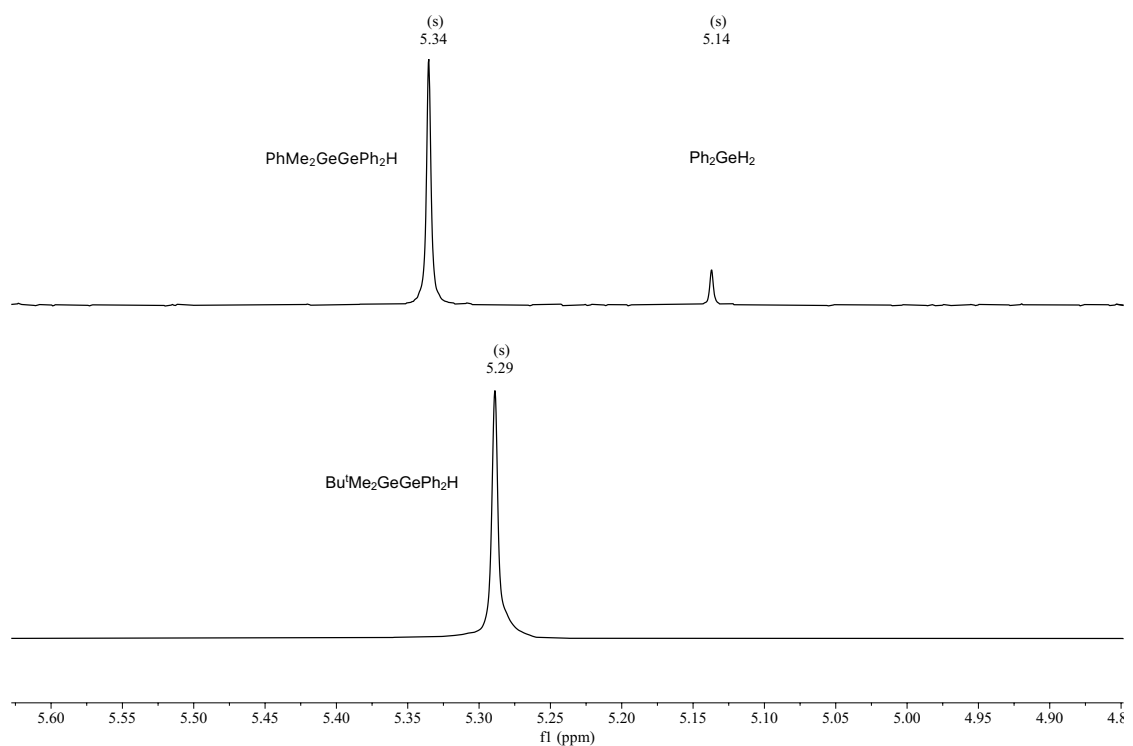
Figure 2.1: Stacked ^{1}H NMR spectra of the digermane derivatives formed in the synthesis of **1** and **2**.

The desired trigermane (**2**) could be obtained, however, by adding an additional equivalent of the germyl amine in acetonitrile and heating the reaction mixture for an additional 24 hours. In the preparation of (**1**), the desired trigermane product could only be obtained after heating for an additional 14 days after adding an additional equivalent of the germyl amine. Pure (**1**) and (**2**) were obtained by removing the residual α-germyl nitrile species R_3GeCH_2CN that remained after the reaction by distillation at 85°C at low pressure (0.005 torr). The trigermane $Bu^n_3GeGePh_2GeBu^n_3$ (**3**) could be isolated using a standard reaction time of 48 hours without the need for a large excess of $Bu^n_3GeNMe_2$, and was prepared according to the literature procedure.[80,81] The overall synthetic pathway for obtaining the trigermanes (**1**) and (**2**) is shown in Scheme 2.2.

15
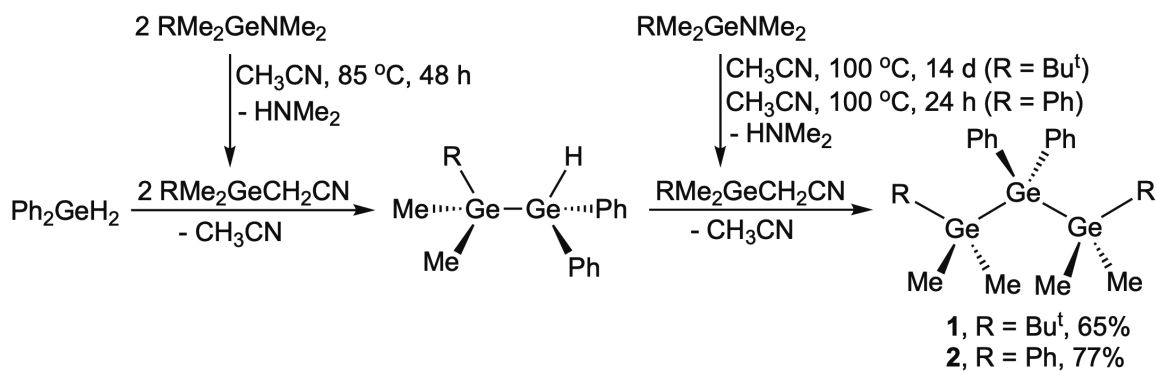
Scheme 2.2: Synthesis of the trigermanes **1** and **2**.[82]

Compounds (**1**), (**2**) and (**3**) were characterized by ^{1}H and ^{13}C NMR spectroscopy and their spectra were consistent with their structures in all three cases. Using the organic substituents on the germanium atoms as references, the spectra could be taken to assure that the solution mixtures did not contain any lingering germyl amine, germanium hydride, or α-nitrile species after a low-pressure distillation purification. The ^{1}H and ^{13}C NMR spectra are shown in Figures 2.3 – 2.8.

7.71
7.70
7.69
7.69
7.68
7.20
7.20
7.19
7.18
7.18
7.16 C6D6
7.15
7.14
7.14
7.13
7.13
7.12
7.11
7.10
7.10
7.10

—0.91

—0.45

4.03

3.57
3.18

18.00
12.01

8.0 7.5 7.0 6.5 6.0 5.5 5.0 4.5 4.0 3.5 3.0 2.5 2.0 1.5 1.0 0.5 0.0
fl (ppm)
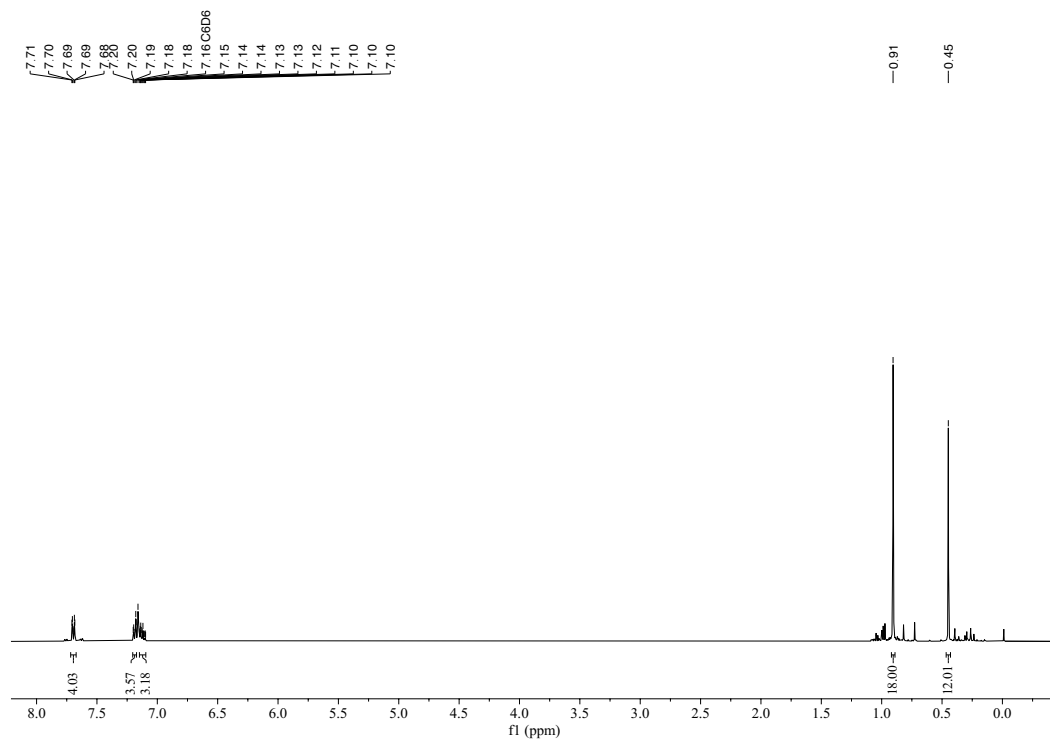
Figure 2.2: ^{1}H NMR spectrum of (**1**).

140.49
136.83
136.23
135.87

128.06 C6D6

28.87
26.85

—3.04

50 140 130 120 110 100 90 80 70 60 50 40 30 20 10 0 -10
fl (ppm)
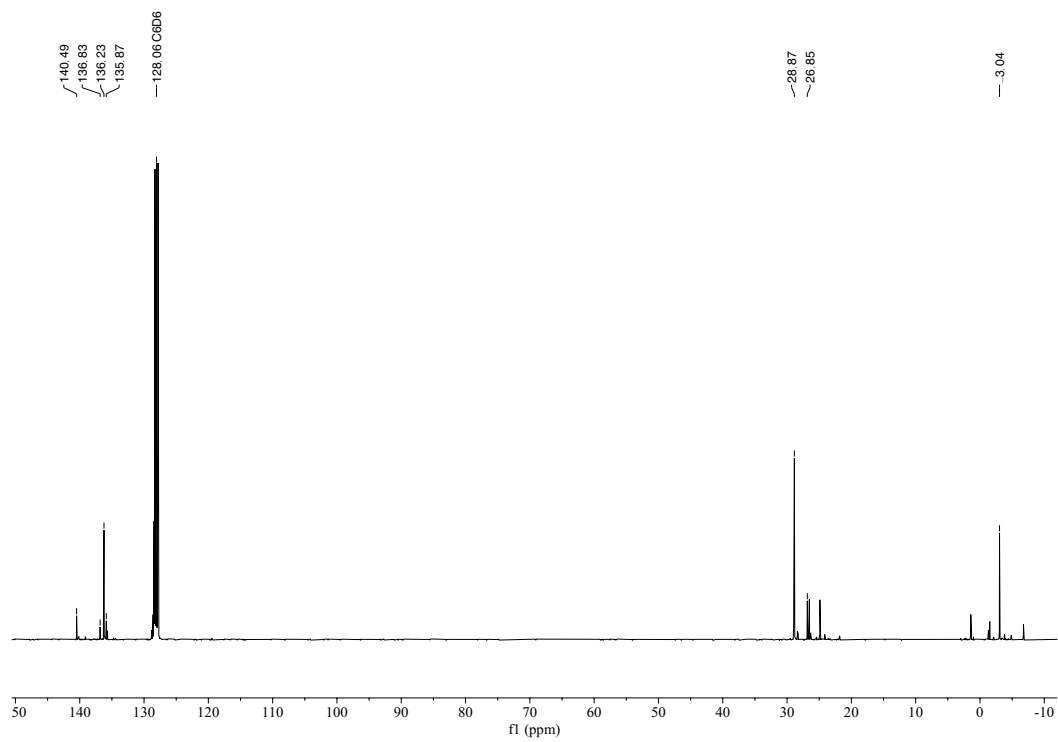
Figure 2.2: ^{13}C NMR spectrum of (**1**).
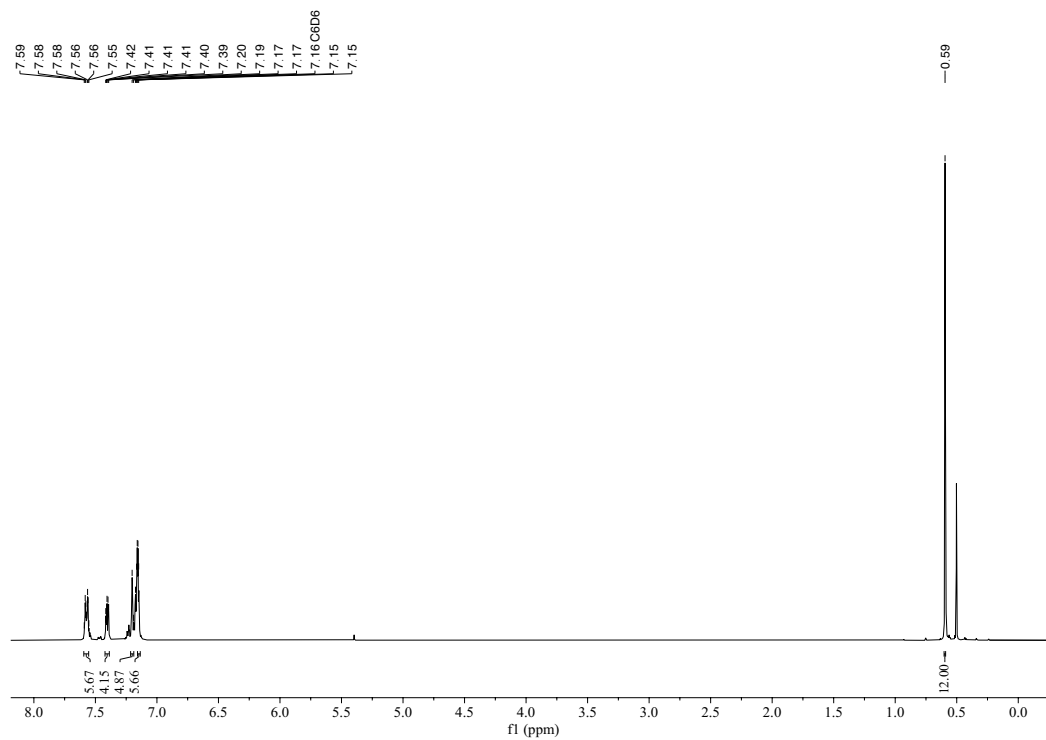
Figure 2.4. ^{1}H NMR spectrum of (**2**).
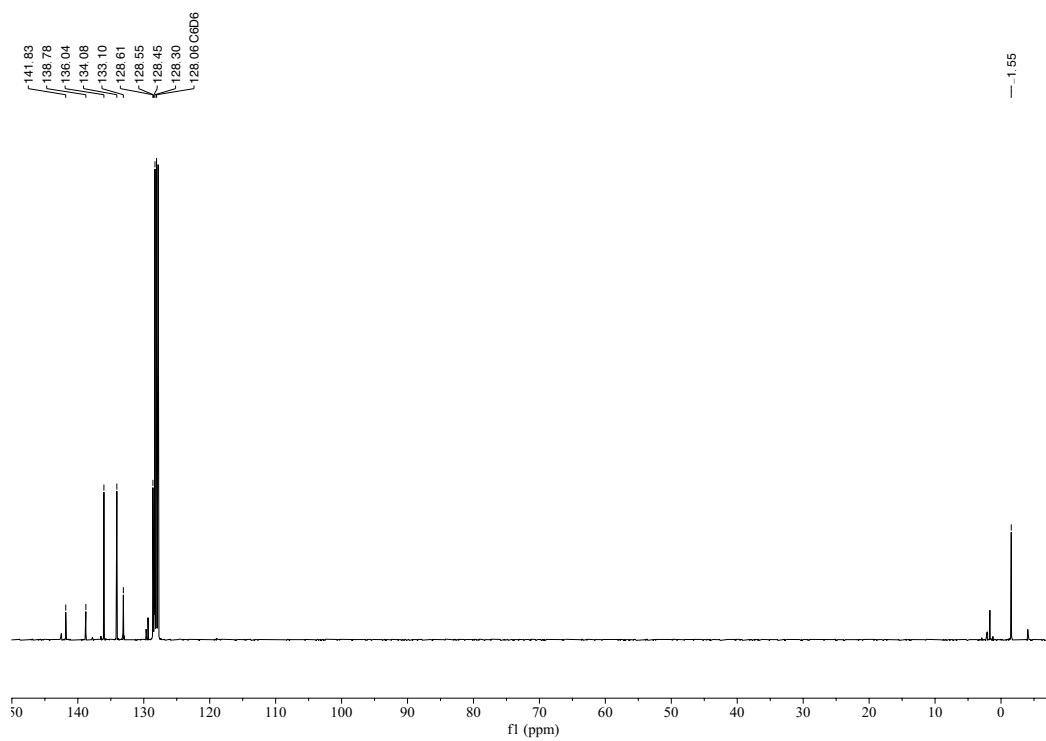
Figure 2.5: ^{13}C NMR spectrum of (**2**).

18
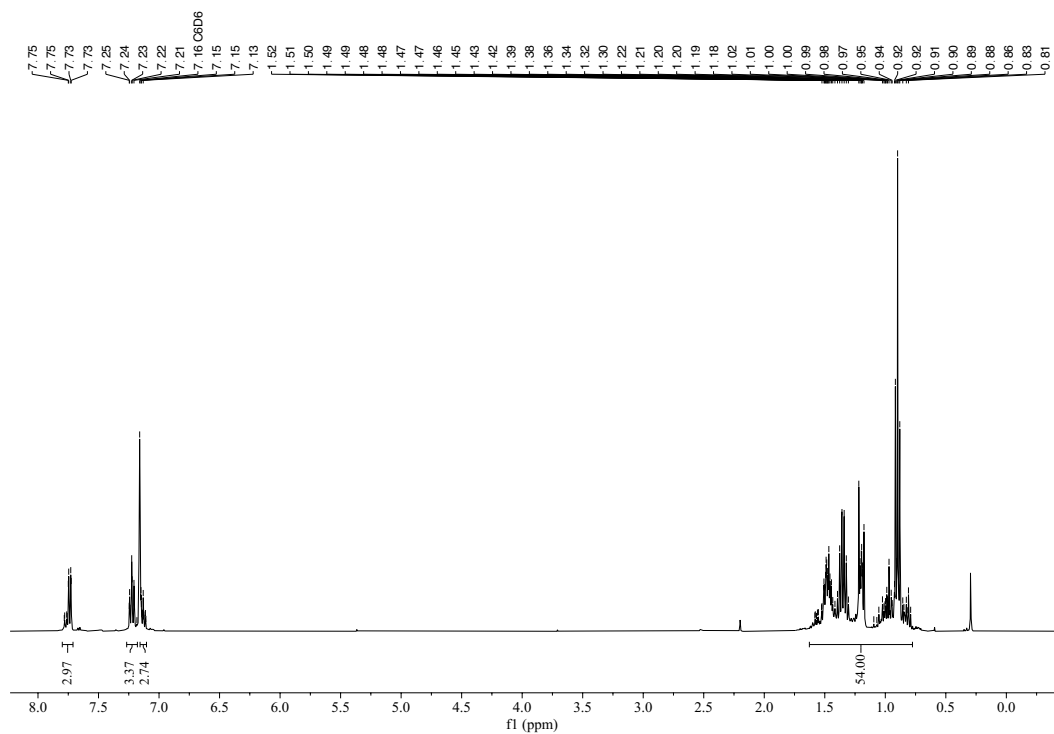
Figure 2.6: ^{1}H NMR spectrum of (**3**).
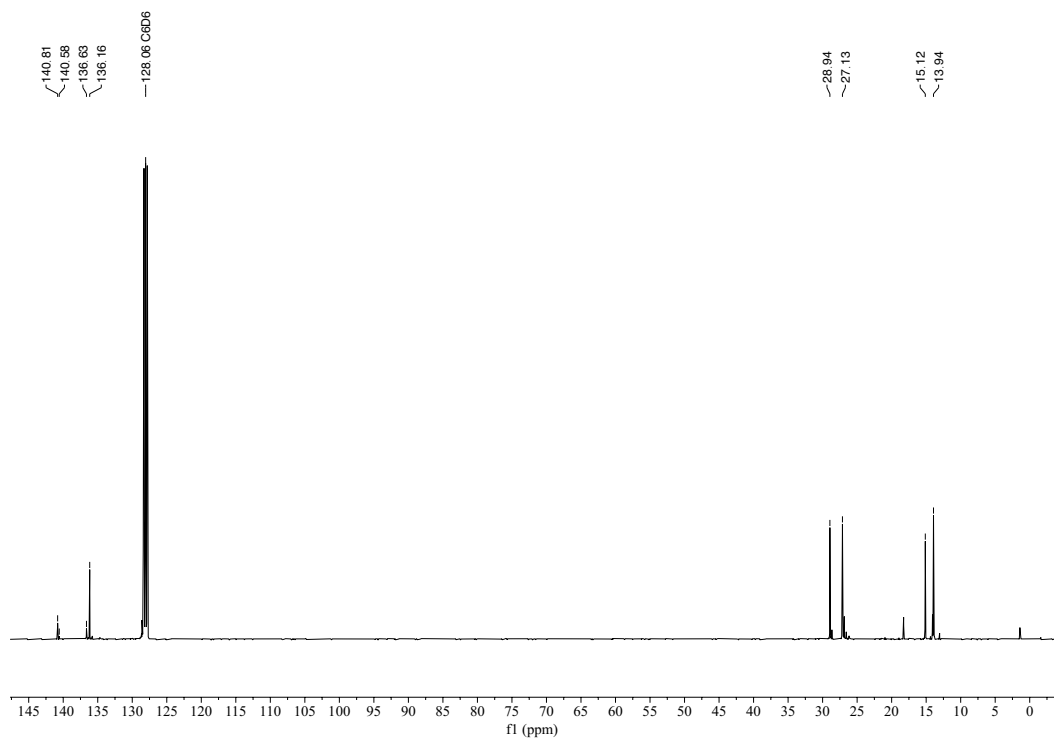
Figure 2.7: ^{13}C NMR spectrum of (**3**).

19

The oxidation potentials of compounds **1 – 3** were obtained using CV and DPV

analysis in dichloromethane (CH_2Cl_2) solvent using 0.1 M [Bu^n_4N][PF_6] as the supporting

electrolyte. The CV and DPV traces for **1 – 3** are shown in Figure 2.9 – 2.10 and the

oxidation potential data that was collected is displayed in Table 2.1.

Table 2.1 Oxidation potential data for trigermanes **1 – 3**.[*82]

Compound	CV E_{ox} (mV)	DPV E_{ox} (mV)
$Bu^tMe_2GeGePh_2GeMe_2Bu^t$ (**1**)	1737, 2015	1540, 2120
$PhMe_2GeGePh_2GeMe_2Ph$ (**2**)	1837	1640
$Bu^n_3GeGePh_2GeBu^n_3$ (**3**)	1604, 1918	1520, 2060

*Errors for the observed oxidation waves are ± 10 mV.

A common trend seen in oligogermanes is that they display an irreversible

oxidation wave in CV and DPV studies. Although **2** exhibits only a single irreversible

oxidation wave in both the CV and DPV, it can be seen that the CV and DPV of **1** and **3**

each display two irreversible oxidation waves. A correlation can be made between the

oxidation potentials of compounds **1 – 3** and the inductive electron donating ability of the

ligands attached to the germanium-germanium backbone. It has been noted that the

energies of the highest occupied molecular orbital (HOMO) and the lowest unoccupied

molecular orbital (LUMO) are affected by the electron donating or withdrawing ability of

the ligands. Between the HOMO and LUMO, the HOMO tends to be affected more

significantly by the variation of the alkyl substituents while the introduction of aryl

substituents can have an effect on the energy of the LUMO. In general, however, it is often

expected that an increase in the inductive electron donating ability of organic substituents

will cause a destabilization of the HOMO of the oligogermane leading to a more facile

oxidation. This trend can be seen in Table 2.2.

Table 2.2 UV/Visible absorption data for trigermanes.[82]

Trigermane	λ_{max} (nm)
Ge_3Me_8	218
$Ph_3GeGe(SiMe_3)GePh_3$	245
$Ph_3GeGeMe_2GePh_3$	245
$Bu^tMe_2GeGePh_2GeMe_2Bu^t$ (**1**)	246
$PhMe_2GeGePh_2GeMe_2Ph$ (**2**)	248
$Bu^n_3GeGePh_2GeBu^n_3$ (**3**)	249
Ge_3Ph_8	249
$Ph_3GeGe(PhMe)GePh_3$	250
$(p\text{-}Tol)_3GeGePh_2Ge(p\text{-}Tol)_3$	251
$(p\text{-}Tol)_3GeGeMe_2Ge(p\text{-}Tol)_3$	251
$Ge_3(p\text{-}Tol)_8$	253
$(p\text{-}Tol)_3GeGe(C_6F_5)_2 Ge(p\text{-}Tol)_3$	258
$(p\text{-}F_3CC_6H_4)GeGe(C_6F_5)_2Ge(C_6H_4CF_3\text{-}p)_3$	264

The Taft parameters σ^* can be used to quantify the inductive electron donating ability of the ligands in the trigermanes synthesized in this chapter.[83–85] Of the trigermanes that were synthesized, **1** – **3** can be envisioned as a series where replacing the *tert*-butyl group in **1** with phenyl groups will give **2**. Similarly, if one were to replace all six of the terminal substituents in **1** and **2** with *n*-butyl groups it would give **3**. The σ^* value for a methyl group is taken as zero, while the σ^* values for a Bu^n, Bu^t, and Ph groups are – 0.166, – 0.300, and + 0.600 respectively. It is also known that negative values are indicative of more electron donating groups, while a positive integer is representative of a more electron withdrawing substituent.[84,85] Taking these values into account, **3** having three *n*-butyl groups would be expected to be the easiest to oxidize in comparison to **1** and **2** since as they both contain two methyl groups. Between **1** and **2**, **2** should be more difficult to oxidize due to the phenyl group being inductively electron withdrawing therefore leading

to a more stabilized HOMO. This is consistent with the CV and DPV data and give a correlation in that the order of ease of oxidation is **3** < **1** < **2**.
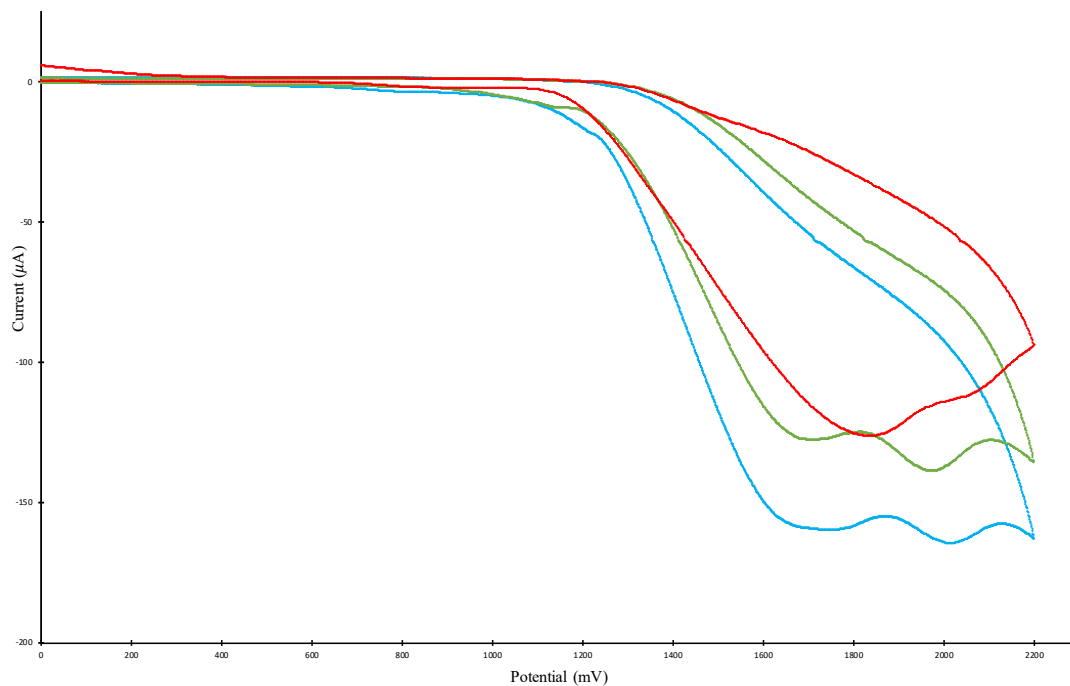
Figure 2.8: Cyclic voltammetry analysis of **1** (blue), **2** (red), and **3** (green) at a scan rate of 50 mV/sec in CH_2Cl_2 solvent with 0.1 M $[Bu^n_4N][PF_6]$ as a supporting electrolyte.[82]
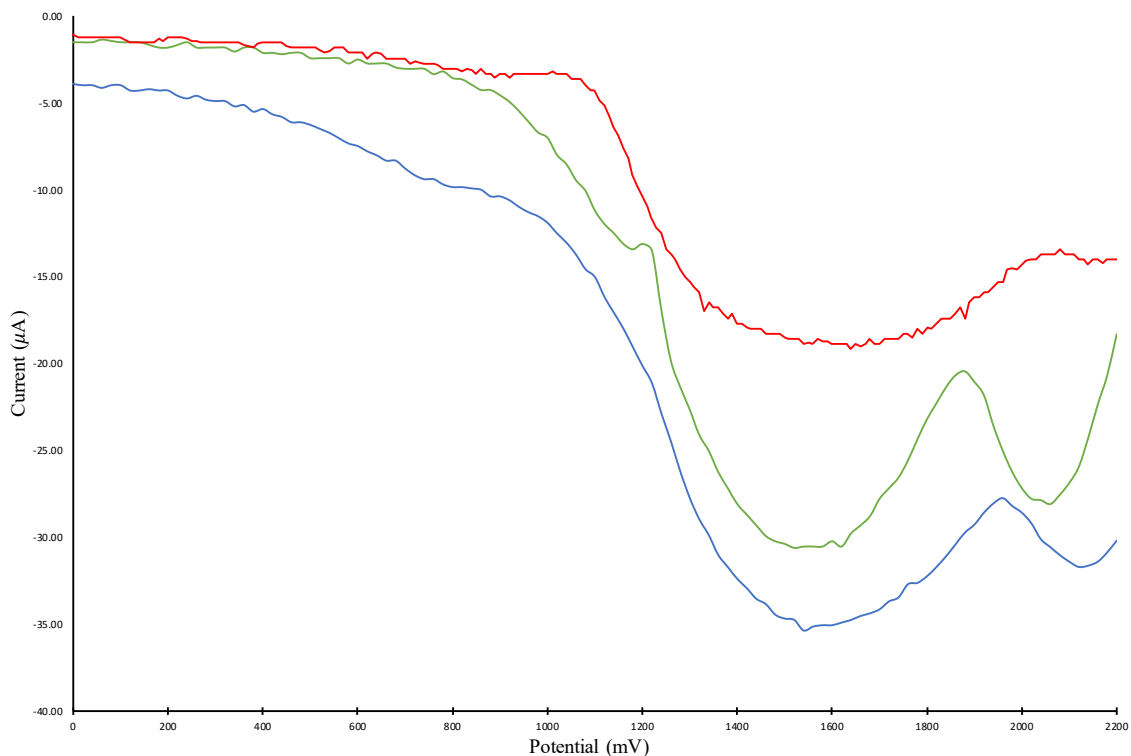
Figure 2.9: Differential pulse voltammetry analysis (pulse period = 0.1 sec, pulse width = 0.05 sec) of **1** (blue), **2** (red), **3** (green) in CH_2Cl_2 solvent with 0.1 M $[Bu^n_4N][PF_6]$ as a supporting electrolyte.[82]

All the trigermanes (**1** – **3**) display one or more irreversible oxidation waves as seen in their CV analysis, as is common for not just linear oligogermanes, but also branched germanium chains with three to six germanium atoms in the Ge – Ge backbone. As for reversible oxidation, no such event has been reported yet even with the use of a microelectrode capable of extremely fast scan times. The irreversible nature of the oxidation events indicate that a chemical reaction is occurring after the trigermane has been oxidized. The trigermanes **1** and **3**, both exhibit a second oxidation wave at a higher potential. This is likely due to the formation and subsequent oxidation of the digermyl radical that forms from the resulting homolytic cleavage of one of the germanium–germanium bonds after the first oxidation occurs.[55] This has been previously observed for

23

oligogermanes when subjected to electrochemical studies through CV and DPV. Some studies have shown reports of oligogermanes having multiple oxidation waves, most notably in the series of oligogermanes (p-CH$_3$C$_6$H$_4$)$_3$Ge(GePh$_2$)$_n$Ge(p-C$_6$H$_4$CH$_3$)$_3$ (n = 1 or 2) and Pr$^i_3$Ge(GePh$_2$)$_n$GePr$^i_3$ as well as for the branched oligogermane (Bu$^n_3$Ge)$_3$GePh.[63–65,46,55,76–79,86] Based on pervious bulk electrolysis studies done on the branched oligogermane (Bu$^n_3$Ge)$_3$GePh,[55] the decomposition of oligogermanes **1** and **3** is proposed to occur as shown in Scheme 2.3. After oxidation, the trigermanes **1** and **3** form a cationic species, followed by a homolytic cleavage occurring between two Ge – Ge bonds to yield a digermyl radical as well as a germylium species. Based on the close proximity of the two oxidation waves in the CV, it is highly unlikely that a positively charged digermane fragment exists in the solution and is subsequently oxidized. The oxidation of the remaining digermane fragment then occurs to yield a second homolytic cleavage of the remaining Ge – Ge bond again yielding a germylium ion and a germylene. Based on the reactivity of the germylene, it is expected that it will polymerize while the cationic species will abstract a halogen atom from the CH$_2$Cl$_2$ solvent to produce corresponding chlorides R$_3$GeCl. Although bulk electrolysis experiments were conducted for the trigermanes **1** and **3**, we were unable to isolate the decomposition products Bu$^n_3$GeCl and Bu^{t}Me$_2$GeCl.
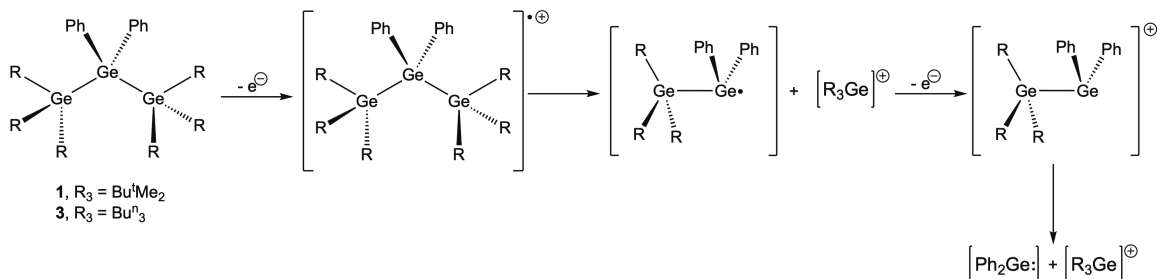
Scheme 2.3: Proposed decomposition pathway for trigermanes **1** and **3**.[82]

24

The UV/visible spectra of compounds **1** – **3** in CH_2Cl_2 are shown in Figure 2.11. The absorption maxima (λ_{max}) of all three trigermanes are similar with values of 246, 248, and 249 nanometers (nm) for **1**, **2**, and **3** respectively. The values are essentially the same within experimental error, and while the λ_{max} for **2** and **3** are well defined, the λ_{max} for **1** appears as a shoulder. The absorption peaks arise due to an electronic transition between the σ-bonding to σ^*-antibonding orbitals of the trigermanes, and this is a result of the σ-delocalization associated with germanium catenates. As shown in Table 2.3, one can make a comparison of the λ_{max} values between conjugated organic compounds having similar absorption maxima and those of the trigermanes **1**, **2**, and **3**. The absorption maxima for **1** – **3** are in the range normally observed for trigermanes having organic alkyl or aryl substituents as shown previously in Table 2.2. The permethylated trigermane Ge_3Me_8 has an λ_{max} at 218 nm, and this is due to the methyl groups having little to no electron donating ability. Trigermanes bearing organic substituents such as *n*-butyl, phenyl, or *para*-tolyl typically exhibit absorption maxima in the range of 245 – 255 nm. However, when the substituents are inductively electron withdrawing such as C_6F_5- and p-$F_3CC_6H_4-$, the λ_{max} of the trigermanes are red – shifted, due to the stabilization of the σ^* - antibonding orbital or the LUMO by the perfluorinated aryl ligands.[62,87]
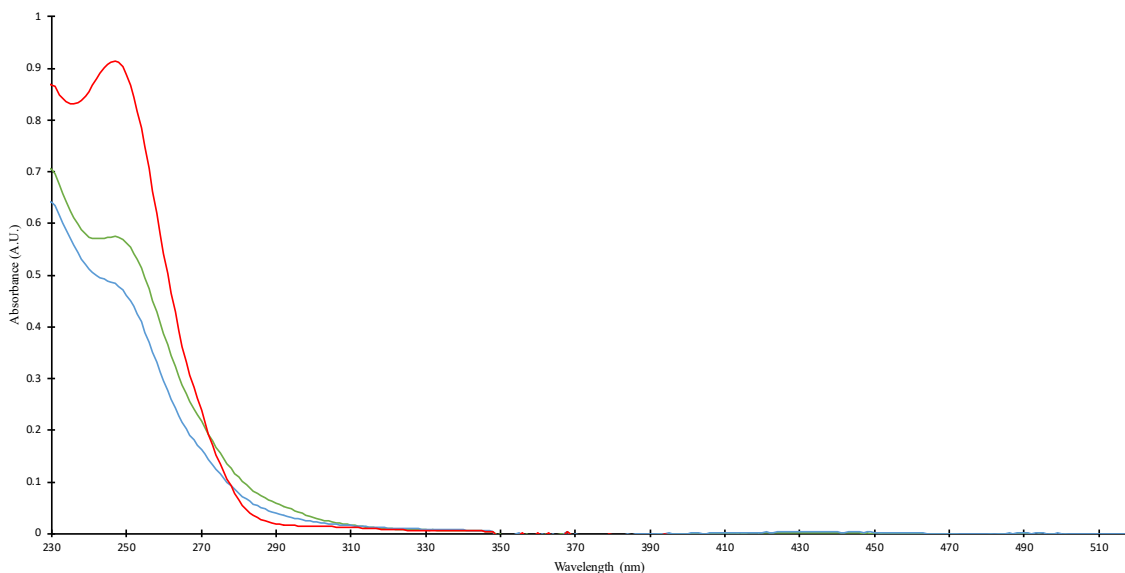
Figure 2.10: Overlaid UV/Visible spectra of trigermanes **1** (blue), **2**, (red), and **3** (green) in CH$_2$Cl$_2$ solution.[82]

Table 2.3 Absorption maxima (λ_{max}) comparison of catenated trigermanes and conjugated organic compounds.[88]

Trigermane	λ_{max} (nm)	Organic Compound	λ_{max} (nm)
Bu^{t}Me$_2$GeGePh$_2$GeMe$_2$Bu^t (**1**)	246	2-Methyl-1,3-butadiene	220
PhMe$_2$GeGePh$_2$GeMe$_2$Ph (**2**)	248	1,3-Cyclohexadiene	256
Bu$^n_3$GeGePh$_2$GeBu$^n_3$ (**3**)	249	1,3,5-Hexatriene	258

The two tetragermanes Et$_3$Ge(GePh$_2$)$_2$GeEt$_3$ (**4**) and Bu$^n_3$Ge(GePh$_2$)$_2$GeBu$^n_3$ (**5**) were synthesized according to Scheme 2.4 again, via the hydrogermolysis reaction. Attempted synthesis of Bu^{t}Me$_2$Ge(GePh$_2$)$_2$GeMe$_2$Bu^t and PhMe$_2$Ge(GePh$_2$)$_2$GeMe$_2$Ph proved to be unsuccessful even with prolonged heating times of two months nor with the addition of excess trialkylgermyl amine. The X-ray crystal structure of **4** was obtained and the molecular structure is shown in Figure 2.12. Selected bond distances and angles for **4** are collected in Table 2.4.
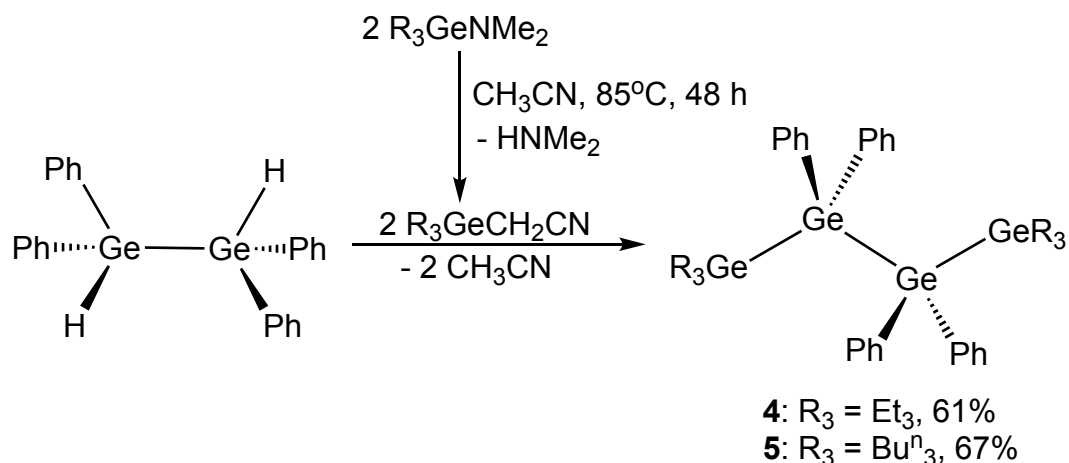
Scheme 2.4: Synthesis of tetragermanes **4** and **5**.[82]

Tetragermane **4** crystallizes with two independent molecules in the unit cell. In Molecule 1 the carbon atoms C(1aa) and C(1) on two of the ethyl substituents attached to Ge(4) are disordered with occupancies of 0.5. Molecule 1 has four crystallographically unique germanium atoms, and the average bond distance measures 2.4420(6) Å. Both terminal Ge – Ge bonds are slightly longer than the central bond by 0.0051 Å. The germanium – carbon bond lengths are close to the typical value of *ca.* 1.95 Å.

In Molecule 2, the central Ge(5)–Ge(5`) bond lies on an inversion center and the average Ge – Ge bond distance is 2.4335(6) Å which is slightly shorter than the average bond distance found in Molecule 1. Due to the presence of the inversion center in Molecule 2, this now renders all four germanium atoms in a *trans*-coplanar configuration. In Molecule 1, considering the plane formed by one of the terminal germanium atoms and both of the internal germanium atoms, the remaining germanium atom is canted slightly out of plane by 6.71(2)°. In Molecule 1, the two Ge – Ge – Ge bond angles average 116.9(2)° in comparison to Molecule 2, where the single unique Ge – Ge – Ge bond angle measures 112.75(2)°, and so the bond angle in Molecule 2 is slightly more acute.

27

Molecule 1   Molecule 2
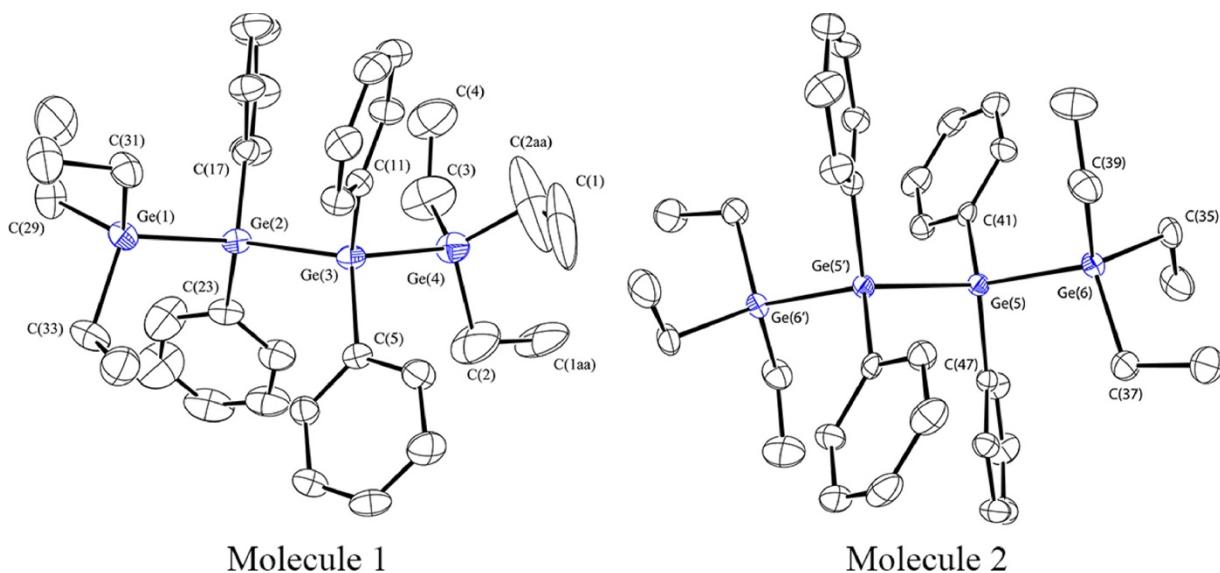
Figure 2.11: X-ray crystal structure of **4**. Thermal ellipsoids are drawn at 50% probability.[82]

Table 2.4 Selected bond distances (Å) and angles (deg) for **4**.[82]

Molecule 1		Molecule 2	
Ge(1) – Ge(2)	2.4437 (6)	Ge(5) – Ge(5`)	2.4319 (7)
Ge(2) – Ge(3)	2.4386 (6)	Ge(5) – Ge(6)	2.4315 (5)
Ge(3) – Ge(4)	2.4437 (6)	Ge(5) – C(41)	1.966 (4)
Ge(1) – C(29)	1.975 (4)	Ge(5) – C(47)	1.970 (4)
Ge(1) – C(31)	1.967 (4)	Ge(6) – C(35)	1.963 (4)
Ge(1) – C(33)	1.969 (4)	Ge(6) – C(37)	1.966 (4)
Ge(2) – C(17)	1.963 (4)	Ge(6) – C(39)	1.962 (4)
Ge(2) – C(23)	1.973 (4)		
Ge(3) – C(5)	1.973 (4)	Ge(6) – Ge(5) – Ge(5`)	112.75 (2)
Ge(3) – C(11)	1.967 (4)	C(41) – Ge(5) – C(47)	108.5 (2)
Ge(4) – C(2)	1.964 (6)	C(35) – Ge(6) – C(37)	107.9 (2)
Ge(4) – C(3)	1.950 (6)	C(35) – Ge(6) – C(39)	108.7 (2)
Ge(4) – C(2aa)	1.867 (8)	C(37) – Ge(6) – C(39)	109.3 (2)
		Ge(5`) – Ge(5) – C(41)	108.7 (1)
Ge(1) – Ge(2) – Ge(3)	118.47 (2)	Ge(5`) – Ge(5) – C(47)	107.0 (1)
Ge(2) – Ge(3) – Ge(4)	115.35 (2)	Ge(5) – Ge(6) – C(35)	109.5 (1)
C(29) – Ge(1) – C(31)	108.3 (2)	Ge(5) – Ge(6) – C(37)	107.4 (1)
C(29) – Ge(1) – C(33)	107.5 (2)	Ge(5) – Ge(6) – C(39)	113.9 (1)
C(31) – Ge(1) – C(33)	108.3 (2)	Ge(6) – Ge(5) – C(41)	112.7 (1)
C(17) – Ge(2) – C(23)	107.7 (2)	Ge(6) – Ge(5) – C(47)	106.7 (1)
C(5) – Ge(3) – C(11)	105.7 (2)		
C(2) – Ge(4) – C(3)	106.1 (2)		
C(2) – Ge(4) – C(2aa)	110.2 (5)		
C(3) – Ge(4) – C(2aa)	109.5 (5)		
Ge(1) – Ge(2) – C(17)	106.8 (2)		

28

Ge(1) – Ge(2) – C(23)	108.1 (2)
Ge(2) – Ge(1) – C(29)	108.4 (2)
Ge(2) – Ge(1) – C(31)	113.2 (2)
Ge(2) – Ge(1) – C(33)	111.1 (2)
Ge(2) – Ge(3) – C(5)	110.9 (1)
Ge(2) – Ge(3) – C(11)	107.9 (1)
Ge(3) – Ge(2) – C(17)	104.8 (1)
Ge(3) – Ge(2) – C(23)	110.4 (1)
Ge(3) – Ge(4) – C(2)	106.1 (2)
Ge(3) – Ge(4) – C(3)	112.5 (2)
Ge(3) – Ge(4) – C(2aa)	110.7 (3)
Ge(4) – Ge(3) – C(5)	106.8 (1)
Ge(4) – Ge(3) – C(11)	109.9 (1)

The environment at each of the germanium atoms in both Molecules 1 and 2 are slightly distorted from the idealized tetrahedral. Among the bond angles in Molecule 2, we see that the average Ge – Ge – C and C – Ge – C bond angles are 109.4º and 108.6º, respectively. In comparison to Molecule 1, the average Ge – Ge – C and C – Ge – C bond angles are 107.9º and 109.1º, respectively. The structure of **4** can be compared to two other similar crystallographically characterized linear tetragermanes. $Ge_4Ph_{10} \cdot 2C_6H_6$ (**6**)[73] and (p-Tol)$_3$Ge(GePh$_2$)$_2$Ge(p-Tol)$_3$ (**7**).[76] The structure of **6** also contains an inversion center and overall is very similar to that of **4**, except for some small differences in the bond angles and distances. We see that the Ge – Ge – Ge bond angle in **6** is 117.8(1)º and is slightly more obtuse than the corresponding angles in **4**, while the Ge – Ge bond distances in **6** are 2.463(2) and 2.461(3) Å and therefore are slightly elongated relative to those in **4**.

In the structure of **7**, similarities are again present with this compound while also having two crystallographically independent molecules in its unit cell. The Ge – Ge – Ge bond angles in the two molecules are 115.53(3)º and 119.9(2)º, with an average value of 117.2º. The Ge – Ge bond distances in **7** are 2.4490(8) and 2.457(1) Å in one molecule and 2.460(3) and 2.448(3) Å in the other. It is noted that if three terminal ethyl groups in **4** are

replaced either by phenyl groups or *p*-tolyl groups, this results in only slight changes in the Ge – Ge – Ge bond angles among all three molecules as well as a slight elongation of the Ge – Ge bond distances in the aryl substituted tetragermanes **6** and **7**.

The effects of varying the substituents on the terminal germanium atoms also affects the differential pulse voltammograms of these two tetragermanes. The DPV of **4** has three clearly defined oxidation waves as shown in Figure 2.13 at 1413, 1695, and 2145 mV. The three oxidation waves are indicative of three homolytic Ge – Ge bond cleavages that occur after the first, second, and third oxidation events. Unlike the trigermanes **1** and **3**, the decomposition of **4** is much more complex in that there are multiple possible pathways for the molecule to completely break apart.
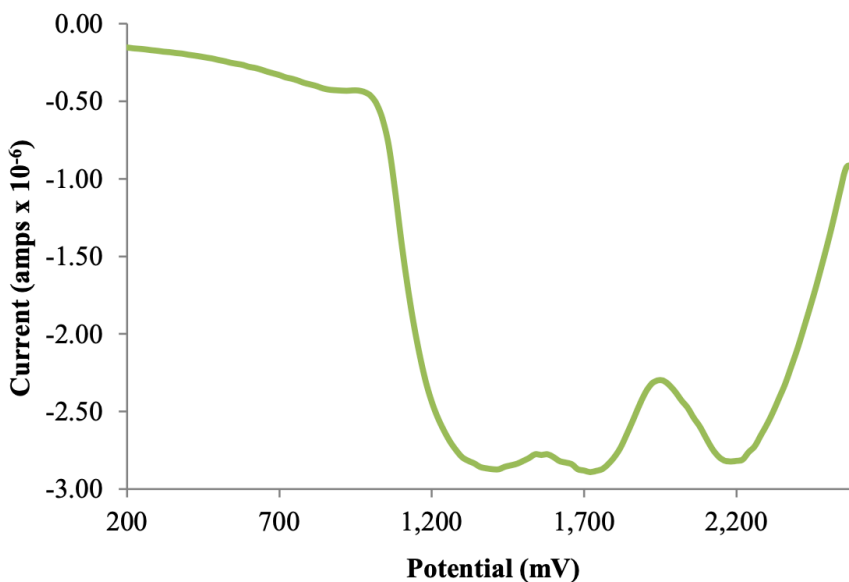
Figure 2.12: Differential pulse voltammogram of **4** in CH_2Cl_2 with $[NH_4][PF_6]$ as the supporting electrolyte (pulse period = 0.1 sec, pulse width = 0.05 sec).[82]

In compound **4**, after the first oxidation takes place it is likely that one of the terminal Ge – Ge bonds is cleaved to yield a germylium ion $[Et_3Ge]^+$ and a trigermyl

radical. The resulting $[Et_3Ge]^+$ species can abstract a chlorine atom from the CH_2Cl_2 solvent to form Et_3GeCl and the trigermyl radical is then subsequently oxidized. The species then continues to decompose via a $Ge - Ge$ bond cleavage, although it is difficult to state with certainty how this occurs, since multiple pathways are available for this species to decompose. Upon completion of the decomposition, the final products are likely Et_3GeCl and the subsequent germylene Ph_2Ge: that will quickly polymerize. The proposed decomposition of **4** is shown in Scheme 2.5.
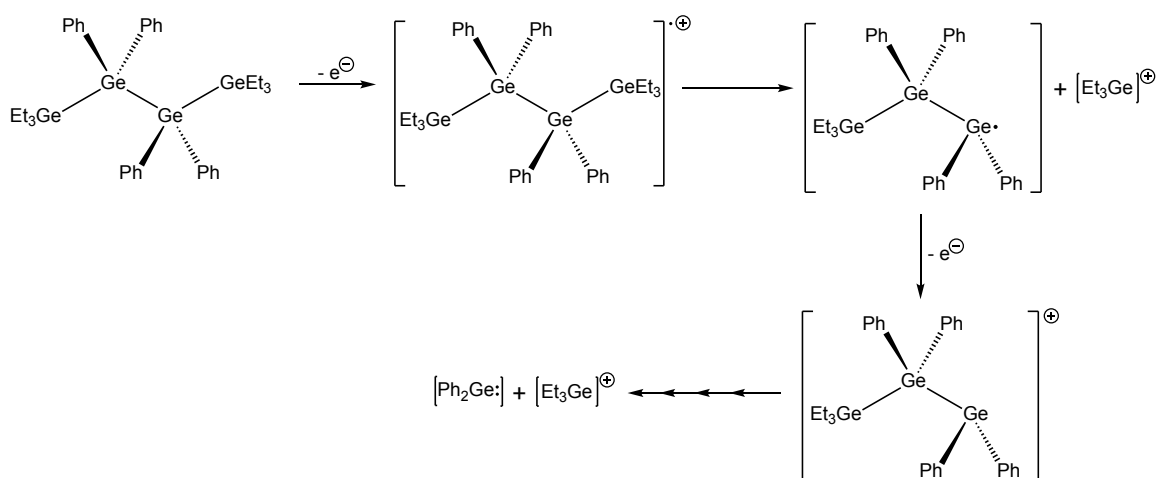
Scheme 2.5: Proposed decomposition pathway of **4** during the DPV electrochemical sweep.[82]

Differential pulse voltammetry studies were also conducted on **5** in CH_2Cl_2, and it was found to only exhibit a single oxidation wave at 1355 mV.[89] It was shown that **5** is easier to oxidize than **4** due to the presence of *n*-butyl groups at the terminal germanium atoms versus the ethyl groups present in **4**. This hypothesis is consistent with the σ^* parameters for an ethyl group versus a *n*-butyl group that are $-$ 0.100 and $-$ 0.166 respectively.[83–85] This indicates that an *n*-butyl group is more inductively donating than an ethyl group based on the data presented.

The UV/visible spectra of **4** and **5** in CH_2Cl_2 solvent are essentially identical within experimental error, with λ_{max} values being 253 and 254 nm, respectively.[89] The perphenyl-tetragermane Ge_4Ph_{10} has an oxidation potential of 1644 mV and shows two additional oxidation waves at 2060 and 2450 mV.[76] These values indicate that the compound is more difficult to oxidize than both **4** and **5**. Additionally, the absorption maximum for Ge_4Ph_{10} is 282 nm, which is a substantially large red shift compared to the λ_{max} values for compounds **4** and **5**, as expected. Of the germanium oligomers synthesized, both **4** and **5** are more facile to oxidize than the trigermanes **1 – 3**, and the oxidation potential in the DPV of **5** is 165 mV more negative than trigermane **3** that was observed to be 1520 mV, largely due to compounds **3** and **5** differing by one $-GePh_2-$ unit.

2.3 Conclusion

The two previously unknown trigermanes $Bu^tMe_2GeGePh_2GeMe_2Bu^t$ (**1**) and $PhMe_2GeGePh_2GeMe_2Ph$ (**2**) as well as the tetragermanes $Et_3Ge(GePh_2)_2GeEt_3$ (**4**) and $Bu^n_3Ge(GePh_2)_2GeBu^n_3$ (**5**) were synthesized via the hydrogermolysis reaction. For trigermanes **1** and **2**, the reactions of the germyl amines $Bu^tMe_2GeNMe_2$ and $PhMe_2GeNMe_2$ with the corresponding hydride Ph_2GeH_2 were very sluggish and required longer reaction times than normal to form these Ge – Ge bonds.

The spectroscopic and electrochemical properties of **1** and **2** were compared with those of the previously synthesized trigermane $Bu^n_3GeGePh_2GeBu^n_3$ (**3**). The λ_{max} values of **1 – 3** in their UV/visible spectra are similar, but their oxidation potentials are measurably different. As presumed by the electron donating or withdrawing nature of the substituents at the terminal germanium atom in these three compounds, the order of ease of oxidation observed was **3 > 2 > 1**. In **1** and **3**, there are two clear irreversible oxidation waves in their

CVs and DPVs indicating that a second species is formed after the first oxidation takes place and is stable enough to undergo a second oxidation. Of these stable secondary products, it can be postulated that it is likely a digermyl radical that formed by homolytic scission of one of the Ge – Ge bonds that then undergoes the second oxidation. In **2** however, there was only a single oxidation wave in both its CV and DPV.

The tetragermanes $Et_3Ge(GePh_2)_2GeEt_3$ (**4**) and $Bu^n_3Ge(GePh_2)_2GeBu^n_3$ (**5**) also displayed similar absorption maxima to one another in their UV/vis spectra. However, their oxidation potentials were different. The *n*-butyl substituted tetragermane **5** was found to be easier to oxidize than the ethyl substituted tetragermane **4**. In **5** it was noted that only a single oxidation wave was exhibited in the DPV of **5**, while in tetragermane **4** the DPV exhibited three irreversible oxidation waves indicating that three successive bond cleavage processes are occurring, one after each subsequent oxidation event. The X-ray crystal structure of **4** was obtained and constitutes a rare example of a crystallographically characterized tetragermane bearing alkyl substituents.

2.4 Experimental Section

General Remarks

All manipulations were carried out under a nitrogen atmosphere using standard Schlenk, syringe, and glovebox techniques. Solvents were dried using a Glass Contour solvent purification system. The reagents $HPh_2GeGePh_2H$,[76] $Bu^tMe_2GeNMe_2$,[79] Et_3GeNMe_2,[46] $Bu^n_3GeNMe_2$,[46] and $PhMe_2GeNMe_2$[90] were prepared using literature procedures. The overall synthesis of these compounds can be seen in Schemes 2.6 and 2.7. Ph_2GeH_2 was purchased from Gelest and used without further purification. NMR spectra were acquired using a Bruker Avance III spectrometer operating at 400.00 MHz (^{1}H) or

100.57 MHz (^{13}C). UV/visible spectra were obtained using an Ocean Optics Red Tide USB650UV spectrometer in CH_2Cl_2 solvent. Electrochemical data (CV and DPV) were obtained using a DigiIvy DY2312 potentiostat with a glassy carbon working electrode, a platinum wire counter electrode, and a Ag/AgCl reference electrode in CH_2Cl_2 solution using 0.1M $[Bu^n_4N][PF_6]$ as the supporting electrolyte. Elemental analyses were conducted by Midwest Microlabs.
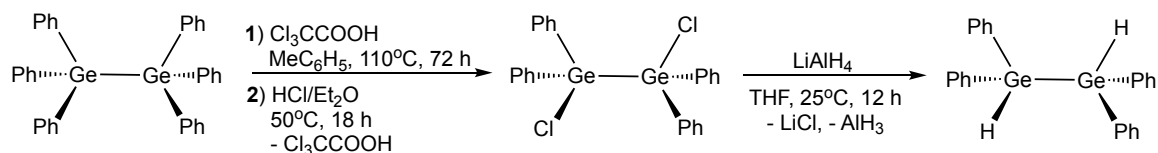
Scheme 2.6: Synthesis of $HPh_2GeGePh_2H$.[82]
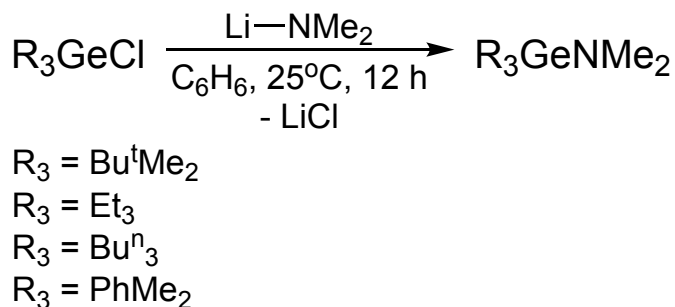
Scheme 2.7: Synthesis of germyl amines with varying substituents.[82]

*Synthesis of Bu^{t}Me$_2$GeGePh$_2$GeMe$_2$Bu^t (**1**)*

A solution of $Bu^tMe_2GeNMe_2$ (2.00 g, 9.81 mmol) in acetonitrile (15 mL) was added to a Schlenk tube followed by a solution of Ph_2GeH_2 (1.12 g, 4.90 mmol) in acetonitrile (10 mL). The Schlenk tube was then sealed with a Teflon stopper and left in an oil bath for 48 hours at 85 °C. The volatiles were removed *in vacuo* (80 °C, 0.005 torr) and ^{1}H NMR indicated the formation of $Bu^tMe_2GeGePh_2H$. The reaction mixture was re-dissolved in acetonitrile (25 mL) in a Schlenk tube and additional $Bu^tMe_2GeNMe_2$ (1.00 g, 4.90 mmol) was added. The reaction mixture was left in an oil bath at 100 °C for 14

days. The volatiles were removed in *vacuo* (80 °C, 0.005 torr) to yield **1** as a colorless liquid (1.75 g, 65%). ^{1}H NMR (C$_6$D$_6$, 25 °C): δ 7.68 (d, J = 8.1 Hz, 4H, *o*-C$_6$H$_5$), 7.22 – 7.13 (m, 6H, *m*-C$_5$H$_5$ and *p*-C$_6$H$_5$), 0.90 (s, 18 H, -C (CH$_3$)$_3$), 0.44 (s, 12H, -CH$_3$) ppm. ^{13}C NMR (C$_6$D$_6$, 25 °C): δ 140.4 (*ipso*-C$_6$ H$_5$), 136.2 (*o*-C$_6$H$_5$), 128.4 (*m*-C$_6$H$_5$), 128.2 (*p*-C$_6$H$_5$), 28.8 (-C(CH$_3$)$_3$), 26.8 (- C(CH$_3$)$_3$), - 3.1 (-CH$_3$) ppm. Anal. Calcd. for C$_{24}$H$_{40}$Ge$_3$: C, 52.75; H, 7.32. Found: C, 52.67; H, 7.41.

Synthesis of PhMe$_2$GeGePh$_2$GeMe$_2$Ph (**2**)

A solution of PhMe$_2$GeNMe$_2$ (2.00 g, 8.93 mmol) in acetonitrile (15 mL) was added to a Schlenk tube followed by a solution of Ph$_2$GeH$_2$ (1.02, 4.47 mmol) in acetonitrile (10 mL). The Schlenk tube that was then sealed with a Teflon stopper and left in an oil bath for 48 hours at 85 °C. The volatiles were removed in *vacuo* (80 °C, 0.005 torr) to yield a yellow oil that was analyzed by ^{1}H NMR spectroscopy, which revealed the presence of PhMe$_2$GeGePh$_2$H. The reaction mixture was re-dissolved in acetonitrile (25 mL) and additional PhMe$_2$GeNMe$_2$ (1.00 g, 4.46 mmol) was added to the solution. The reaction mixture was placed in an oil bath at 100 °C and left for 24 hours. The volatiles were removed *in vacuo* (80 °C, 0.005 torr) to yield the **2** as a yellow liquid (2.02 g, 77%). ^{1}H NMR (C$_6$D$_6$, 25 °C): δ 7.52 (d, J = 7.6 Hz, 4H, *o*-aromatics), 7.35 (d, J = 6.8 Hz, 4H, *o*- aromatics), 7.20 – 7.16 (m, 6H, *m*- aromatics and *p*-aromatics), 7.13 – 7.09 (m, 6H, *m*- aromatics and *p*- aromatics), 0.54 (s, 12H, -CH$_3$) ppm. ^{13}C NMR (C$_6$D$_6$, 25 °C): δ 141.8 (*ipso*-aromatics), 138.7 (*ipso*-aromatics), 136.0 (*o*-aromatics), 134.0 (*o*-aromatics), 128.6 (*m*-aromatics), 128.5 (*m*-aromatics), 128.4 (*p*- aromatics), 128.2 (*p*-aromatics), - 1.6 (-CH$_3$) ppm. Anal. Calcd. for C$_{28}$H$_{32}$Ge$_3$: C, 57.35; H, 5.50. Found: C, 57.26; H, 5.43.

Synthesis of Et$_3$Ge(GePh$_2$)$_2$GeEt$_3$ (**4**)

To a solution of $HPh_2GeGePh_2H$ (0.250 g, 0.549 mmol) in CH_3CN (15 mL) was added a solution of Et_3GeNMe_2 (0.224 g, 1.10 mmol) in CH_3CN (15 mL) under an atmosphere of nitrogen. The reaction mixture was sealed in a Schlenk tube under nitrogen and stirred for 48 hours at 85 °C. The acetonitrile was removed *in vacuo* (80 °C, 0.005 torr) and the resulting thick oil was vacuum distilled (80 °C, 0.005 torr) to yield **4** (0.259 g, 61%) as a white solid. ^1H NMR (C_6D_6, 25 °C): δ 7.72 - 7.56 (m, 8H, *meta*-C_6H_5), 7.22 - 6.88 (m, 12H, *ortho*-C_6H_5 and *para*-C_6H_5), 1.05 (m, 12H, - CH_2CH$_3$), 0.94 (m, 18H, - CH$_2$CH_3) ppm. ^{13}C NMR (C_6D_6, 25 °C): δ 139.2 (*ipso*-C_6H_5), 137.1 (*o*-C_6H_5), 136.5 (*m*-C_6H_5), 136.0 (*p*-C_6H_5), 10.3 (-CH$_2$CH_3), 6.6 (-CH_2CH$_3$) ppm. Anal. Calcd. for $C_{36}H_{50}Ge_4$: C, 55.91; H, 6.52. Found: C, 55.84; H, 6.44.

Synthesis of $Bu^n_3Ge(GePh_2)_2GeBu^n_3$ (**5**)

To a solution of $HPh_2GeGePh_2H$ (0.400 g, 0.878 mmol) in CH_3CN (15 mL) was added a solution of $Bu^n_3GeNMe_2$ (0.506 g, 1.76 mmol) in CH_3CN (15 mL) under an atmosphere of nitrogen. The reaction mixture was sealed in a Schlenk tube under nitrogen and stirred for 48 hours at 85 °C. The acetonitrile was removed *in vacuo* and the resulting thick oil was vacuum distilled (80 °C, 0.005 torr) to yield **5** (0.554 g, 67%) as a white solid. ^1H NMR (C_6D_6 , 25°C): δ 7.75 - 7.64 (m, 8H, *meta*-C_6H_5), 7.25 - 7.10 (m, 12H, *ortho*-C_6H_5 and *para*-C_6H_5), 1.60 - 0.90 (m, 36H, -CH_2CH_2CH_2CH$_3$), 0.81 (t, *J* = 6.9 Hz, 18H, - CH$_2$CH$_2$CH$_2$CH_3) ppm. ^{13}C NMR (C_6D_6, 25°C): δ 139.8 (*ipso*-C_6H_5), 137.1 (*o*-C_6H_5), 136.5 (*m*-C_6H_5), 136.0 (*p*-C_6H_5), 28.9 (-CH$_2$CH$_2$CH_2CH$_3$), 26.5 (-CH$_2$CH_2CH$_2$CH$_3$, 14.0 (-CH$_2$CH$_2$CH$_2$CH_3), 12.2 (-CH_2CH$_2$CH$_2$CH$_3$) ppm. Anal. Calcd. for $C_{48}H_{74}Ge_4$: C, 61.23; H, 7.92. Found: C, 61.36; H, 7.84.

X-ray structure determination of $Et_3Ge(GePh_2)_2GeEt_3$ (**4**)

Single crystals of $C_{36}H_{50}Ge_4$ (**4**) were obtained by recrystallization from toluene at 35°C. A suitable crystal was selected and mounted on a Bruker APEX-II CCD diffractometer. The crystal was kept at 100.15 K during data collection. Using Olex2,[91] the structure was solved with the ShelXS[92] structure solution program using Direct Methods and refined with the XL[92] refinement package using Least Squares minimization. Disordered ethyl groups were modeled with substantial restraint on the thermal ellipsoids of the terminal methyl groups.

Crystal data for $C_{36}H_{50}Ge_4$ (M =773.20 g/mol): monoclinic, space group $P2_1/c$ (no. 14), a = 27.193(1) Å, b = 10.6491(4) Å, c = 18.6622(8) Å, β = 90.853(2)°, V = 5403.5(4) Å^3, Z = 4, T = 100.15 K, μ(MoKα) = 3.327 mm^{-1}, $Dcalc$ = 1.426 g/cm^3, 77117 reflections measured (2.996° $\leq 2\Theta \leq$ 52.834°), 11066 unique (R_{int} = 0.0588, R_{sigma}= 0.0434) which were used in all calculations. The final R_1 was 0.0408 (I > 2σ(I)) and wR_2 was 0.0876 (all data). CCDC Deposition Number: 2015113.

CHAPTER III

REACTIONS OF POLYFUNCTIONAL PHENOL AND PHENOXIDE

SUBSTITUENTS WITH GERMANIUM(II) AMIDES AND GERMANIUM(IV)

HALIDES FOR HYDROGERMYLATION

3.1 Introduction

Carbenes have been recognized as important conduits between organic and inorganic chemistry. Owing to their unique reactivities, they have been noted to play key roles as transient intermediates in complex reactions. Carbene chemistry has been extensively studied for decades and is now a well understood area in the field. It is this level of exploration and analysis of carbenes that have led researchers to investigate the reactivities and similarities of the heavier elements in Group 14. Analogous silylenes (R_2Si:), germylenes (R_2Ge:), stannylenes (R_2Sn:), and plumbylenes (R_2Pb:) are considered to be the heavier analogues of carbenes have great importance in applied chemistry due to their differences and similarities to carbenes as well as each other.[93,94] Although some metalenes may exhibit more reactive properties than others, there are instances where they display similar reactivities when reacted with metal carbonyls.

An example of this is seen in Schemes 3.1 and 3.2 with the stannylene ($SnNR_2$) and the germylene ($GeNR_2$) ($R = SiMe_3$) that both undergo a CO ligand substitution with transition metal carbonyls.[95]

$$Sn[N(SiMe_3)_2]_2 \xrightarrow[\substack{M = Cr, Mo, W \\ - CO}]{M(CO)_6} M(CO)_5[Sn(N(SiMe_3)_2)_2]$$
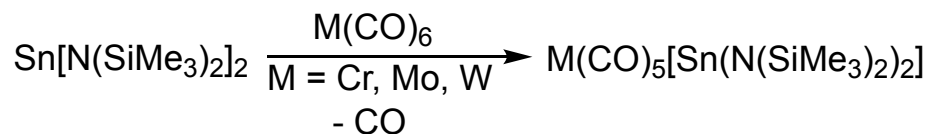
Scheme 3.1: Reaction of $M(CO)_6$ (M = Cr, Mo, W) with $Sn[N(SiMe_3)_2]_2$ to yield a CO ligand substitution.[95]

$$Ge[N(SiMe_3)_2]_2 \xrightarrow[\substack{M = Cr, Mo, W \\ - CO}]{M(CO)_6} M(CO)_5[Ge(N(SiMe_3)_2)_2]$$
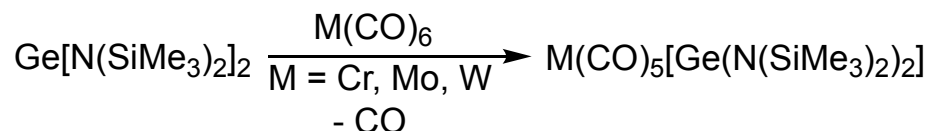
Scheme 3.2: Reaction of $M(CO)_6$ (M = Cr, Mo, W) with $Ge[N(SiMe_3)_2]_2$ to yield a CO ligand substitution.[95]

The chemistry centered around germylenes was pioneered by M. Lesbre and J. Satagé at the University of Toulouse, France in 1948.[96] However, difficulties with their characterization and isolation was problematic due to the high reactivity of these compounds as well as the meager spectroscopic methods available at the time. The high reactivity of these compounds potentially stems from the oxidation state of a germylene being +2. A trend is seen in the Group 14 compounds that correlates stability of the +2 oxidation state with the increasing of the principal quantum number (n). This is noted in compounds containing atoms that are towards the bottom of Group 14, such as $PbCl_2$ and $SnCl_2$, that are air and moisture stable ionic compounds. As seen in Figure 3.1, two electrons exist as a singlet pair in the ns orbital, making the germylene ground state a singlet. This electron pair centered in the sp^2 orbital can effectively allow for germylenes to act as a Lewis base and donate its electron density to other species. These differ from

carbenes which have the ground state found normally in a triplet state.[93,94,96] This singlet state in germylenes also leaves an empty p-orbital that is susceptible to a nucleophilic attack given its Lewis acid character as well. It is noted that in order to stabilize germylenes, as well as other Group 14 analogues, there is a requirement of either thermodynamic and/or kinetic stabilizing ligands. The physical properties and variety in stabilizing ligands could give reason as to why germylenes have been shown to exhibit several structural motifs such as monomers, dimers, and polymers.[97]
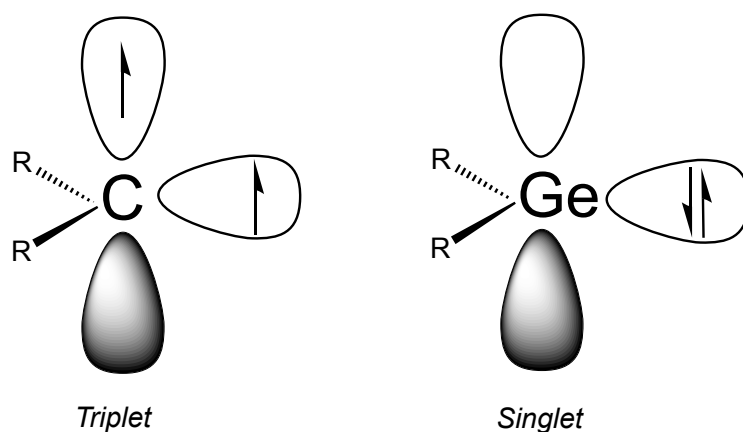
Figure 3.1: Differences in the ground states of a carbene and a germylene.

Currently there exists multiple methods for the synthesis of germylenes. Most of these methods involve the use of ultraviolet (UV) irradiation to induce a homolytic cleavage of a Ge – Ge bond to produce an alkyl or aryl substituted germylene. This is seen in the reaction between tetraphenylgermoles and benzyne which leads to the formation of a 7,7–disubstituted – 7–germabenzonorbornadiene intermediate that produces a dialkyl substituted germylene and tetraphenylnaphthalene upon heating or by UV irradiation. Germylene synthesis using UV irradiation is also known in diaryl and bis(silyl) germanium compounds, photochemical deazotization of dimethyldiazidogermane, and the photolytical

cleavage of strained cyclogermanes containing Ge – Ge bonds.[96] Schemes 3.3 – 3.6 display the overall reaction processes for these germylenes.

R = Me, Et, Bu, Ph, 4-MePh
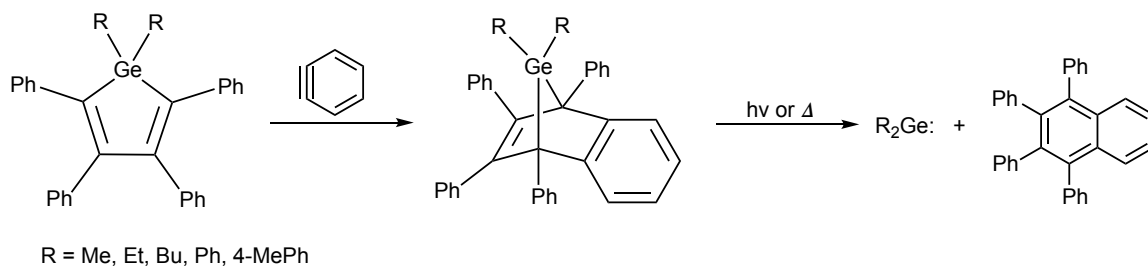
Scheme 3.3: Germylene formation upon UV irradiation after a reaction between tetraphenylgermoles and benzyne.[96]

Ar = Ph, 4-MePh, 2,6-Me$_2$Ph, 2,6-Et$_2$Ph, Mes, 2,4,6-Pr$^i_3$Ph
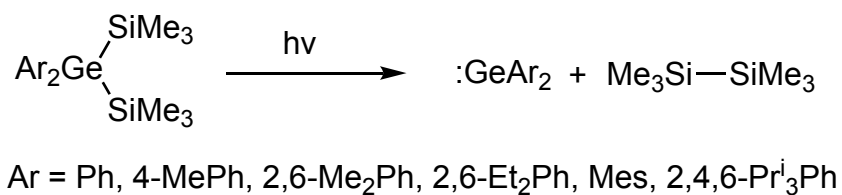
Scheme 3.4: Germylene synthesis via UV irradiation of a bis(silyl) germanium compound.[96]
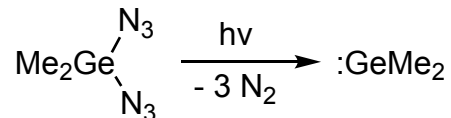
Scheme 3.5: Germylene synthesis via photochemical deazotization of dimethyldiazidogermane.[96]
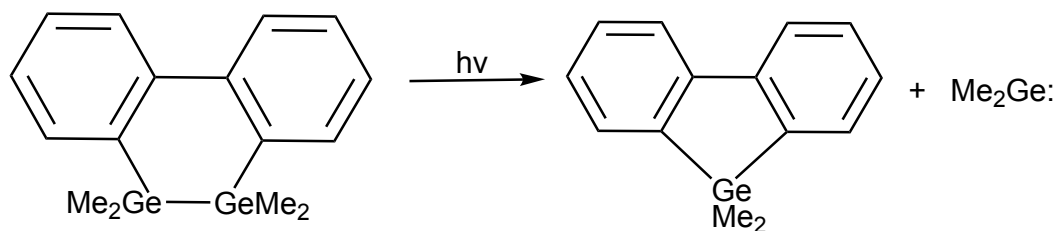
Scheme 3.6: Germylene synthesis via photolytical splitting of strained cyclogermanes.[96]

While there exist several synthetic methods for the production of alkyl and aryl substituted germylenes, the isolation and characterization of germylenes, as mentioned previously, has proved to be complicated due to the high reactivity of these species and

41

their ability to undergo rapid polymerization. In order to characterize these compounds, they must be isolated either in a hydrocarbon matrix at 77 K, or they can be detected by the use of chemical trapping methods using 1,3–dienes or benzil.

While it has been noted that most germylenes are unstable, there has been success in synthesizing germylenes that resist polymerization. This is achieved via the attachment of bulky ligands such as amido, aryloxo, arylthiolato, alkyl and aryl groups to the germanium(II) center. These ligands have been shown to kinetically and/or thermodynamically stabilize the germylene compound such that it does not allow polymerization to occur, and they exist in a monomer–dimer equilibrium state or in a monomeric state alone.[98] Of the variety of ligands used to stabilize germanium(II) compounds, the most common are the disyl ($CH(SiMe_3)_2$) and trimethylsilylamido ($[N(SiMe_3)_2]$) groups which produce the bis[bis(trimethylsilyl)methyl] germanium (II) and bis[bis(trimethylsilyl)amido] germanium(II) germylenes, respectively. Both of these germylenes exist as monomers and this is due to the nature of the ligands bonded to the germanium(II) center. The absence of β–hydrogens and the presence of a β–silicon impedes metal–ligand decomposition through a β–elimination pathway. The bulky ligands also inhibit access to the germanium(II) center through steric effects therefore limiting the reactivity. Additionally, these ligands contain a significant number of methyl groups that not only provide steric bulk, but also provide the benefit of enhancing the solubility of the germylenes in hydrocarbon solvents. The added features of having the ligands listed attached to the germanium(II) center have allowed for their manipulation.

Although the two germylenes mentioned previously are similar in bulk, they are synthesized by different methods, exist with different solid–state structures, and have

exhibited a wide range of reactivity. The compound bis[bis(trimethylsilyl)methyl] germanium(II) (Ge[CH(SiMe$_3$)$_2$]$_2$) can be prepared via the reaction of bis(trimethylsilyl)methyl lithium and a germanium(II) amide as seen in Scheme 3.7.[99]

$$2 \text{ Li[CH(SiMe}_3)_2] \xrightarrow[\text{Et}_2\text{O, 0 to -20°C}]{\text{Ge[N(SiMe}_3)_2]_2} \text{Ge[CH(SiMe}_3)_2]_2 + 2 \text{ Li [N(SiMe}_3)_2]$$
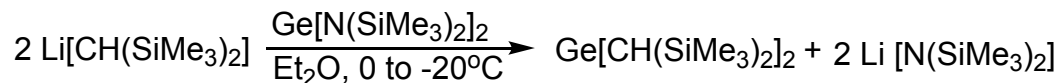
Scheme 3.7: Synthesis of Ge[CH(SiMe$_3$)$_2$]$_2$ via a reaction of Li[CH(SiMe$_3$)$_2$] and a germanium(II) amide.[99]

Ge[CH(SiMe$_3$)$_2$]$_2$ has been shown to be dimeric in the crystalline state as displayed in Figure 3.2, but interestingly reacts in solution as if it were monomeric. This behavior can be most likely attributed to the weak nature of a Ge – Ge bond. A typical Ge – Ge bond measures 2.347(2) Å, which is indicative of a Ge – Ge double bond, while the average Ge – C bond distance measure 2.011(3) Å and the Ge – Ge – C bond angles are 113.7(3)° and 122.3(2)°.[100]
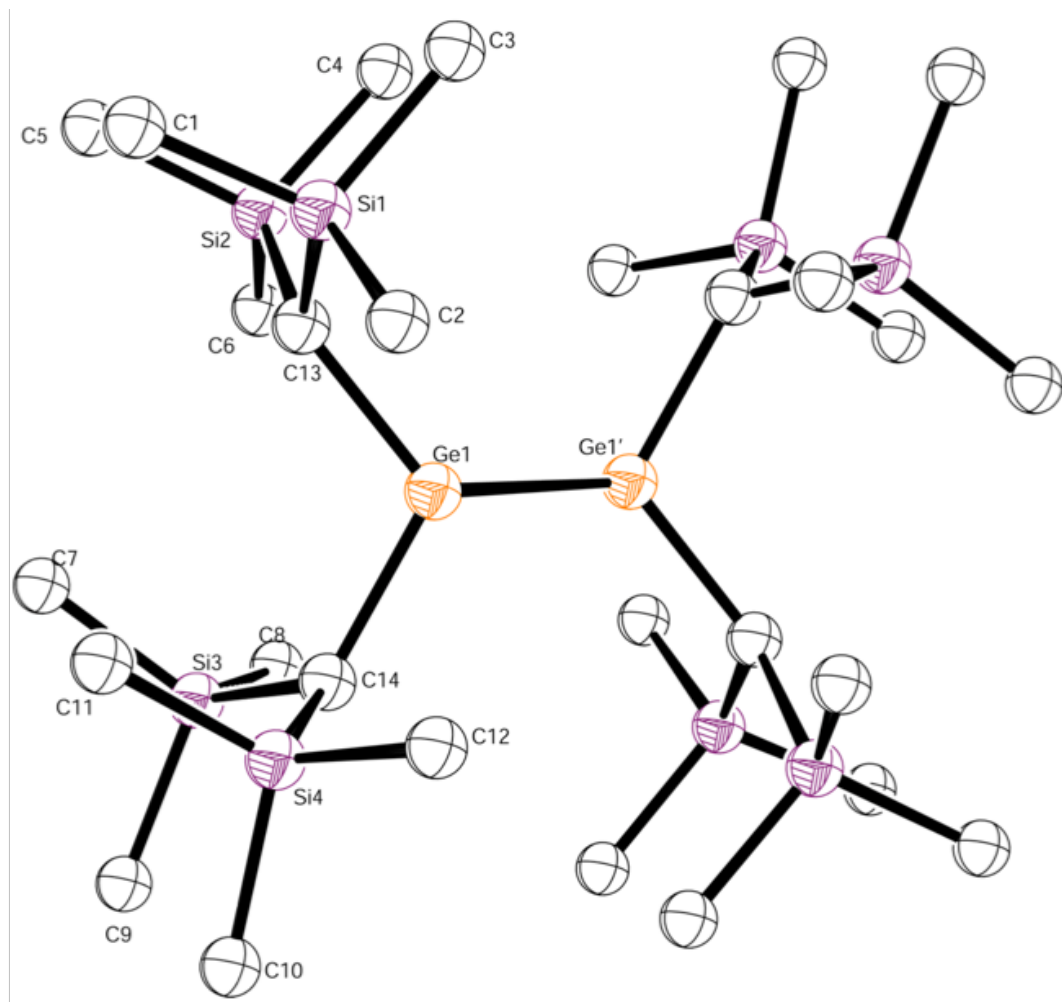
Figure 3.2: X-ray crystal structure of Ge[CH(SiMe$_3$)$_2$]$_2$.[100]

The germylene Ge[CH(SiMe$_3$)$_2$]$_2$ has been used in the CH activation of compounds including alkanes,[101] ethers,[101] cyanides,[102] amines,[103] and ketones[104] however, typically the reactions require the use of MgCl$_2$ or PhI. Several reaction examples can be seen in Schemes 3.8 – 3.12 showing the unique reactivity of Ge[CH(SiMe$_3$)$_2$]$_2$.

Scheme 3.8

(Me$_3$Si)$_2$HC—Ge—I / dioxane adduct

(Me$_3$Si)$_2$HC / Ge / I / cyclopentyl

(Me$_3$Si)$_2$HC—Ge—I / (tetrahydrofuran)

Ge[CH(SiMe$_3$)$_2$]$_2$ + PhI

(Me$_3$Si)$_2$HC—Ge—I / ether (O-CH(CH$_3$))

Slow

(Me$_3$Si)$_2$HC—Ge—I—Ph

(Me$_3$Si)$_2$HC—Ge—I / cyclohexyl
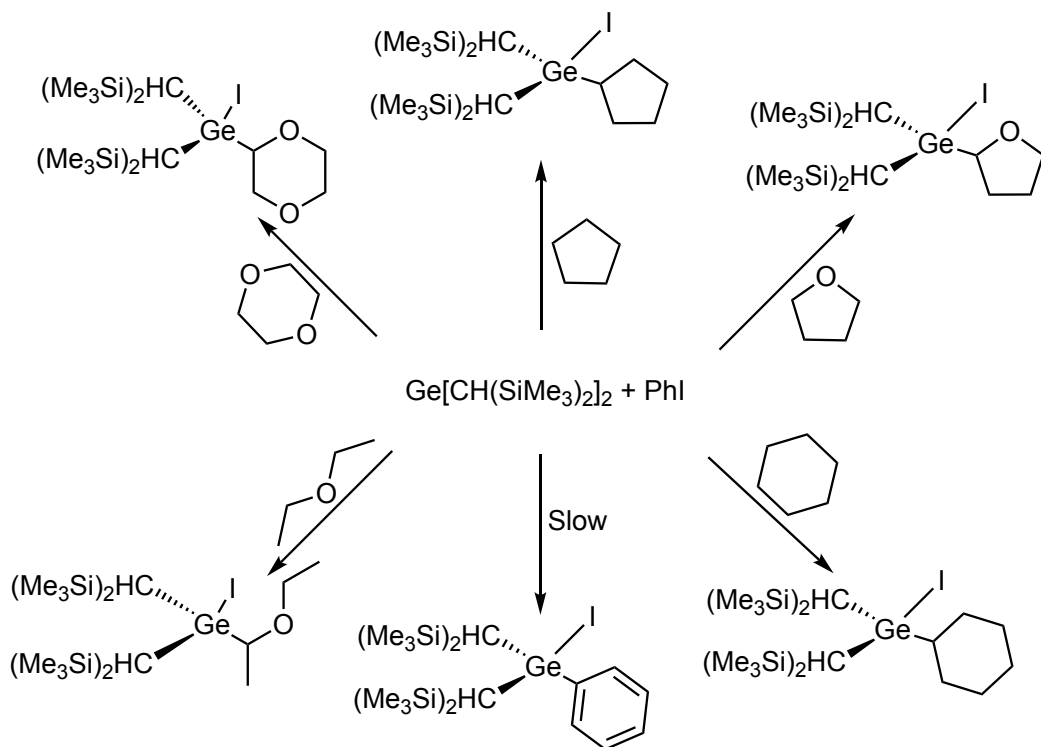
Scheme 3.8: CH activation of some alkanes and ethers with Ge[CH(SiMe$_3$)$_2$]$_2$ and PhI.[101]

Scheme 3.9

(Me$_3$Si)$_2$HC—Ge—H—CH$_2$CN

(Me$_3$Si)$_2$HC—Ge—H—CH(CH$_3$)CN

CH$_3$CN

(Me$_3$Si)$_2$HC—Ge—H—CH(CN)CH$_2$CN

CH$_3$CH$_2$CN

NC(CH$_2$)$_2$CN

Ge[CH(SiMe$_3$)$_2$]$_2$

C$_6$H$_5$CH$_2$CN

NC(CH$_2$)$_4$CN

(Me$_3$Si)$_2$HC—Ge—CN / NH (cyclopentenyl)

Δ

(Me$_3$Si)$_2$HC—Ge—CN / N (cyclopentylidene)

(Me$_3$Si)$_2$HC—Ge—H—CH(C$_6$H$_5$)CN
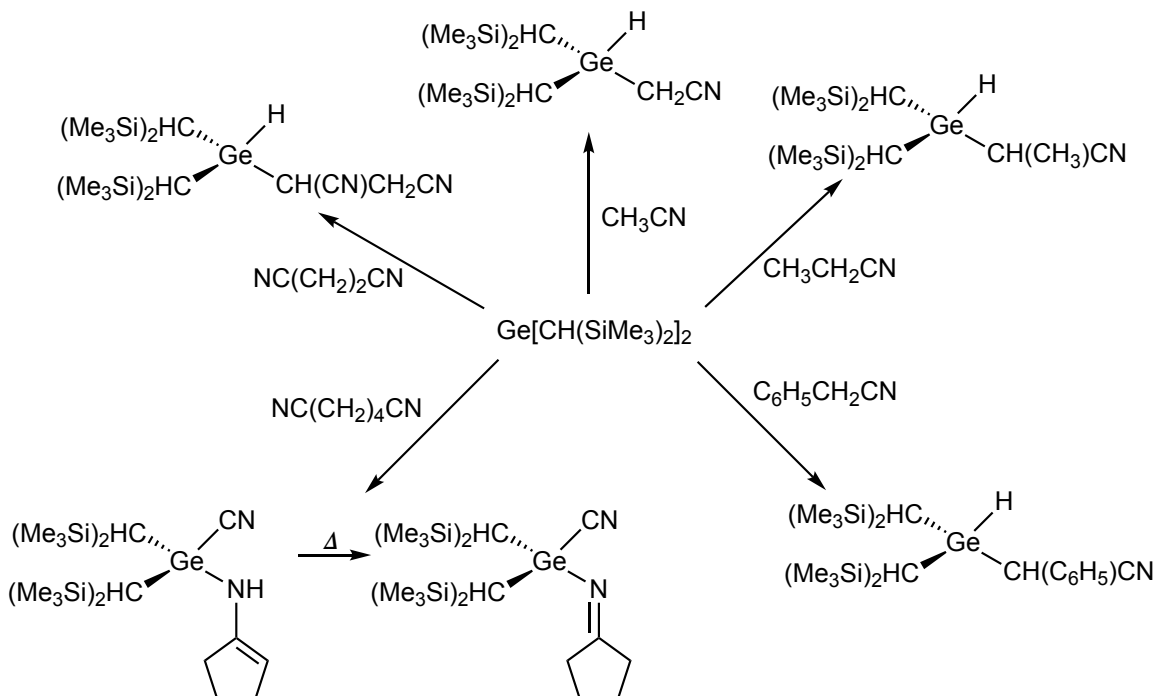
Scheme 3.9: CH activation of some cyano containing alkyl compounds with Ge[CH(SiMe$_3$)$_2$]$_2$. Reactions were performed using MgCl$_2$ or LiCl in THF.[102]
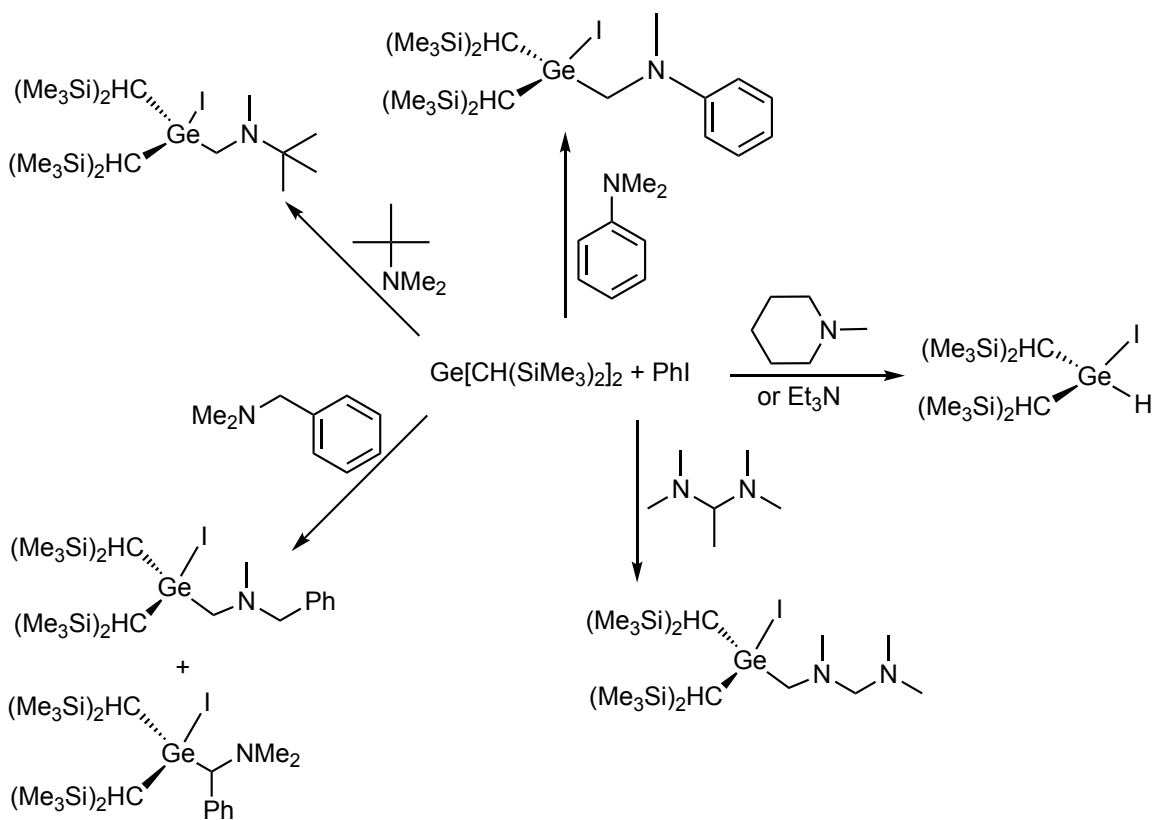
Scheme 3.10: CH activation of compounds containing amine groups with Ge[CH(SiMe₃)₂]₂ in the presence of PhI.[103]
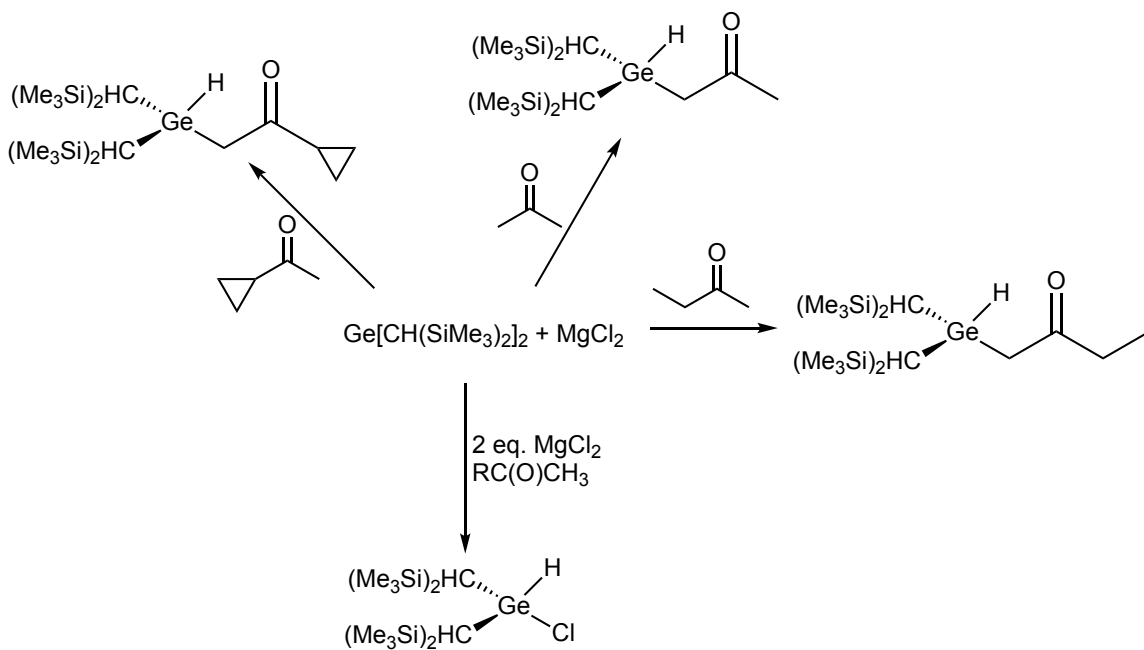
Scheme 3.11: CH insertion reactions of Ge[CH(SiMe₃)₂]₂ with ketones in the presence of MgCl₂.[104]
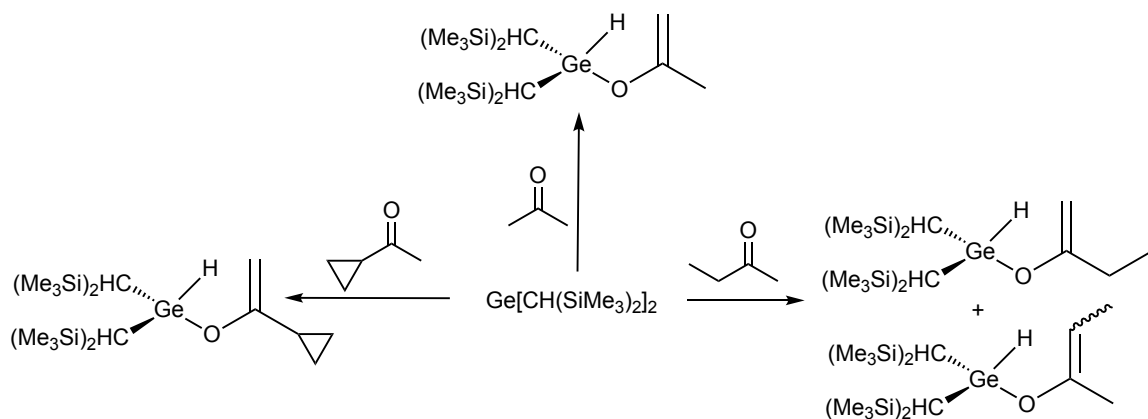
Scheme 3.12: CH insertion reactions of Ge[CH(SiMe$_3$)$_2$]$_2$ without MgCl$_2$ resulting in OH insertion.[104]

Initially reported by Lappert *et al,* in 1974[105] the second most common germanium(II) compound utilizes the bulky nature of the electron withdrawing trimethylsilylamido ligand to kinetically stabilize the germylene and this compound is isolated in a monomeric state. This is likely due to the nitrogen atoms being directly bonded to the germanium, and since they have some electron withdrawing ability, can result in an electron deficient germanium center rendering the electron lone pair to be less reactive. Additionally, another reason for this compound to exist in a monomeric state is that the trimethylsilylamido ligands lacks β-hydrogens and the presence of bulky β-silicon atoms.[105–109]

When synthesized, the germylene Ge[N(SiMe$_3$)$_2$]$_2$ exhibits a yellow/orange thermochromatic color existing as a liquid at room temperature and becomes colorless upon cooling to -192°C. The schematic synthesis of this reaction can be seen in Scheme 3.13, where germaniumdichloride•1,4–dioxane is reacted with two equivalents of lithium hexamethyldisilazane producing the desired germylene as well as two equivalents of lithium chloride and 1,4–dioxane.[105]

$$GeCl_2 \cdot (1,4\text{ - dioxane}) + 2\ LiN(SiMe_3)_2 \longrightarrow\ :Ge[N(SiMe_3)_2]_2 + 2\ LiCl +$$
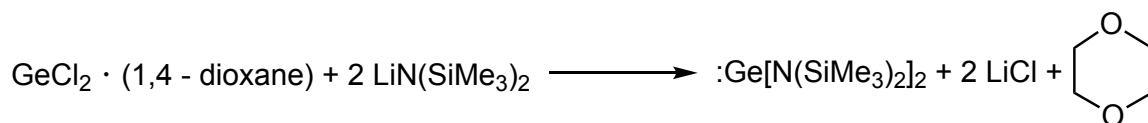
Scheme 3.13: Synthesis of Germanium Bis[bis(trimethylsilyl)amide].[105]

X-ray crystal structure analysis of the germanium (II) amide shown in Figure 3.3 reveals a bent geometry with the germanium–nitrogen bond distances measuring 1.873(5) and 1.878(5) Å while the N–Ge–N angle measures 107.1(2)°.[98,109]
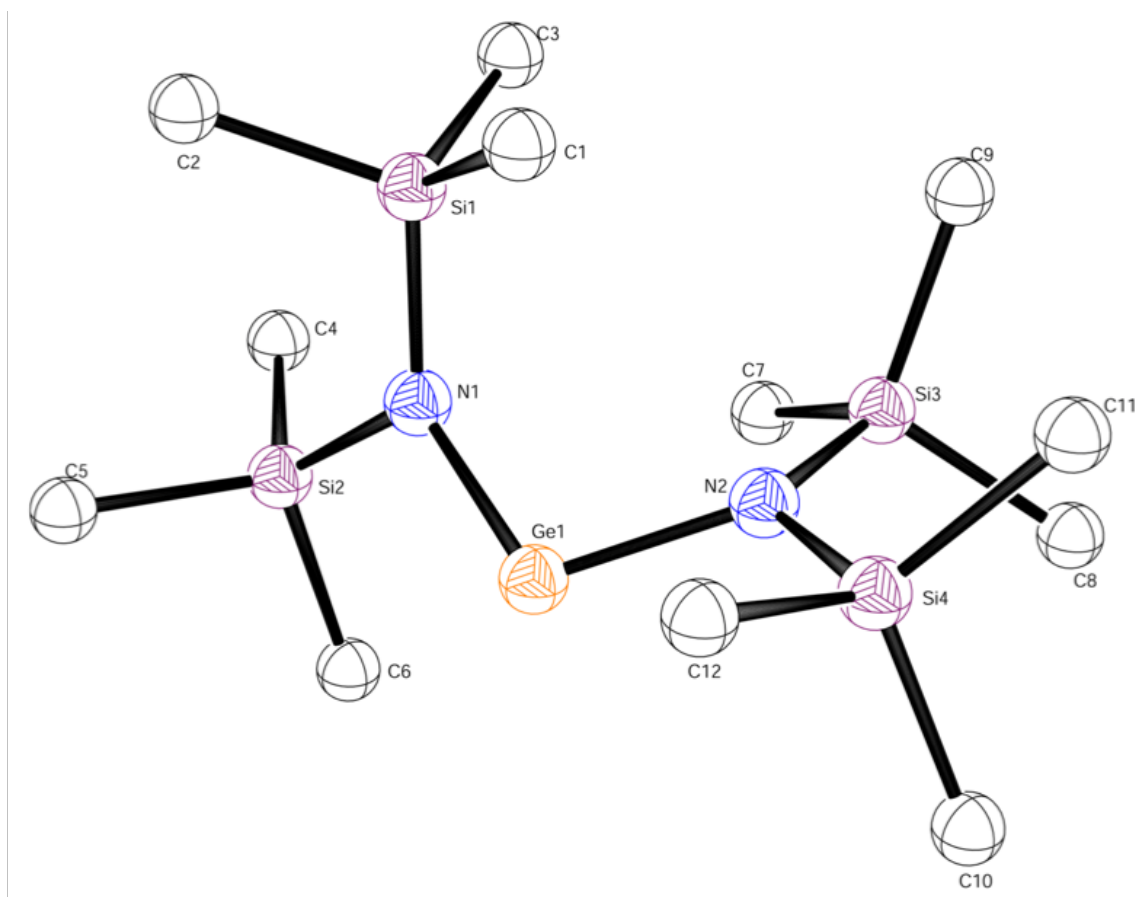
Figure 3.3: X-ray crystal structure of Ge[N(SiMe_3)_2]_2.[98]

While achievable however, the synthesis of Ge[N(SiMe_3)_2]_2 via the reaction of germaniumdichloride•1,4–dioxane and lithium hexamethyldisilazane results in only moderate yields ranging up to 67%.[105] The reason for this resides in the formation of the

highly acidic trichlorogermanium hydride intermediate, shown in Scheme 3.14, that is produced during the synthesis of the germanium dichloride•1,4–dioxane precursor compound.[100,110]

$$GeCl_4 + Bu_3SnH \xrightarrow[\text{Et}_2\text{O}]{} [HGeCl_3] \xrightarrow{-HCl} GeCl_2 \cdot dioxane$$
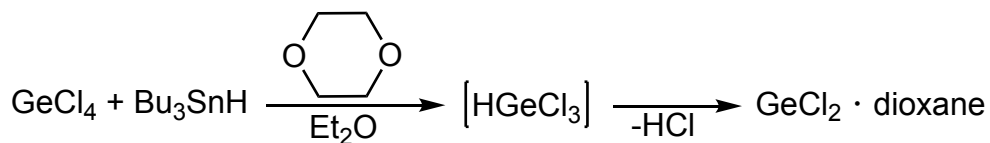
Scheme 3.14: Synthesis of the germaniumdichloride•1,4–dioxane precursor compound with the highly acidic trichlorogermanium hydride intermediate required for the formation of Ge[N(SiMe$_3$)$_2$]$_2$.[110]

Efforts to improve on the efficiency and yield of this synthesis route were developed by Roskamp *et al.* where Ge[N(SiMe$_3$)$_2$]$_2$ was synthesized via a stabilized triphenylphosphonium–trichlorogermanate intermediate in 1992.[110] This method involved a multistep synthesis beginning with reacting a solution of triphenylphospine and germanium tetrachloride with tributyltin hydride in diethyl ether at room temperature to yield the triphenylphosphonium–trichlorogermanate complex as well as tributyltin chloride. The triphenylphosphonium–trichlorogermanate was then crystallized out and further reacted with triethylamine to yield triethylammonium–trichlorogermanate and triphenylphosphine. Lastly, the triethylammonium–trichlorogermanate was reacted with three equivalents of lithium hexamethyldisilazane to yield the final product Ge[N(SiMe$_3$)$_2$]$_3$ in a 70–77% yield as well as triethylamine, lithium chloride, and hexamethyldisilazane as by–products. This reaction scheme is shown in Scheme 3.15. Further adding to the efficiency of this reaction was the fact that the stabilized intermediate reduced the number of side reactions and most of the final by–products of these reaction were volatile allowing for a facile work–up.[110]

$$\text{Ph}_3\text{P} + \text{GeCl}_4 \xrightarrow[\substack{\text{Et}_2\text{O, 25°C} \\ -\text{Bu}^n_3\text{SnCl}}]{\text{Bu}^n_3\text{SnH}} \text{Ph}_3\overset{\oplus}{\text{P}}\text{H}\text{—}\overset{\ominus}{\text{GeCl}_3} \xrightarrow[\substack{\text{CH}_2\text{Cl}_2, 25°C \\ -\text{Ph}_3\text{P}}]{\text{Et}_3\text{N}} \text{Et}_3\overset{\oplus}{\text{N}}\text{H}\text{—}\overset{\ominus}{\text{GeCl}_3} \xrightarrow[\substack{\text{THF, 25°C} \\ -\text{LiCl, } -\text{NEt}_3 \\ -\text{HN(SiMe}_3)_2}]{\text{3 LiN(SiMe}_3)_2} \text{Ge[N(SiMe}_3)_2]_2$$
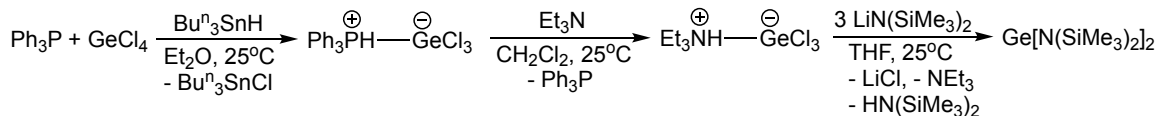
Scheme 3.15: Complete synthetic pathway for the formation of Ge[N(SiMe₃)₂]₂.[110]

The reactivity of Ge[N(SiMe₃)₂]₂ has been shown to be quite versatile in CH insertion and activation reactions, similar to the previous germylene presented (Ge[CH(SiMe₃)₂]₂). What has been explored more in the relative ability of Ge[N(SiMe₃)₂]₂ versus Ge[CH(SiMe₃)₂]₂ is to be used as a ligand for transition metal elements. Studies have shown that Ge[N(SiMe₃)₂]₂ can act as a ligand for copper,[111] ruthenium,[112] nickel,[113] chromium, molybdenum, tungsten, platinum, and palladium.[95] A few examples of these reactions can be seen in Scheme 3.16.
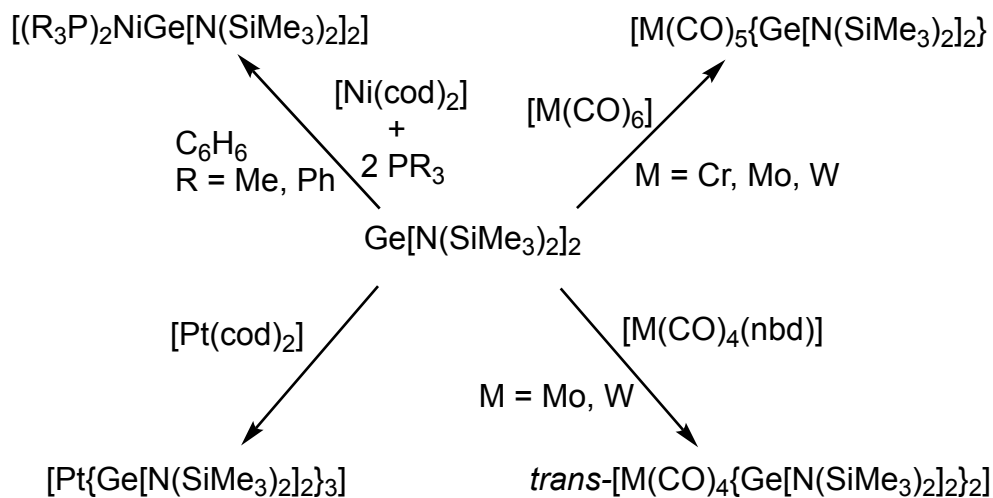
Scheme 3.16: Example reactions of Ge[N(SiMe₃)₂]₂ with transition metal compounds.[95,113]

The ability of Ge[N(SiMe₃)₂]₂ to react with organic compounds and main group elements has also been observed, and includes the formation of Ge–Si,[114] Ge–O,[115] Ge–N,[116] Ge–S,[117] Ge–Se,[117] and Ge–Te[117] bonds. These reaction schemes can be seen in Schemes 3.17 – 3.19.
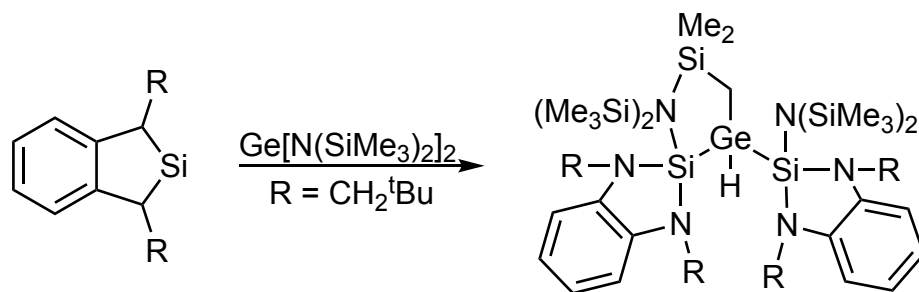
Scheme 3.17: Formation of a Ge – Si bond.[114]
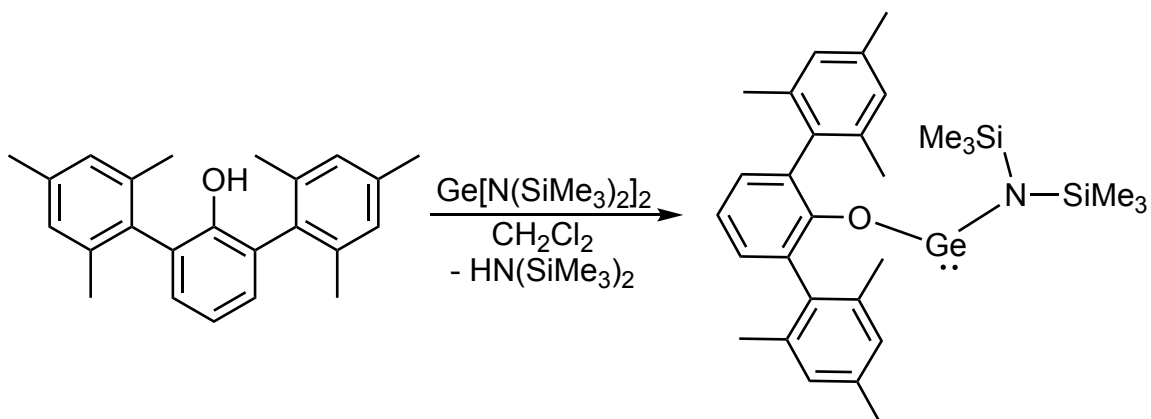
Scheme 3.18: Formation of a Ge–O bond.[115]
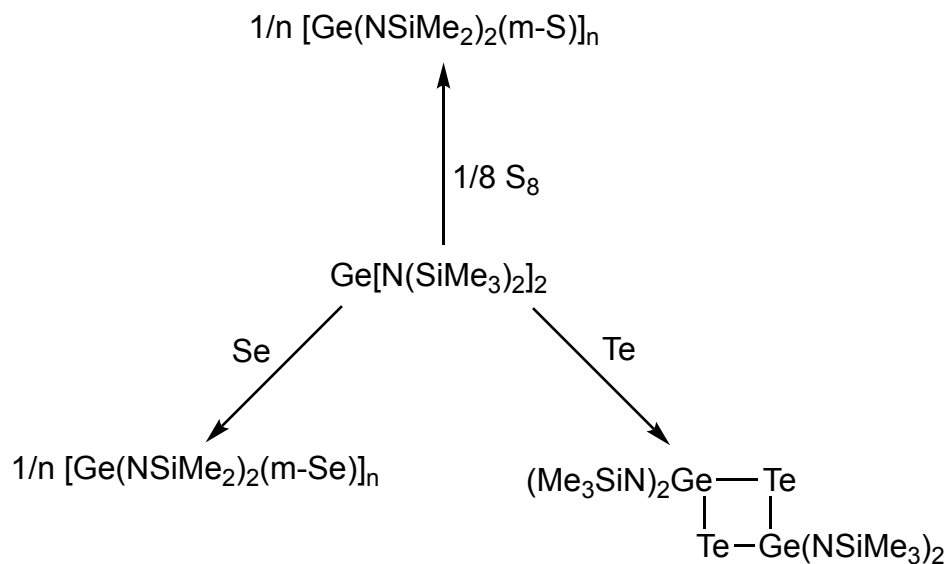
Scheme 3.19: Formation of sulfur, selenium, and tellurium germanium bonds.[117]

Reactions involving transition metal ligand substitution and main group metals have demonstrated the unique reactive properties of Ge[N(SiMe$_3$)$_2$]$_2$. However, this species has also been applied in the synthesis of germanium (II) aryloxides (aryloxygermylenes). Germanium aryloxides contain a single germanium atom bonded to two or more phenolic oxygens with the aromatic rings on the oxygen having varying substitution patterns at the *ortho-, meta-, and para-* positions. Typically synthesized via a protonolysis reaction with Ge[N(SiMe$_3$)$_2$]$_2$ and two equivalents of a phenol, the product structure is dependent on the steric bulk of the ligands bonded to the germanium(II) center. Depending on the degree of substitution variability and steric bulk of the phenol, the germanium aryloxide can potentially exist in a monomeric or dimeric state. Dimeric species have been prevalent when aryl groups are used such as (OC$_6$H$_2$Me$_3$–2,4,6,) or (OC$_6$H$_3$^{i}Pr$_2$–2,6).[118] Monomeric species are formed when the aryl groups that are used are (OC$_6$H$_3$Mes$_2$–2,6),[115] (OC$_6$H$_2$Me–4–Bu$^t_2$–2,6),[118] and (OC$_6$HPh$_4$–2,3,5,6).[118] Reaction schemes for the synthesis of these aryl oxide germanium (II) compounds can be seen in Schemes 3.20–3.22.
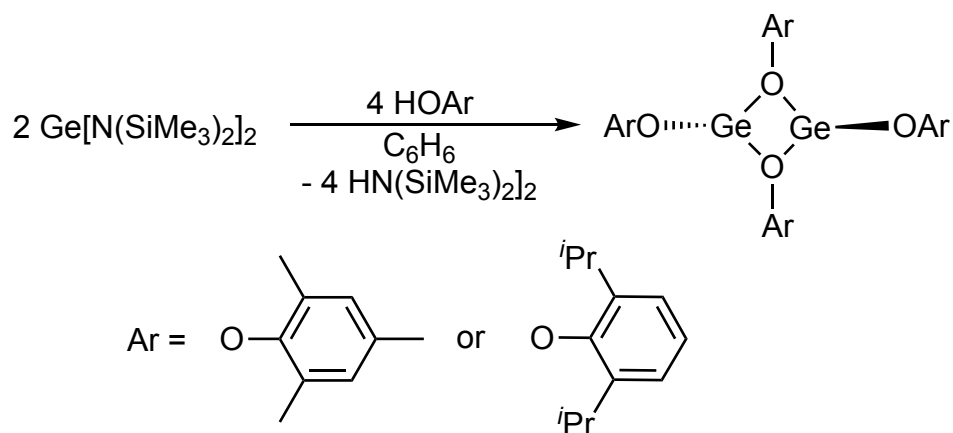
Scheme 3.20: Dimeric germanium aryloxide synthesis with OC$_6$H$_2$Me$_3$–2,4,6 and OC$_6$H$_3$^{i}Pr$_2$–2,6.[118]
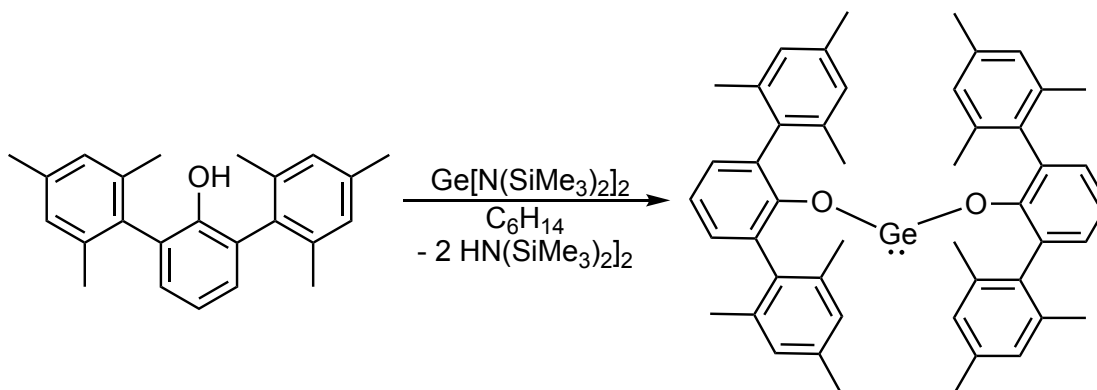
Scheme 3.21: Synthesis of a monomeric germanium aryloxide with $OC_6H_3Mes_2$–2,6.[115]
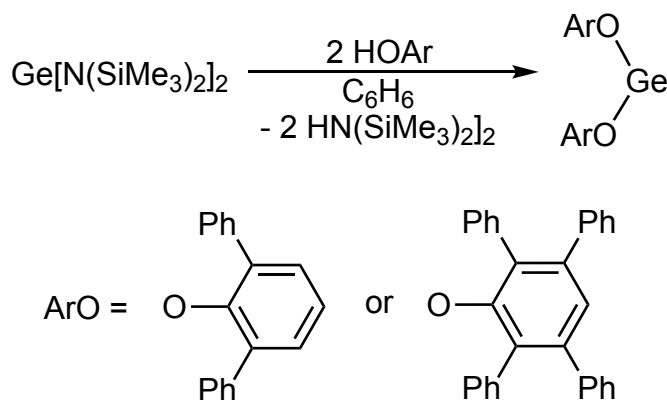
Scheme 3.22: Synthesis of a monomeric germanium aryloxide with OC_6HPh_4–2,3,5,6 and $OC_6H_3Ph_2$–2,6.[118]

The monomeric germanium(II) aryloxide [$Ge(O_6HPh_4$–2,3,5,6)$_2$] has been isolated and additionally, the reactivity of this compound can be further explored by reacting it with methyl iodide via an oxidative addition of the germanium (II) center into the C-I bond to yield a germanium(IV) aryloxide complex [$Ge(OC_6HPh_4$–2,3,5,6)$_2$(Me)(I)] as shown in Scheme 3.23.[118] This compound is only seen as the major product when the ligand bonded to the germanium(II) center is OC_6HPh_4–2,3,5,6 and not with OC_6HPh_2–2,6. When OC_6HPh_2–2,6 is used, a trisubstituted derivative is formed as shown in Scheme 3.24, and it is believed that this derivative is formed with OC_6HPh_2–2,6 and not OC_6HPh_4–2,3,5,6 because the extra phenyl rings are more sterically encumbering and shielding the

53

germanium(II) center. The trisubstitution is observed after oxidative addition of methyl iodide onto the germanium (II) center has occurred, thus making the sole isolation of [Ge(OC$_6$HPh$_2$–2,6)$_2$(Me)(I)] quite difficult.[89] This has then lead to the exclusive use of OC$_6$HPh$_4$–2,3,5,6 as the main ancillary ligands to synthesize the germanium(IV) compound [Ge(OC$_6$HPh$_4$–2,3,5,6)$_2$(Me)(I)]. It is expected that the steric and electronic properties at the germanium(IV) center can be altered by variation of the methyl group to other substituents. The germanium–iodide bond potentially can be reduced to form a germanium–hydride species that could then be used as a hydrogermylation reagent for alkenes, alkynes, and ketones in the presence or absence or a radical initiator. It is also expected that the hydrogenating ability of the hydrides [Ge(OC$_6$HPh$_4$)$_2$(R)(H)] will be dependent on the nature of the organic substituent bonded to the germanium(IV) center, and also that asymmetric hydrogermylation reactions might be possible under the right reaction conditions. The synthetic pathway for the formation of these compounds is shown in Scheme 3.25 and the attempted synthesis, characterization, and application will be the foci of the following chapters.
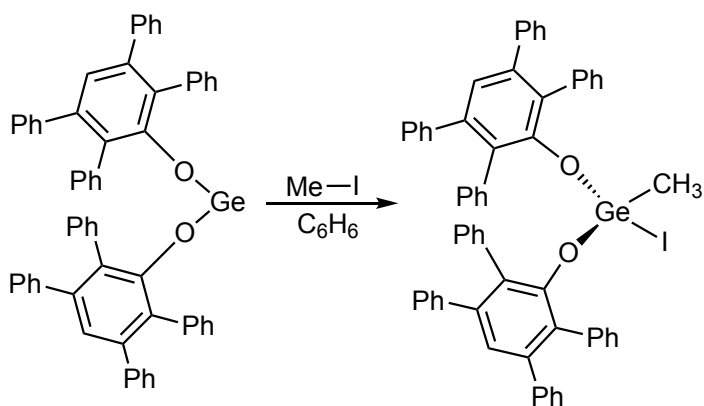
Scheme 3.23: Oxidative addition of methyl iodide onto the germanium (II) center.[118]
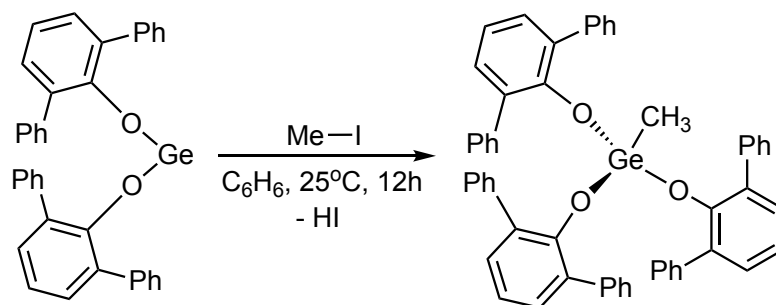
Scheme 3.24: Formation of a tris substituted germanium aryloxide complex with OC$_6$HPh$_2$–2,6 as the supporting

ligand.[89]
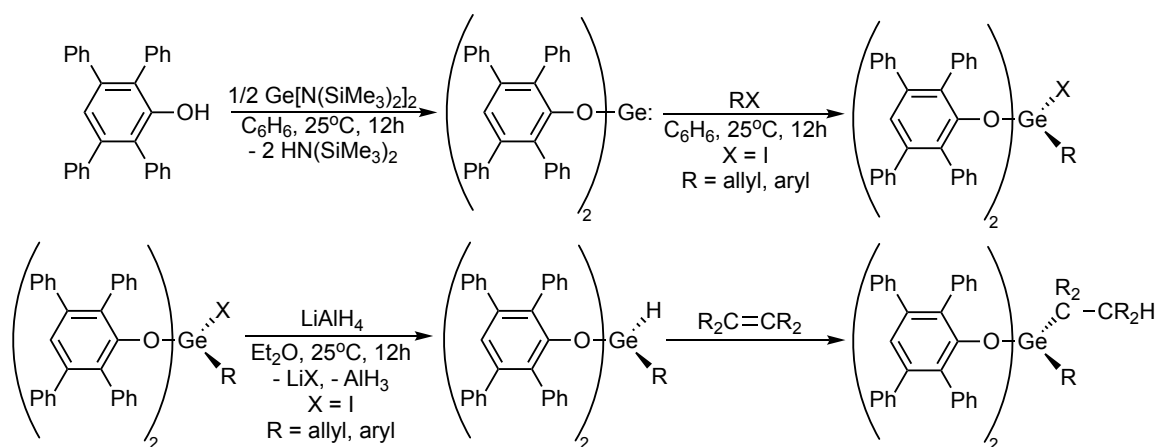
Scheme 3.25: Overall reaction scheme for the synthesis of the germanium aryloxide [Ge(OC$_6$HPh$_4$)$_2$(R)(H)] for
hydrogermylation of an alkene.

3.2 Results and Discussion

Synthesis of HOC$_6$HPh$_4$–2,3,5,6 (**1c**) was prepared via two different literature

methods, one involving the use of *n*-butyl lithium reported by Hoveyda and co-workers.[119]

The multi–step synthetic process for obtaining compound **1c** is shown in Scheme 3.26 and

began with a condensation reaction between 1,3–diphenylacetone and (*E*)–1,3–diphenyl–

2–propanone in a solution of sodium methoxide and methanol refluxed for 16 hours to

yield 2,3,5,6–tetraphenyl–2–cyclohexanone (**1a**). Compound **1a** was then reacted with

bromine (Br$_2$) in glacial acetic acid and refluxed for 14 hours to yield 4–bromo–2,3,5,6–

tetraphenylphenol (**1b**). Lastly, the brominated phenol is reacted with ^{n}butyl lithium at -78°C in tetrahydrofuran (THF) and quenched with methanol to yield compound **1c**.
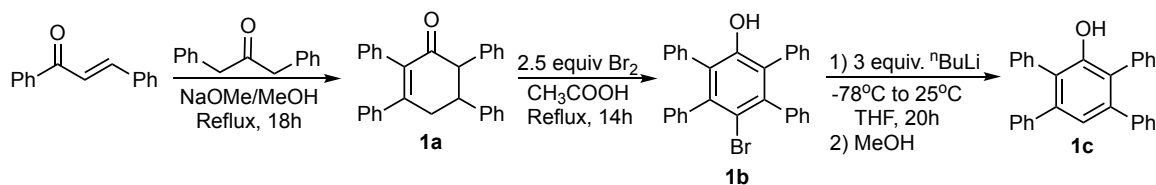
Scheme 3.26: Synthetic pathway for obtaining compounds **1a,1b**, and **1c**.[119]

While this synthetic pathway did produce the desired phenol in high yields of up to 80%, obtaining compound **1c** in a pure form was a consistent problem. In the final step, compound **1b** was never fully debrominated to the desired phenol as shown by the ^{1}H NMR spectra in Figure 3.4, which resulted in a 1:4 ratio of compounds **1b** and **1c** respectively. A resonance at δ 5.00 ppm due to the hydroxyl group on **1b** is present as well as a resonance at δ 5.23 ppm belonging to the hydroxyl group of **1c**. Due to the chemical similarities of compounds **1b** and **1c**, column chromatography, low vacuum distillation (0.005 torr), and extraction all proved to be ineffective for separating compounds **1b** and **1c**, often resulting in a homogeneous mixture of both compounds.
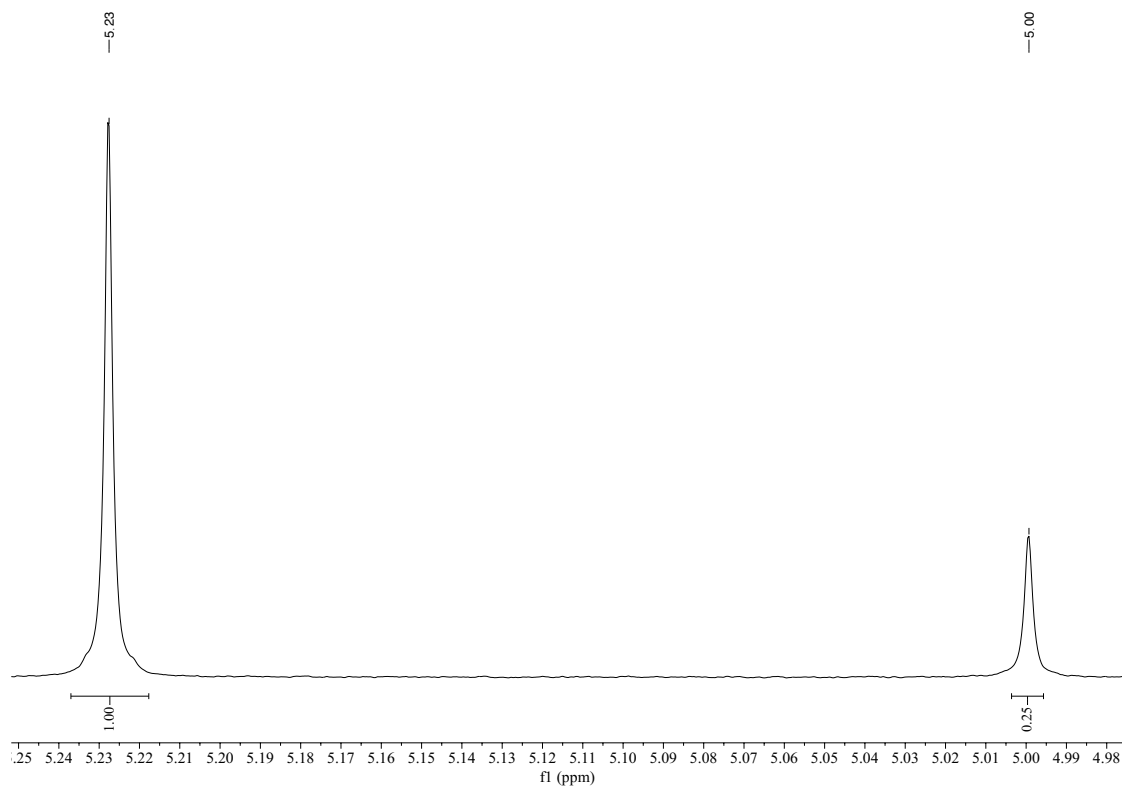
Figure 3.4: ^{1}H NMR spectrum displaying the hydroxyl group resonances of compounds **1b** and **1c**.

This problem of purity was resolved by using a different synthetic route constructed by Yates and co-workers[120] that used similar methods, but a different stoichiometry. Similar to the steps shown in Scheme 3.26 the addition of Br_2 was carefully measured out as one equivalent to prompt a tautomerization reaction in compound **1a** that induces aromatization of the center ring and shifts equilibrium to the products allowing the enol product to form. As long as there is no more than one equivalent of Br_2 in the solution mixture, the reaction proceeds to exclusively form compound **1c** without any traces of the brominated compound **1b**, as shown in the ^{1}H NMR in Figure 3.5.
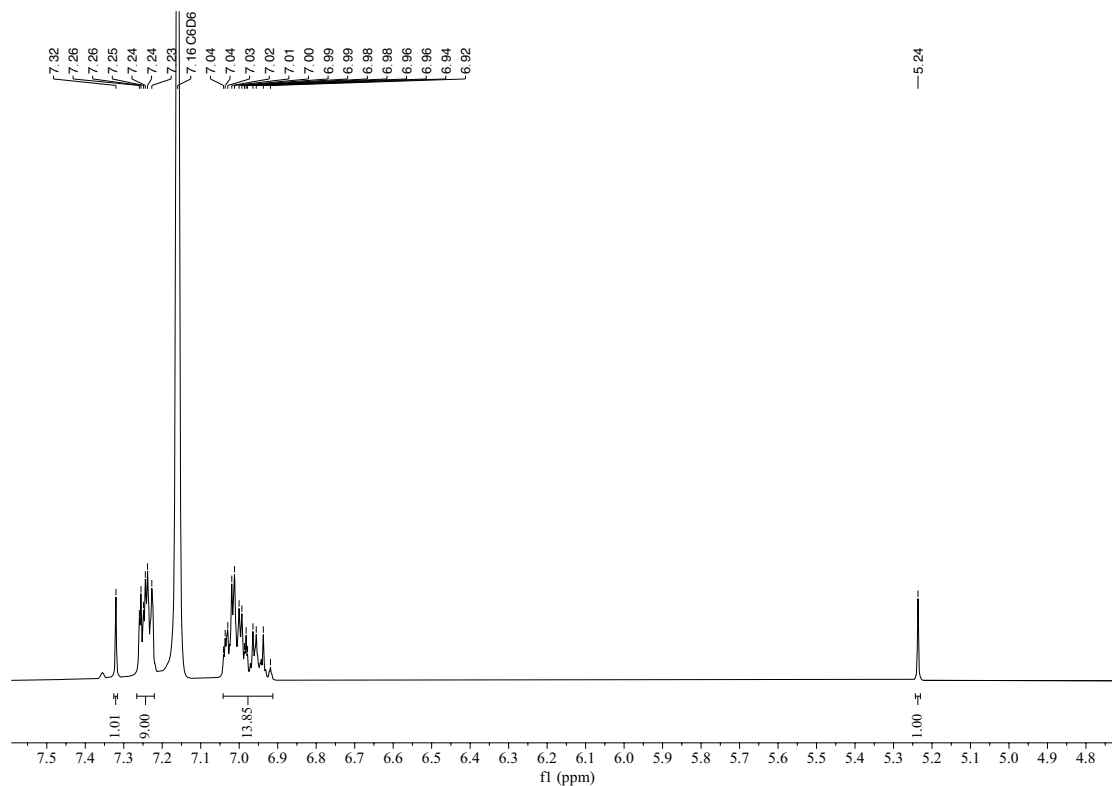
Figure 3.5: ^{1}H NMR spectrum of compound **1c**.

With the successful formation of the precursor for the ancillary ligands, the next step was the reaction of compound **1c** with the germanium(II) amide Ge[N(SiMe₃)₂]₂. Successful formation of the germylene aryloxide [(OC₆HPh₄)₂Ge:] (**2**) was detected using ^{1}H NMR spectroscopy with the disappearance of the hydroxy resonance at δ 5.24 ppm as well as the –SiMe₃ resonance at δ 0.3 ppm. Based on previous studies done by Weinert and co-workers,[118] the oxidative addition of methyl iodide to compound **2** would produce the compound [(OC₆HPh₄)₂Ge(Me)(I)] (**3**). An indication of a successful germanium-methyl bond is seen in the ^{1}H NMR spectra in the range of δ –0.5 to –0.2 ppm based on previous results using a germanium aryloxide having 2,6–diphenylphenoxy ligands.[89] These results, however, could not be reproduced. While there appeared to be a negative singlet resonance

well within the range expected for a germanium–methyl bond, as shown in Figure 3.6, the hydroxy resonance as well as the trimethyl silyl resonance did not diminish. While the reaction appears to proceed at room temperature, it was clear that the hydroxy resonance and trimethylsilyl resonances were still not diminishing in intensity even after the reaction mixture was refluxed. Hexane washes as well as a low pressure (0.001 torr) kugelrohr distillation were performed in an attempt to remove any unwanted impurities or starting material as well as to isolate compound **3**, but this also proved to be unsuccessful.
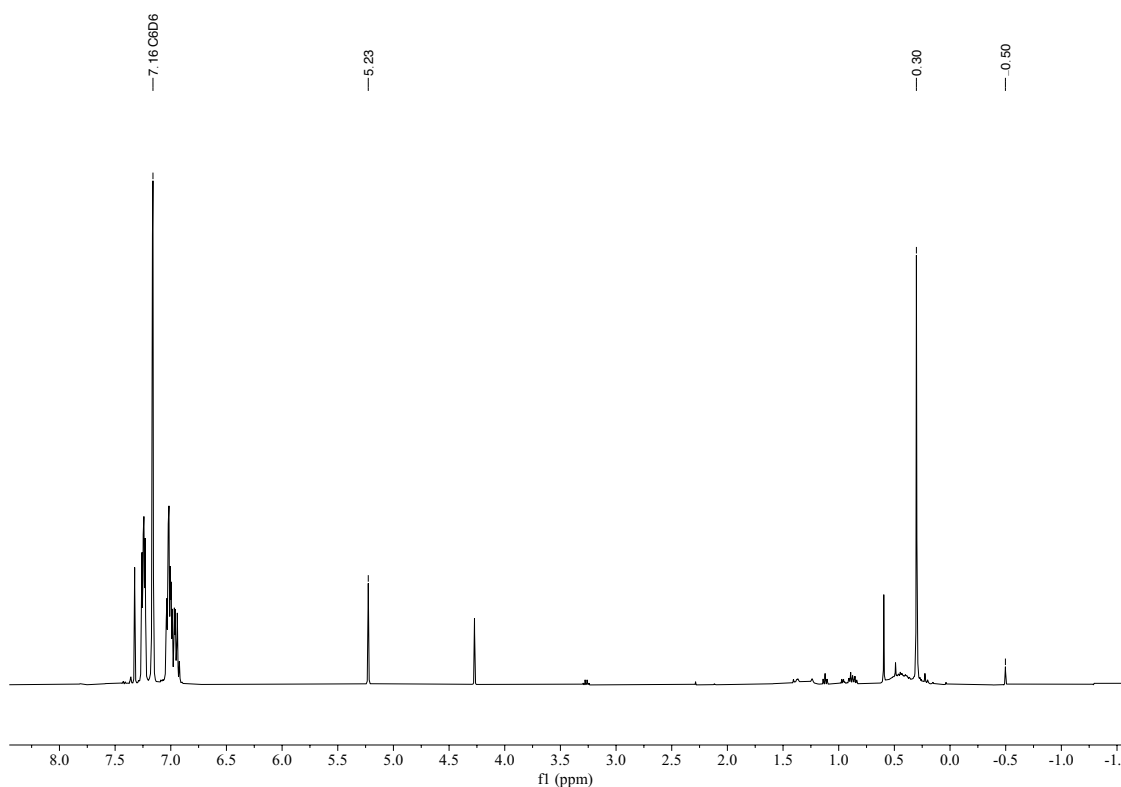
Figure 3.6: ^{1}H NMR spectrum of the mixture of **3**, **1c**, and Ge[N(SiMe$_3$)$_2$]$_2$ after attempted isolation and purification.

Other phenols were also reacted with Ge[N(SiMe$_3$)$_2$]$_2$ in an attempt to gain a better understanding as to why the reactions with compound **1c** were not producing the intended product, as well as to provide different steric attributes on the germylene species. The commercially available 2,4,6–tri–*tert*–butylphenol and 2,6–di–*tert*–butyl–4–ethylphenol

were reacted with $Ge[N(SiMe_3)_2]_2$ to form the products $[(OC_6H_2Bu^t_3)_2Ge:]$ (**4**) and

$[(OC_6H_2Bu^t_2Et)_2Ge:]$ (**5**) as shown in Scheme 3.27.

$$R = Bu^t \ (\textbf{4})$$
$$Et \ (\textbf{5})$$
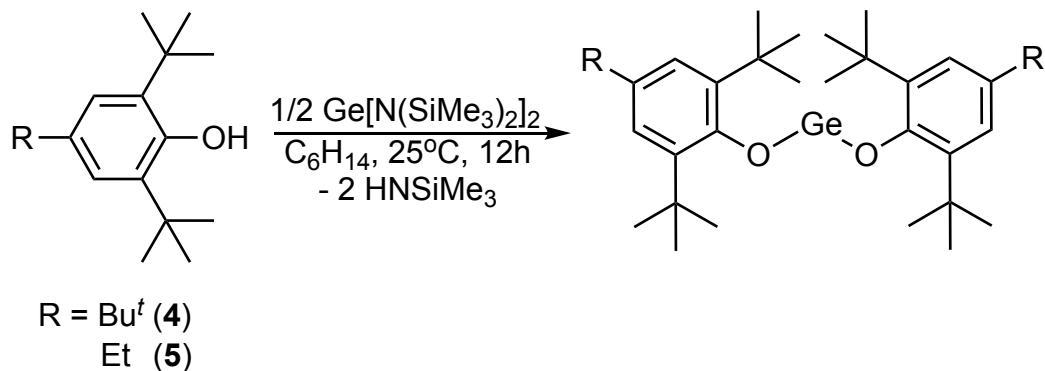
Scheme 3.27: Attempted synthesis scheme of compounds **4** and **5**.

The ^{1}H NMR spectra of these products again indicated that the hydroxy resonance persisted

as well as the trimethylsilyl resonance. There also appeared to be several new resonances

that may be attributed to the formation of both **4** and **5**; however, these compounds could

not to be purified or isolated. Multiple *tert*–butyl resonances were present in the ^{1}H NMR

spectra of **4** and **5** indicating that both the desired product as well as staring material were

present. Based on further analysis of the spectra as shown in Figures 3.7 and 3.8, it was

deduced that $Ge[N(SiMe_3)_2]_2$ had been oxidized or hydrolyzed in some manner rendering

it unavailable for protonolysis reactions with phenols.
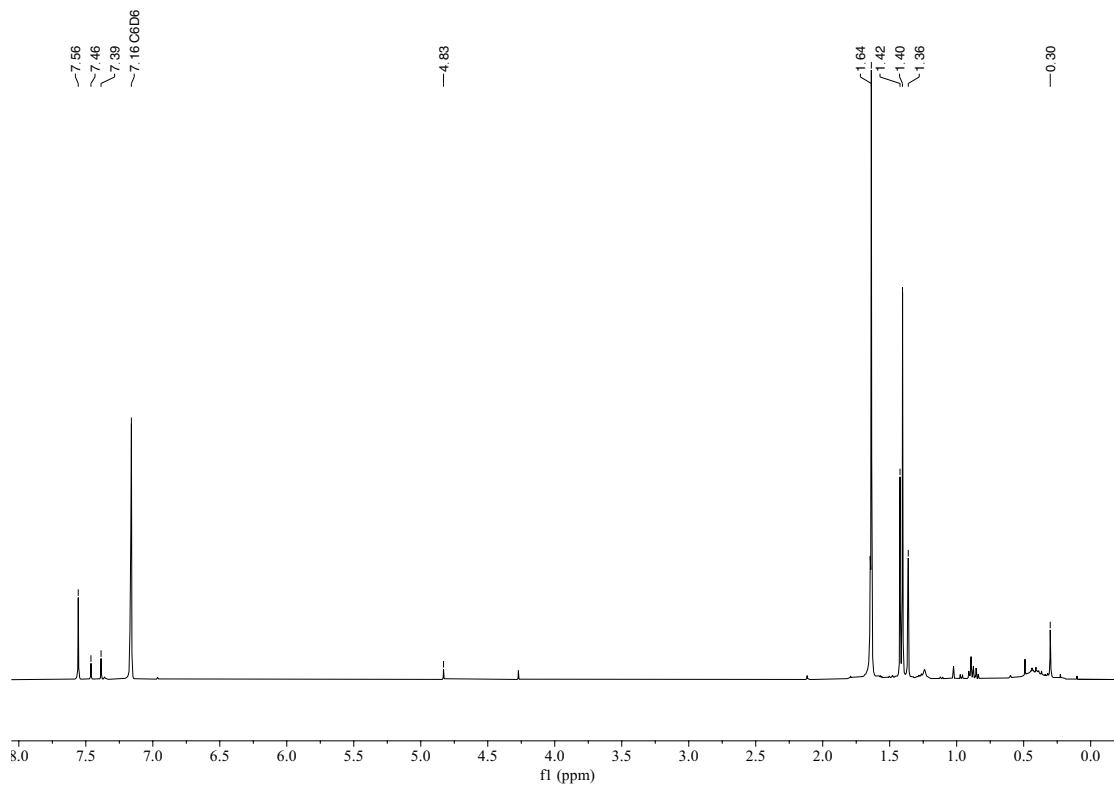
Figure 3.7: ^{1}H NMR spectrum of the product from the attempted synthesis of compound **4**.
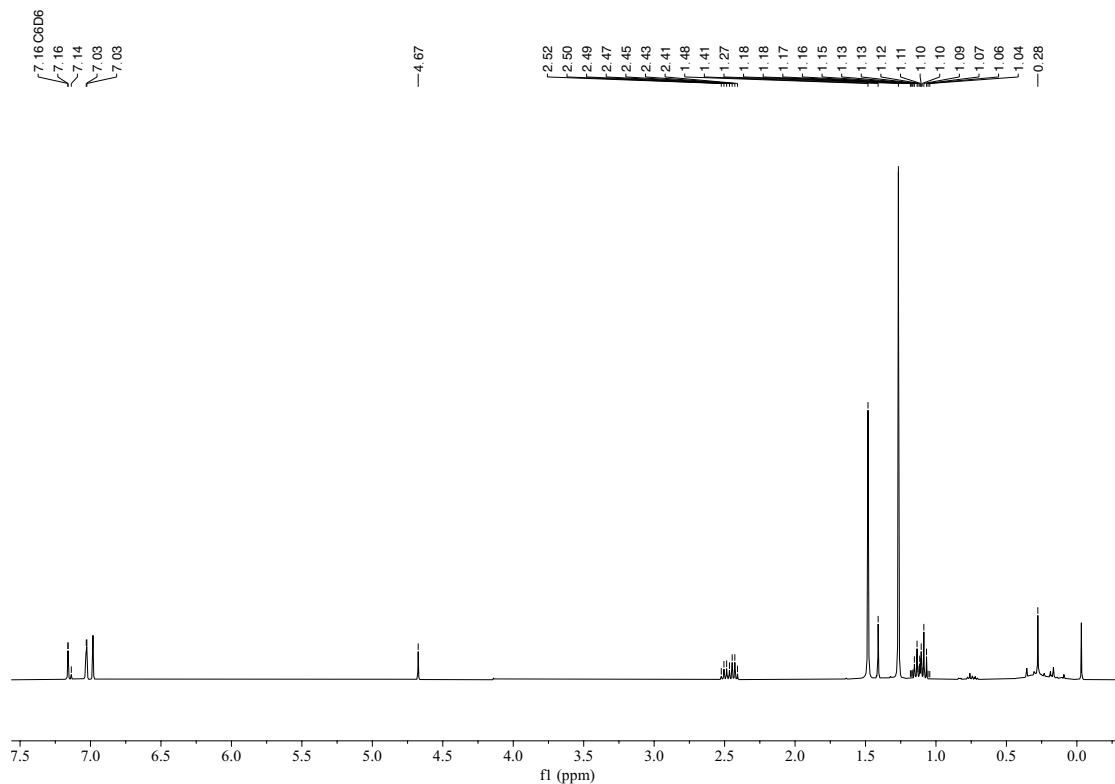
Figure 3.8: ^{1}H NMR spectrum of the product from the attempted synthesis of compound **5**.

With the unsuccessful synthesis of previous germanium aryloxides using Ge[N(SiMe$_3$)$_2$]$_2$, a different synthetic pathway was developed that involved preparing the desired aryloxide through a series of nucleophilic attacks and reductions. Rather than using Ge[N(SiMe$_3$)$_2$]$_2$, allyl germanium trichloride (C$_3$H$_5$GeCl$_3$) was used instead. This change in reagent was prompted by the idea that because compound **1c** is such a sterically encumbering ligand, it would only be possible for the compound to be bonded to the germanium(IV) center twice. This steric hindrance capability would then yield the compound [(OC$_6$HPh$_4$)$_2$Ge(C$_3$H$_5$)(Cl)] (**6**) that can then be reduced to a hydride yielding the compound [(OC$_6$HPh$_4$)$_2$Ge(C$_3$H$_5$)(H)] (**7**). To create a nucleophile that can displace chloride atoms off C$_3$H$_5$GeCl$_3$, compound **1c** was first reacted with potassium hydride to

deprotonate the hydroxy group thereby localizing the electron density around the oxygen and creating a stronger nucleophile in the process. Once the reaction mixture stopped producing H_2 gas, an orange solid remained likely owing to the increased conjugation throughout the phenyl rings of the compound ($K^+O^-C_6HPh_4$) (**1d**). Compound **1d** was then dissolved in THF and added dropwise via an addition funnel to a solution of $C_3H_5GeCl_3$ in THF to yield compound **6**. This reaction scheme as shown in Scheme 3.28.
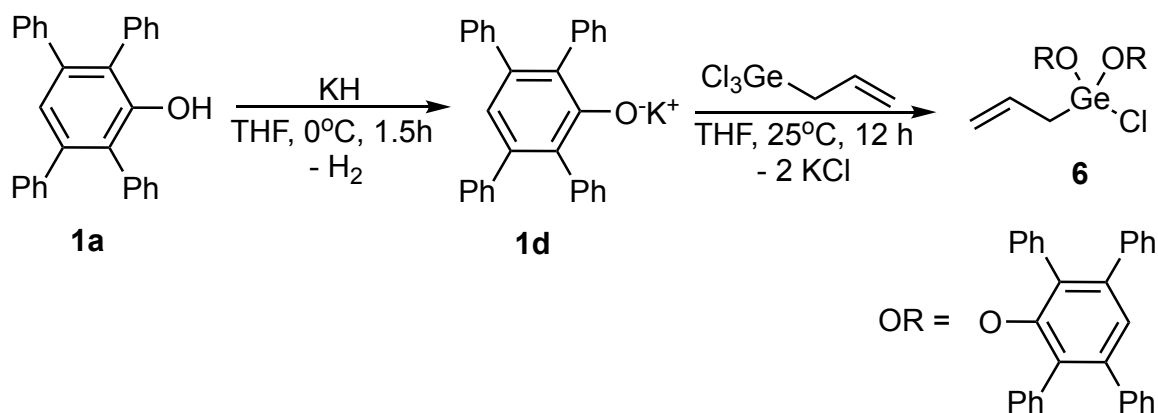
Scheme 3.28: Preparation of compound **1d** using potassium hydride for the nucleophilic attack on $C_3H_5GeCl_3$ for the formation of compound **6**.

The ^1H NMR spectrum of the product revealed several resonances that appeared downfield indicating the reaction may have produced several unknown products. Due to the nucleophilic nature of the allyl substituent, possible side reactions could have occurred and causing several products to form. This was noted in the ^1H NMR spectra as there were several multiplets ranging from δ 4.4 ppm to δ 5.9 ppm. Due to this uncertainty, a definitive conclusion could not be made on whether compound **6** was produced. The spectra are shown in Figure 3.9. The singlet at δ 5.25 ppm also suggests that compound **1d** may have been protonated in the process of the nucleophilic attack.
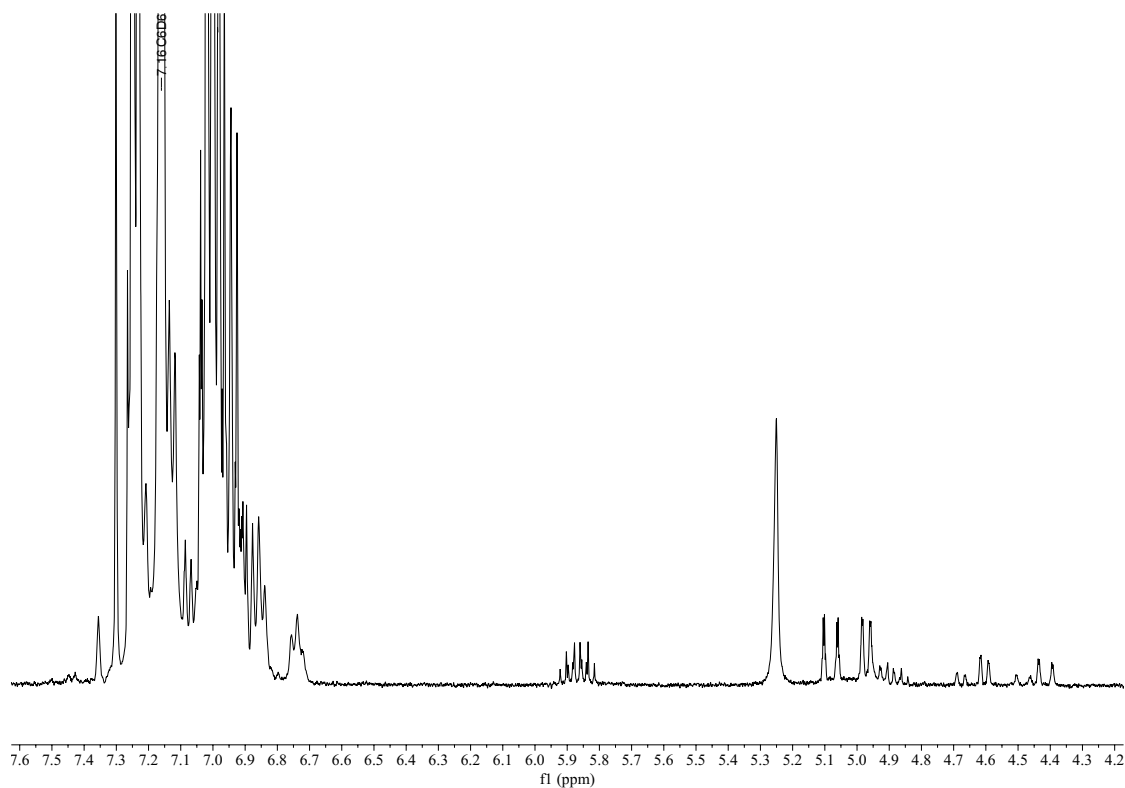
Figure 3.9: ^{1}H NMR spectrum of the attempted synthesis of **6**.

With the possibility of several compounds being produced in this reaction and a possible reformation of compound **1c**, the allyl germanium trichloride was deemed not useful for nucleophilic attacks and was not considered any further. Instead, phenylgermanium trichloride (PhGeCl$_3$) was used in an attempt to introduce a greater steric hinderance around the germanium(IV) center and allow compound **1d** to only attack twice. Similar to the allylgermanium trichloride, the phenoxide salt was dissolved in THF and added dropwise to a solution of PhGeCl$_3$ in THF. The presumed product [(OC$_6$HPh$_4$)$_2$Ge(Ph)(Cl)] (**7**) was then reacted with lithium aluminum hydride to produce [(OC$_6$HPh$_4$)$_2$Ge(Ph)(H)] (**8**). The reaction scheme can be seen in Scheme 3.29.
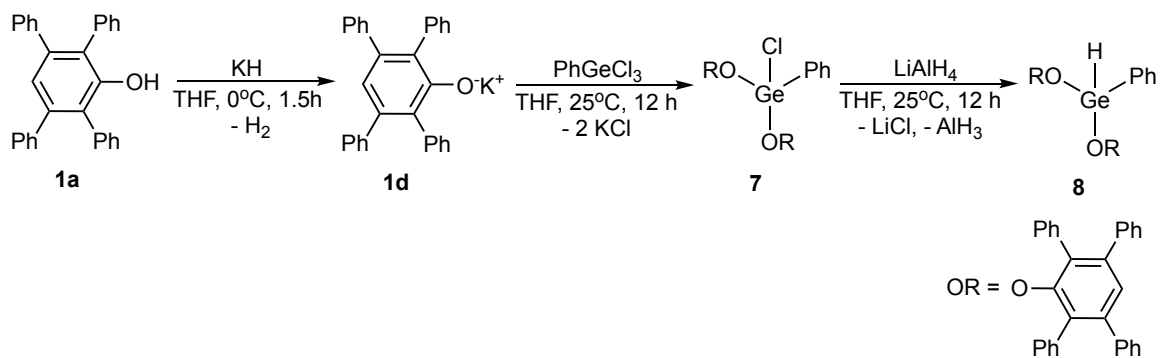
Scheme 3.29: Synthetic pathway for the attempted synthesis of **7** and **8**.

Compound **8** was characterized using ^{1}H NMR spectroscopy to reveal what appeared to be an uncharacteristically upfield hydride resonance at δ 4.24 ppm as shown in Figure 3.10. The peak also appeared to be small in comparison to the phenyl region and was suspiciously close to the region in which dichloromethane appears at (δ 4.27 ppm). ^{1}H and ^{13}C NMR analysis alone was not sufficient enough to determine if a mono-, di-, or tri-substitution process was occurring at the germanium(IV) center or whether the hydride resonance was in fact a dichloromethane impurity. To investigate this, slow evaporation of the compound in a toluene/hexane mixture was attempted in efforts to obtain suitable crystals for x-ray diffraction that could confirm the substitution pattern that was achieved on the germanium (IV) center. The crystals obtained however, were revealed to be compound **1c** upon X-ray crystallographic analysis.
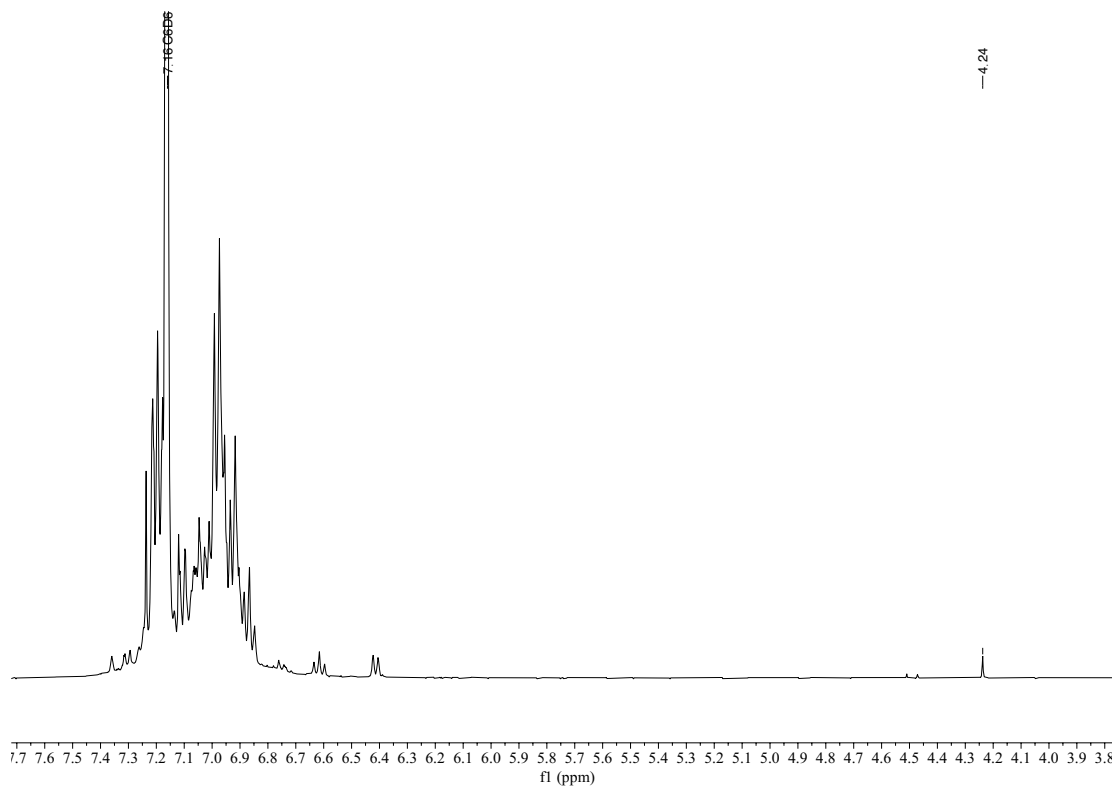
Figure 3.10: ^{1}H NMR spectrum of the suspected compound **8**.

3.3 Conclusion

Formation of compound **2** using synthetic techniques that have been previously reported did not produce the intended result. While it was clear that a germanium–methyl bond did form to produce compound **3** as noted by the resonance at $\delta - 0.5$ ppm, the reaction did not reach completion even after refluxing overnight. Purification could also not be achieved either through low pressure distillation or extraction. Based on the experiments done with compounds **4** and **5**, the starting material Ge[N(SiMe$_3$)$_2$]$_2$ could be responsible for the irregularities associated with the reaction. This compound can be quickly oxidized or hydrolyzed if not handled correctly. Due to these unforeseen

66

circumstances, a new synthetic pathway was attempted with the goal of producing the same intended germanium aryloxide.

The results that were realized during the attempted synthesis of sterically encumbered germanium aryloxides has shown that using the anion of **1c** for nucleophilic attacks on germanium(IV) compounds is too reactive to produce a single dominant product. This was noted primarily when $C_3H_5GeCl_3$ was used as there were multiple resonances appearing in the ^1H NMR spectra. This may be in due part to the lack of rigidity associated with compounds **1c** as well as **1d**, owing to the rotation of the phenyl rings. This lack of rigidity may be a reason as to why there may appear to be mono-, di-, and tri- substitution of the chloride atoms on $C_3H_5GeCl_3$.

This did not appear to be the case when the compound $PhGeCl_3$ was used instead of $C_3H_5GeCl_3$. This may be related to the phenyl group being much larger and sterically bulkier than the allyl group, suggesting that a more sterically hindered compound is needed for a di–substitution to occur exclusively. While the reduction of compound **7** to form compound **8** does appear to form a hydride due to a resonance at δ 4.24 ppm in the ^1H NMR spectrum of the products, there is still a level of uncertainty pertaining to how close it is in the region of being CH_2Cl_2. Proceeding with the next step of reacting compound **8** with an alkene did not seem reasonable seeing as there were multiple indistinguishable products present.

Overall, the experiments performed made it clear that a more rigid ligand, potentially with bidentate properties, would be a more suitable option for a di–substitution to occur exclusively. Such rigidity is found in binaphthol compounds and can be attributed

to the axial chirality contributing to a more stable compound that resists racemization. Using binaphthol as a ligand will be the focus of the following chapter.

3.4 Experimental Section

General Remarks

Handling and manipulation of air and moisture sensitive compounds were carried out under a nitrogen atmosphere using standard Schlenk, syringe, and glovebox techniques. Solvents were dried using a Glass Contour solvent purification system. Compounds that are not sensitive to air or moisture were done on a benchtop using standard glassware. The reagents $C_3H_5GeCl_3$, $PhGeCl_3$, $LiAlH_4$, iodomethane, bromine, potassium hydride, 2,4,6–tri–*tert*–butylphenol, 2,6–di–*tert*–butyl–4–ethylphenol, and $Ge[N(SiMe_3)_2]_2$ were purchased from Gelest and were used without further purification. Preparation of 2,3,5,6 – tetraphenylphenol was prepared according to the procedure of Yates and the spectral data matched with Hoveyda's reports.[119,120] NMR spectra were acquired using Bruker Avance III spectrometer operating at 400.0 MHz (^{1}H) or 100.57 MHz (^{13}C).

Synthesis of Compound 1a

This procedure was based on Hoveyda's report.[119] An oven-dried round bottomed flask was charged with a magnetic stir bar along with 1,3–diphenylacetone (5.0 g, 23.78 mmol) and dissolved in 25 mL of methanol. To this solution (*E*)–1,3–diphenyl–2–propanone (4.95 g, 23.78 mmol) was also added and allowed to dissolve. Excess sodium methoxide in methanol (20 mL of 25 *wt*. %) was then added dropwise to the solution and monitored via thin layer chromatography for consumption of the starting material. Upon completion, the now yellow solution was refluxed for 18 hours after which the solution was black with a white precipitate. The crude reaction mixture was cooled in an ice bath,

filtered through a single sided glass frit, and washed with cold methanol. The white precipitate was recrystallized from a hot toluene/methanol mixture to give white crystals. Filtration and washing with cold toluene yielded 6.99 g (73%) of 2,3,5,6–tetraphenyl–2–cyclohexanone. ^{1}H NMR (C_6D_6, 25°C): δ [ppm] 7.25 – 7.23 (2H, aryl), 7.10 – 6.89 (18H, aryl), 3.70 (d, J = 12.4 Hz, 1H, CH *ortho* to carbonyl), 3.54 – 3.48 (m, 1H, CH *meta* to carbonyl), 2.89 – 2.76 (m, 2H, CH_2 *para* to carbonyl). ^{13}C NMR (C_6D_6, 25°C): δ [ppm] 198.10, 152.0, 146.72, 142.82, 138.45, 137.77, 136.69, 131.55, 129.88, 128.76, 128.62, 128.58, 128.44, 128.20, 127.8, 127.59, 126.99, 126.80, 126.71, 59.61, 47.79, 40.95.

Synthesis of 1b

This procedure was based on Hoveyda's report.[119] An oven-dried round-bottomed flask was charged with a stir bar and compound **1a** (1.5 g, 3.75 mmol) along with 25 mL of glacial acetic acid. Br_2 (0.5 mL, 9.76 mmol) was added dropwise and the reaction was refluxed for 14 hours after which the solution was a bright orange color. The flask was allowed to cool, and 50 mL of deionized H_2O was added followed by a filtration through a single sided glass frit. The filtration gave a pale–yellow solid that was recrystallized from a hot toluene/methanol mixture to yield 1.34 g (75%) of 4–bromo–2,3,5,6–tetraphenylphenol as white crystals. ^{1}H NMR (C_6D_6, 25°C): δ [ppm] 7.22 – 7.20 (5 H, aryl), 7.02 – 6.81 (15 H, aryl), 5.00 (s, 1H, OH). ^{13}C NMR (C_6D_6, 25°C): δ [ppm] 152.01, 143.45, 141.75, 138.33, 137.89, 131.04, 130.76, 129.42, 128.50, 127.39, 124.50, 122.92.

Synthesis of 1c

This procedure was based on the procedure of Yates.[120] An oven-dried round-bottomed flask was charged with a stir bar and compound **1a** (3.5 g, 8.74 mmol) along with 50 mL of glacial acetic acid. Br_2 (0.45 mL, 8.74 mmol) was added dropwise and the

reaction was refluxed for 9.5 hours. Upon completion the compound, was cooled in an ice bath and filtered through a single sided glass frit to reveal a white solid. The white solid was washed several times with deionized H_2O and was recrystallized in hot toluene to yield 3.34 g (95%) of 2,3,5,6–tetraphenylphenol as white crystals. ^1H NMR (C_6D_6, 25°C): δ [ppm] 7.32 (s, 1H, central aryl C*H*), 7.24 (m, 8H, aryl), 7.04 – 6.82 (12H, aryl), 5.24 (s, 1H, O*H*). ^{13}C NMR (C_6D_6, 25°C): δ [ppm] 150.45, 142.88, 141.20, 136.0, 131.50, 130.14, 128.65, 127.92, 127.52, 126.68, 126.25, 124.52.

Synthesis of **1d**

An oven-dried Schlenk flask was charged with a stir bar, compound **1c**, (1.13 g, 2.84 mmol) along with 15 mL of THF, and stirred to dissolve the solid. A separate oven-dried Schlenk flask was charged potassium hydride (3 equivalents, 30 *wt.* %, 1.15 g) along with a stir bar, 15 mL of THF, and was cooled to 0°C in an ice bath. With both flasks under a flow of nitrogen gas, quick vacuum pulls were utilized to cannulate compound **1c** into the potassium hydride solution dropwise with vigorous stirring and a needle to vent off H_2 gas. Once the formation of H_2 gas had stopped, the reaction was filtered through a double–sided frit under a nitrogen atmosphere and the volatiles were removed *in vacuo*. The product was washed with hexane to remove excess mineral oil from the potassium hydride and revealed to be an orange solid with a mass of 1.16 g (93%). ^1H NMR (C_6D_6, 25°C): δ [ppm] 7.38 (m, 5H, aryl), 7.19 (s, 2H, aryl), 7.05 (dd, J = 8.3, 6.8 Hz, 5H, aryl), 7.00 – 6.92 (m, 2H, aryl), 6.88 (s, 1H, aryl), 6.75 (t, J = 7.5 Hz, 4H, aryl), 6.62 (t, J = 7.3 Hz, 2H, aryl). ^{13}C NMR (C_6D_6, 25°C): δ [ppm] 152.02, 142.79, 136.80, 136.0, 129.31, 127.85, 127.52, 123.20, 120.03.

Attempted synthesis of **2**

Under a nitrogen atmosphere, a vial equipped with a stir bar was charged with 15 mL of benzene, and compound **1c**, (3.00 g, 7.53 mmol). The mixture was stirred to dissolve the solid. In a second vial, Ge[N(SiMe$_3$)$_2$]$_2$ (1.41 g, 3.58 mmol) was dissolved in 10 mL of benzene. The solution of compound **1c** was added dropwise to the vial containing Ge[N(SiMe$_3$)$_2$]$_2$ with stirring and allowed to react for 12 hours. The solution was then transferred to a Schlenk flask, and the volatiles were removed *in vacuo*. After NMR analysis showed there was still staring material present, the mixture was redissolved in 25 mL of benzene and left to reflux for 12 hours. After removal of the volatiles again, a white solid was left that was analyzed via NMR spectroscopy to show that starting material was still present in the mixture. The mixture was washed with hexane and was distilled at low pressure (0.001 torr) in an effort to purify product that may have formed. The mixture could not be separated. The partially formed compound **2** was still reacted further to determine if there were trace amounts of the desired germylene produced.

Attempted synthesis of 3

Under a nitrogen atmosphere compound **2** (0.09 grams, 0.1 mmol) was charged to a vial along with 5 mL of benzene and a stir bar. To this solution, methyl iodide (15 mg, 0.1 mmol) that had previously been dried over molecular sieves and MgSO$_4$, was added dropwise and left to react for 12 hours. Removal of the volatiles *in vacuo* revealed a white solid with a resonance indicative of a germanium–methyl bond however starting material was still present in the mixture. The mixture was distilled at low pressure (0.001 torr) as well as washed with hexane in an effort to purify the desired product **3**. The mixture could not be separated. The impure compound **3** was not reacted further.

Attempted synthesis of 4

Under a nitrogen atmosphere Ge[N(SiMe₃)₂]₂ (1.0 g, 2.54 mmol) was charged to a vial along with 10 mL of hexane and a stir bar. The mixture was stirred to dissolve the solid. A solution of 2,4,6–tri–*tert*–butylphenol (1.4 grams, 5.33 mmol) in 10 mL of hexane was added dropwise to the solution containing the germylene with stirring and left to react for 12 hours. The solution was transferred to a Schlenk flask, and the volatiles were removed *in vacuo* to reveal a yellow solid. NMR spectroscopic analysis showed starting material was still present along with multiple *tert*–butyl resonances indicating there may be product in the mixture. The mixture was washed with hexane, filtered, and distilled at low pressure (0.001 torr), but pure compound **4** could not be separated.

Attempted synthesis of 5

Under a nitrogen atmosphere Ge[N(SiMe₃)₂]₂ (1.0 g, 2.54 mmol) was charged to a vial along with 10 mL of hexane and left to dissolve. A solution of di–*tert*–butyl–4–ethylphenol (1.26 g, 5.37 mmol) in 10 mL of hexane was added dropwise to the solution containing the germylene with stirring and left to react for 12 hours. The solution was transferred to a Schlenk flask, and the volatiles were removed *in vacuo* to reveal a white solid. NMR spectroscopy analysis showed starting material was still present. The ethyl resonances also appeared as multiplets and there were multiple *tert*–butyl resonances as well indicating that some product may be present. The mixture was washed with hexane, filtered, and distilled at low pressure (0.001 torr), but pure **5** could not be separated.

Attempted synthesis of 6

C₃H₅GeCl₃ (252 mg, 1.15 mmol) was charged to an oven-dried Schlenk flask, along with a stir bar and 10 mL of THF under a nitrogen atmosphere. In an oven-dried addition funnel was placed a solution of compound **1d** (1.00 g, 2.3 mmol) in 10 mL of THF. The

addition funnel was attached to the opening of the Schlenk flask and allowed to slowly drip into the solution of $C_3H_5GeCl_3$ with vigorous stirring and left to react for 12 hours. Upon completion the volatiles were removed *in vacuo* to reveal a white solid. NMR spectroscopy revealed several multiplets suggesting the reaction produced several unknown compounds. Compound **6** was not reacted any further.

Synthesis of 7

PhGeCl_3 (200 mg, 0.78 mmol) was charged to an oven dried Schlenk flask under a nitrogen atmosphere along with a stir bar and 10 mL of THF. In an oven dried addition funnel was placed a solution of compound **1d** (682 mg, 1.56 mmol) in 10 mL of THF. The addition funnel was attached to the opening of the Schlenk flask, allowed to slowly drip into the solution of PhGeCl_3 with vigorous stirring, and left to react for 12 hours. Upon completion the volatiles were removed *in vacuo* to reveal 560 mg (74%) as a white solid. ^{1}H NMR (C_6D_6, 25°C): δ [ppm] 7.24 – 6.85.

Synthesis of 8

Compound **7** (500 mg, 0.51 mmol) was charged to a vial under a nitrogen atmosphere along with a stir bar and 10 mL of THF. LiAlH_4 (30 mg, 0.79 mmol) was added directly to the vial containing compound **7** slowly with vigorous stirring. The solution was left to react overnight for 12 hours and upon completion was transferred to a Schlenk flask where the volatiles were removed *in vacuo*. A hot benzene extraction was done followed by a filtration through a double–sided glass frit with celite. The volatiles were once again removed *in vacuo* to reveal 400 mg (83%) as a white solid. ^{1}H NMR (C_6D_6, 25°C): δ [ppm] 7.24 – 6.85, 4.24.

CHAPTER IV

SYNTHESIS, CHARACTERIZATION, AND FUNCTIONALITY STUDIES OF A C_2–

SYMMETRICAL CHIRAL GERMANIUM SPECIES FOR

HYDROGERMYLATION AND GERMYLIUM ION FORMATION

4.1 Introduction

The formation of chiral main group compounds has been explored due to the fact that they may be used for other potentially powerful synthetic processes. Radical reactions involving chiral tin compounds in particular have developed significantly due to the compounds produced and proceed with high stereoselectivity.[121,122] This can be attributed mainly to the stereocontrol of the compound and is accomplished through the use of chiral auxiliaries linking to the radical center.[123] Stereocontrol of a tin compound can occur via an atom- or group–transfer reaction between a prostereogenic radical and a chiral radical to produce a new chiral tin compound. Through this method, a chiral tin compound can be converted to a tin hydride compound and can exist as a nonracemic mixture through the intermediacy of diastereomeric transition states.

Through the use of tin hydride compounds, free-radical based processes can be used to create a multitude of compounds some of which include the tandem construction of multi-ring systems of biological importance.[124–126]

Formation of chiral main group compounds have also been realized through the use of chiral auxiliaries. The axially chiral binaphthyl compound has been used extensively as an auxiliary ligand in main group chiral compounds. Being first pioneered by Curran *et al* in 1996, the use of a bidentate chiral binaphthyl ligand was used to synthesize a chiral tin hydride compound through a stepwise synthetic method displayed in Scheme 4.1.
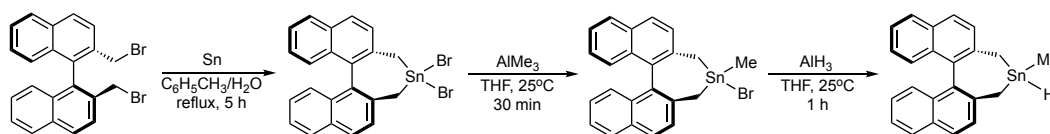
Scheme 4.1: Synthesis of the chiral tin hydride compound (*S*)-4,5-Dihydro-4-methyl-3*H*-dinaphtho[2,-*c*: 1',2'-e]stannepin.[127]

The chiral tin hydride was then used in the reduction of (*R*) – (–) –1,2–diphenylpropan–1–one, as shown in Scheme 4.2, under a variety of different reaction conditions bearing low to moderate yields, and varying enantiomeric excess (ee) values that are collected in Table 4.1.[127]
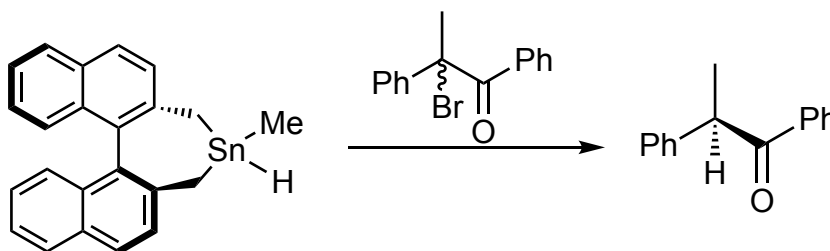
Scheme 4.2: A chiral tin hydride is employed for the reduction of (R) – (–) –1,2–diphenylpropan–1–one.[127]

Entry	Conditions	Yield (%)	Ee (%)[a]
1	AIBN, 80°C	70	11
2	AIBN, - 78°C	54	20
3	Et$_3$B, - 78°C, air[b]	12	30
4	Et$_3$B, - 78°C, air[c]	13	32
5	Et$_3$B, - 78°C, N$_2$[d]	45	25
6	Et$_3$B, - 78°C, air[e]	35	11
7	Et$_3$B, - 78°C, air[f]	30	41

Table 4.1. Reaction conditions, yields, and enantiomeric excess results for the reduction of (*R*) – (–) –1,2–diphenylpropan–1–one using a chiral tin hydride. a) Determined by chiral HPLC. b) Addition of 30% Et$_3$B every 2 h for 16 h. c) Addition of 30% Et$_3$B every 30 min for 4 h. d) Addition of 30% Et$_3$B every 10 min for 90 min. e) Addition of Et$_3$B (10 eq) together with the other reagents f) Addition of 30% Et$_3$B every 1 min for 30 min, then 1 h at -78°C.[127]

The results produced from these experiments led other research from Schiesser[128] and Metzger[129] to further explore the free-radical reactivity associated with chiral tin hydride compounds.

More studies were performed on the free-radical reactivity of tin hydrides, but now with the inclusion of Lewis acids. As is typical in many enantioselective reductions, the addition of a Lewis acid or an increase in steric bulk of the reagent or the substrate, can lead to advances in enantioselectivity. This was seen in studies done by Hoshino who reported an 88% yield and a 62% ee with the reduction of an iodo-coumarin with Bu$_3$SnH in the presence of a chiral Lewis acid (Scheme 4.3).[130]
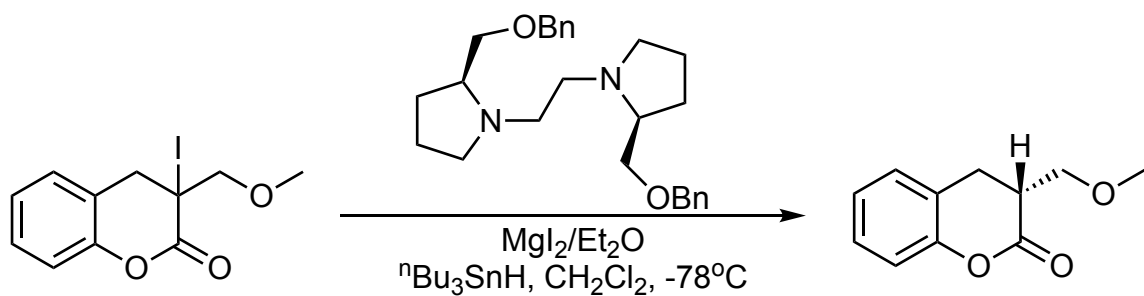
Scheme 4.3: Reduction of methoxymethyl–α–iodolactone in the presence of a chiral Lewis acid giving a 62% ee.[130]

Further reduction studies were performed with enantiopure chiral tin hydrides by Schiesser in which several Lewis acids were screened across an array of substrates reporting enantioselectivities in excess of up to 90%.[128] Selected reactions with yield and ee percentage can be seen in Table 4.2.

Tin hydride	Substrate	Lewis Acid	Product	Ee, Conv. (%)
				86, 75
				90, 73
				96, 75
		MgBr$_2$		92, 96
		MgI$_2$		95, 76

| | | MgI₂ | | 99, 96 |

Reagent structures (left to right): Sn(H)Ph (bis-menthyl tin hydride, subscript 2); HN–C(O)CF₃, OBn, Br, O (bromo substrate); MgI_2; HN–C(O)CF₃, OBn, H, O (reduced product); 99, 96
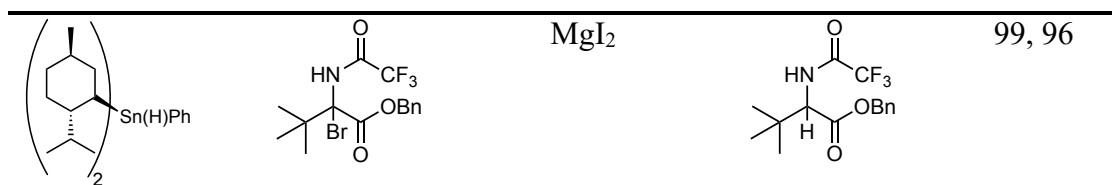
Table 4.2 Selected reduction reactions performed by Schiesser with chiral tin compounds in the presence of Lewis acids in toluene at -78°C.[128]

The continued use of stannanes has proven to be ubiquitous when used as stereoselective radical reducing agents, either alone or in conjunction with chiral Lewis acids. However, continued studies using these reagents have also led to unfortunate difficulties with their isolation, stability, and potential toxicity. In order to circumvent these complications, efforts were placed into the development of silicon and germanium containing hydrides for free-radical reductions.[131–133] The use of trialkylsilanes were initially proposed for free-radical reductions due to their ability to abstract halogen atoms more efficiently than stannanes, however, their ability to support radical chain reactions was not as prevalent as stannanes.[134] This property stems from the fact that silanes are poor hydrogen atom donors toward alkyl radicals unless subjected to high temperatures.[135] This problem was mitigated with the synthesis of a branched silyl compound (($Me_3Si)_3SiH$) that lowered the bond dissociation energy of the silicon–hydrogen bond to 79 kcal/mol therefore allowing it to perform radical chain reductions of alkyl halides in a manner similar to stannanes.[132] The reaction scheme and results of these reactions is shown in Scheme 4.4 and in Table 4.3.

$$4 \ Me_3SiCl \xrightarrow[\substack{- 8 \ LiCl \\ THF}]{\substack{1) \ 8 \ Li \\ 2) \ SiCl_4}} (Me_3Si)_4Si \xrightarrow[\substack{2) \ H_3O^+ \\ - Li^+, - H_2O}]{\substack{1) \ LiCH_3 \\ - Me_4Si}} (Me_3Si)_3SiH$$
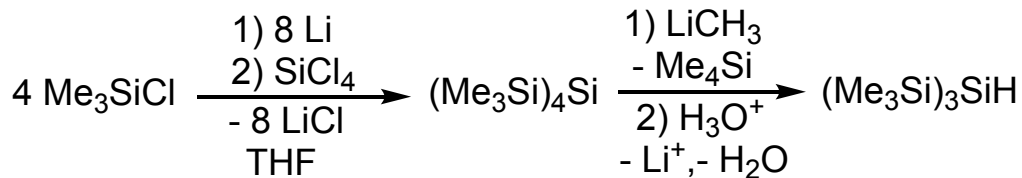
Scheme 4.4. Synthesis of the permethylated silyl hydride for halide reduction.[132]
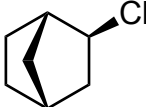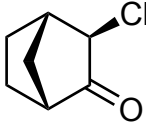
RX	Method	Reaction time, h	Yield, RH (%, via GC)
$C_{18}H_{37}Cl$	A	5	93
	A	2.5	95
	A	0.25	100
$PhCH_2Br$	B	1.0	100
$C_{16}H_{33}Br$	A	0.5	100
$C_{16}H_{33}Br$	B	1.0	100
$C_{18}H_{37}I$	A	0.1	100

Table 4.3 Reduction of organic halides by tris(trimethylsilyl)silane. Method A: Photolysis of samples in quartz tubes containing equimolar amounts (ca. 0.2 m) of RX and $(Me_3Si)_3SiH$ in hydrocarbon or monoglyme solvent. Method B: Reaction initiated with benzoyl peroxide at 50 °C, no solvent.[132]

Being first reported in 1965 by Gilman and co-workers,[136] the compound tris(trimethylsilyl)silane $((Me_3Si)_3SiH)$ was not further analyzed until nearly 20 years later. This analysis revealed $(Me_3Si)_3SiH$ to be a strong hydrogen donor capable of sustaining radical chain reduction of organic substrates similarly to tin hydride compounds. Several substrates were screened that included halides,[132,137] selenides,[132,137] thiono esters,[138–140] isocyanides,[138] acid chlorides,[137] and sulfides with a heteroatom in the β-position.[141,142] The reduction reactions and products are shown in Scheme 4.5 and followed similar

reaction procedures as noted in Table 4.3, with the inclusion of a radical initiator involving higher temperatures in either toluene or benzene. More importantly, however, the results of these reactions, as well as the reagent $(Me_3Si)_3SiH$ and its by-products, proved to be less toxic than the corresponding tin containing compounds.[140]
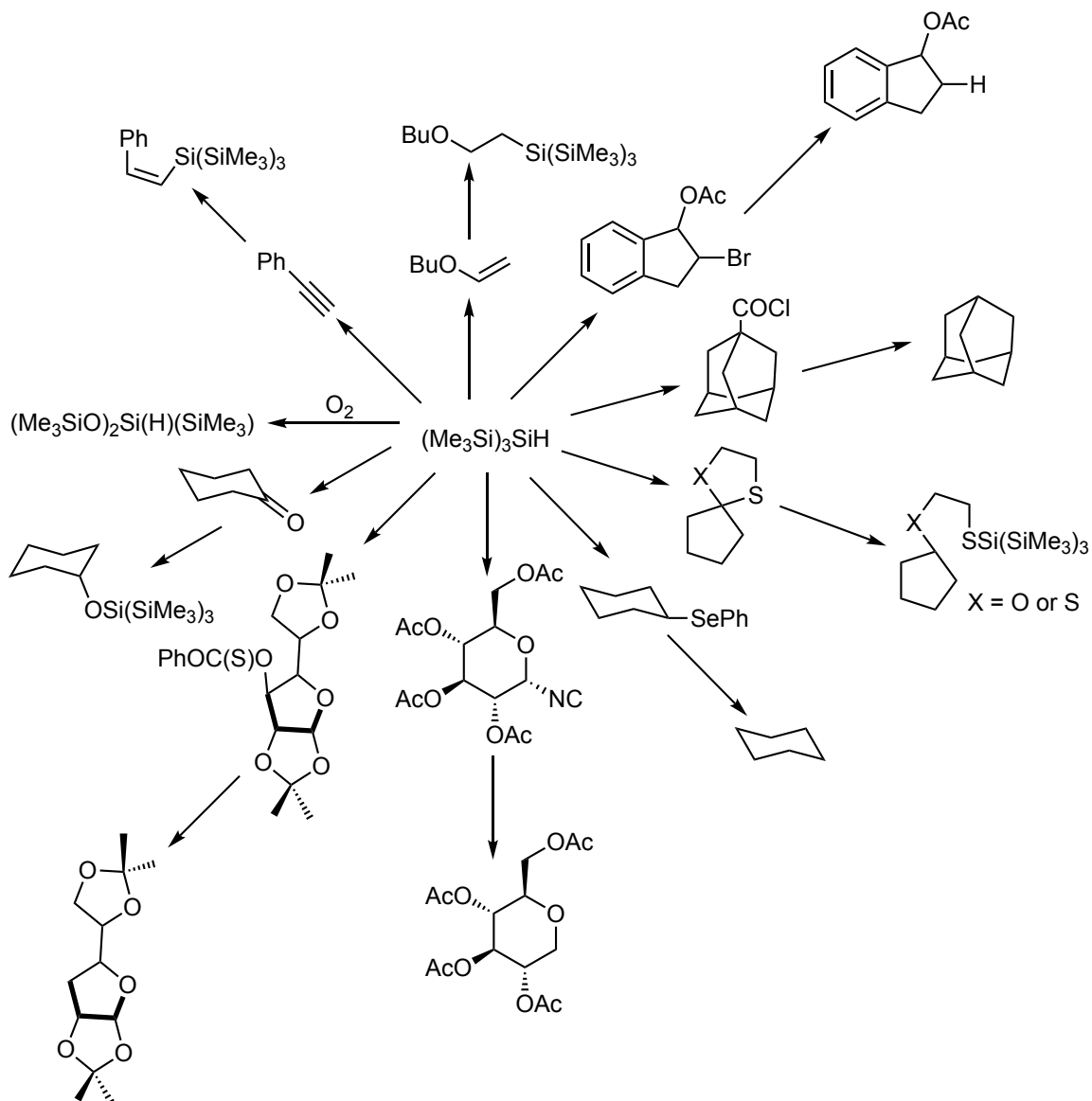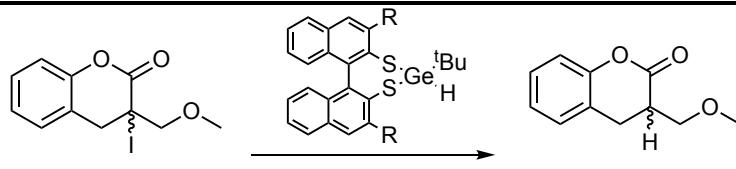
Scheme 4.5: A series of reduction reactions involving $(Me_3Si)_3SiH$.[137]

The reductions involving $(Me_3Si)_3SiH$ as a new reagent, along with perceived results of lowered levels of toxicity, allowed for further analysis of other main group

elements such as germanium to be explored. With the use of chiral auxiliaries, a series of chiral germanium compounds have been synthesized by Curran[143] and Schiesser[131] and rate studies were carried out with data supporting the reduction of organic compounds through radical chain processes was obtained. Similar to silicon, the germanium based chiral compounds mimic the reduction ability that is known for tin-based compounds. While Curran has synthesized these compounds through the use of reduction techniques to generate a germanium-sulfur bond, that was shown to improve the stability of these chiral compounds when compared to germanium-carbon bonds, Schiesser has explored the synthesis of these compounds through the use of uncontrolled Grignard reactions with bulky substituents to generate a germanium-carbon bond. The reaction schemes for these compounds are shown in Scheme 4.6 and while Schiesser's method does produce the desired chiral germanium hydride species, the overall yield of these compounds suggest that Curran's method of synthesis is more sustainable. As displayed by Curran, obtaining a chiral germanium hydride species can be done in two steps and the data collected in Table 4.4 shows the hydrides have radical chain reduction capabilities.
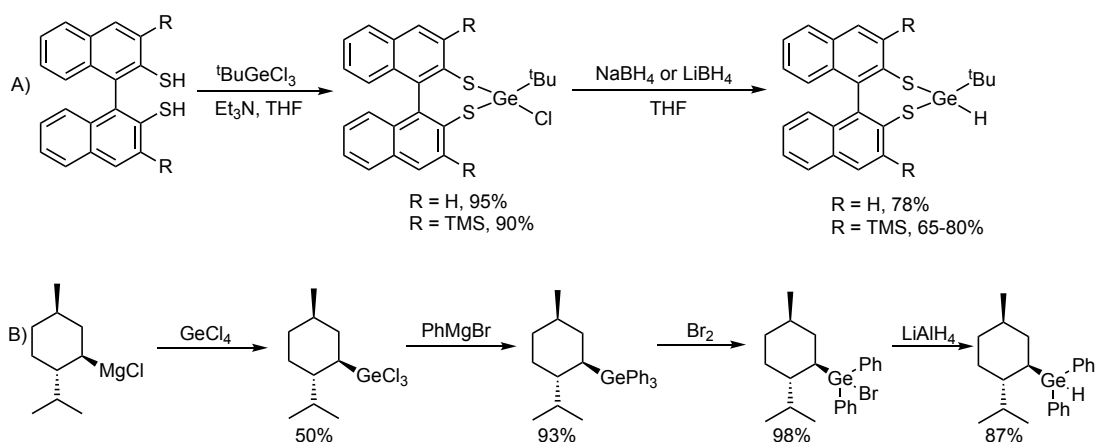
Scheme 4.6: In Scheme 4.6a, the reaction schematic can be seen for synthesizing a chiral germanium hydride species through a series of reductions. In Scheme 4.6b, the reaction schematic can be seen for synthesizing a different chiral germanium hydride species through the use of Grignard reactions.[131,143]

Hydride Conformer	R Group	Temperature (°C)	Initiator	Yield (%)	Ee (%)
(R)	H	−78	Et$_3$B/Ar	97	20 (R)
(R)	H	−78	Et$_3$B/hv	96	26 (R)
(R)	TMS	−78	Et$_3$B/Ar	70	41 (S)
(S)	TMS	−78	Et$_3$B/O$_2$	41	40 (R)

Table 4.4 Selected radical chain induced reduction of iodo-organic species.[143]

While the use of sulfur-containing chiral auxiliaries is primarily focused on the synthesis of chiral germanium hydrides, an avenue that has not been explored is the use of oxygen groups on the chiral auxiliaries to form a germanium-oxygen bond. The use of oxygen groups rather than sulfur to attach to germanium could potentially have an impact in solubility, reactivity, and characterization of these chiral germanium species. This new method of using germanium(IV) halides versus a germanium(II) species also presents a more facile method for the formation of the desired hydride species without the unwanted formation of side-products or an incomplete reaction. The focus of this chapter will be the synthesis, characterization, and functionalization studies associated with reacting a axially chiral binaphthol compound with a germanium(IV) species and forming a chiral germanium complex. This chapter will also advance on a proposed mechanism for the

formation of a chiral germanium complex, as well as its susceptibility to form a germylium ion, in an effort to lead into future studies associated with chiral Lewis acid-base adducts.

4.2 Results and Discussion

Synthesis of the binaphthol ligand began with the enantiopure commercially available binaphthol as either the R or S conformer. Due to the probability of potential polymerization occurring during the formation of the desired chiral germanium species, functionalization of the binaphthol ligand was performed in an effort to make the compound bulkier. This was accomplished by first protecting the hydroxy groups with trimethylchlorosilane, followed by using ^{n}butyllithium (^{n}BuLi) to deprotonate and lithiate the 3 and 3′-positions of the now protected binaphthol compound. After these first two steps, the lithiated compound was reacted with trimethylchlorosilane again to add trimethylsilyl (TMS) groups onto the 3 and 3′-positions followed by the subsequent deprotection of the oxygens. The final product was compared to other literature reports and was confirmed to be pure.[144] The stepwise reaction scheme for the binaphthol compound can be seen in Scheme 4.7.
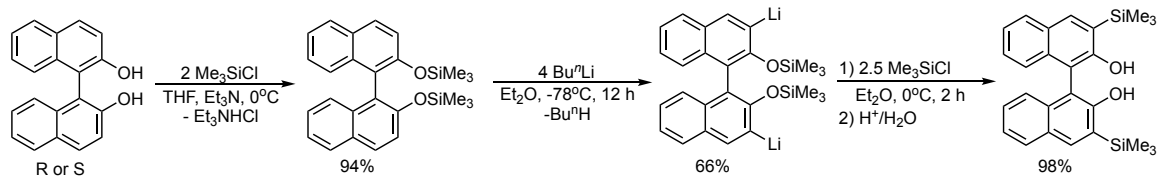
Scheme 4.7: Overall reaction schematic for the synthesis of the chiral auxiliary ligand 3,3'-bis(trimethylsilyl)-[1,1'-binaphthalene]-2,2'-diol.

When analyzed via ^{1}H NMR the final product exhibited a single upfield resonance at δ 0.47 ppm with an integration of 18 hydrogens that can be assigned to the -*SiMe₃* group, as shown in Figure 4.1.
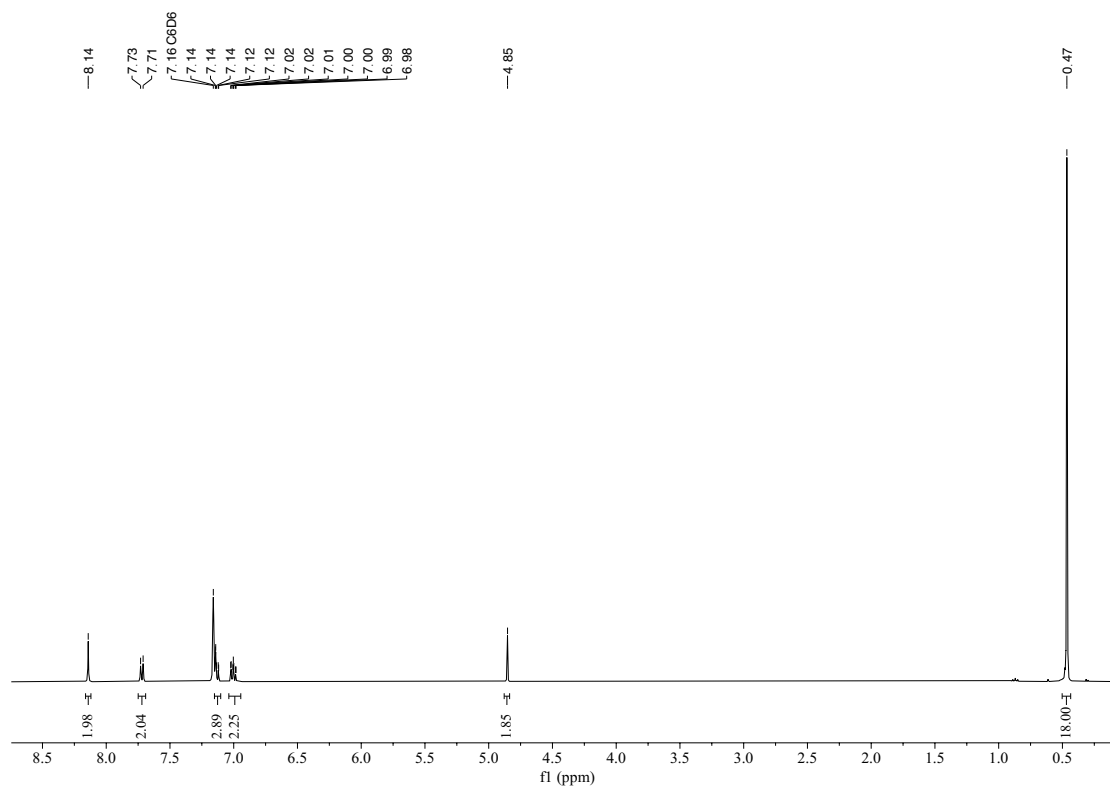
Figure 4.1: ^{1}H NMR spectrum of 3,3'-bis(trimethylsilyl)-[1,1'-binaphthalene]-2,2'-diol.

This is observed as a singlet and not a doublet due to the C_2 symmetry of the compound. With the successful formation of the desired chiral auxiliary ligand precursor, a series of different germanium (IV) compounds were reacted with both the R and S conformers of the binaphthol derivative with and without the TMS groups. Phenylgermaniumtrichloride, benzylgermaniumtrichloride, and methylgermaniumtrichloride were all used for the formation of chiral germanium compounds. Using synthetic methods similar to those of Curran,[143] the germanium (IV) compounds were reacted with both the R and S enantiopure TMS-substituted and unsubstituted binaphthol ligands at 0° C, with the dropwise addition of excess triethylamine. Upon addition of the triethylamine a white solid immediately precipitated out of solution which was confirmed to be triethylamine hydrochloride

indicating the reaction was producing the desired chiral species. The overall schematics for these reactions can be seen in Scheme 4.8.

1a) R` = Ph, 97%, R = SiMe₃
1b) R` = Ph, 93%, R = H
2a) R` = Me, 87%, R = SiMe₃
2b) R` = Me, 84%, R = H
3a) R` = Bn, 91%, R = SiMe₃
3b) R` = Bn, 93%, R = H
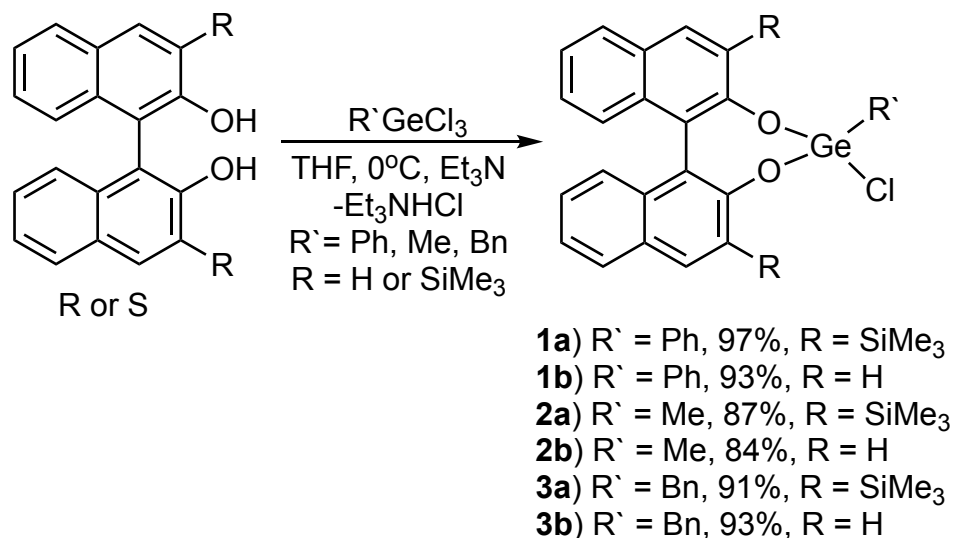
Scheme 4.8: The reaction conditions for producing the desired chiral germanium species with different germanium(IV) compounds and variations at the ortho positions of the binaphthol.

While the reactions did produce a series of different chiral germanium species, there were irregularities observed in the synthesis of compounds **2a** and **2b**. Based on the ^{1}H spectroscopic data, there appear to be multiple methyl and TMS resonances indicating that several different products were formed. This also suggests that the reaction for compounds **2a** and **2b** could have undergone a tri-substitution on the germanium(IV) center. A perceived reason for this possible outcome stems from the fact that the methyl group on the germanium(IV) center is not as large or bulky as a benzyl or a phenyl group. Therefore, this suggests that the size of the R` group plays a role in the reaction in that it can allow for only a di-substitution to occur on the germanium center and prevents a tri-substitution from occurring. Based on this hypothesis, the reaction of methylgermaniumtrichloride with the binaphthol compound would yield a mixture of both the desired chiral species **2a** and **2b** as well as a tri-substituted derivative, examples of which are shown in Figure 4.2.
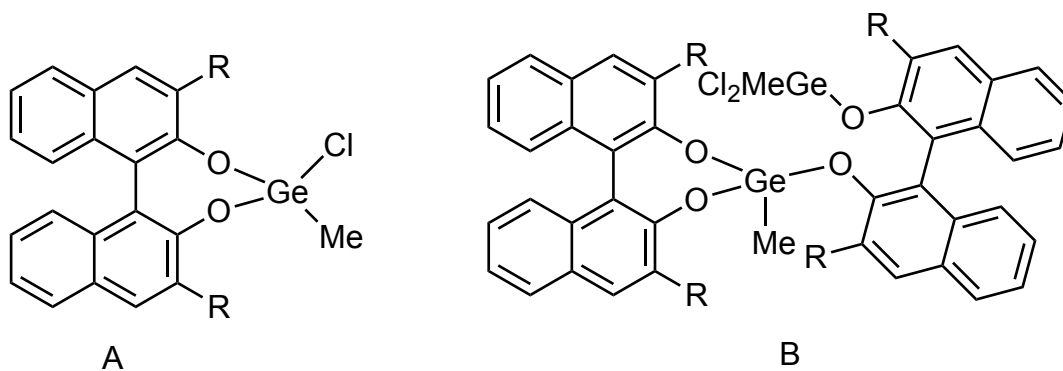
Figure 4.2: Compound A represents the desired chiral germanium species and compound B which is a possible by-product.

Due to the high air and moisture sensitivity, similar chemical properties and solubility, and high boiling point the purification of compounds **2a** and **2b** proved to be too difficult using column chromatography, low pressure distillation, or solvent extraction. For these reasons, compounds **2a** and **2b** were not reacted further. ^{1}H NMR analysis of compounds **3a** and **3b** appeared to be consistent with the intended result however, upon integration of the resonances the spectra did not give the expected relative intensities of the peaks. In order to solve this problem, attempted recrystallization of compounds **3a** and **3b** were carried out from a series of different solvents in order to form crystals suitable for X-ray crystallography. These attempts did not give suitable crystals using either polar solvents, nonpolar solvents, or the combination of both and as such the products could not be isolated in pure form. This led to compounds **3a** and **3b** not being reacted any further.

The formation of compounds **1a** and **1b** proceeded the most efficiently with little to no starting material left upon completion of the reaction, and their ^{1}H NMR spectra agreed with the expected structure of the product. As expected with the TMS group resonances, the signal of the *-SiMe₃* resonance in compound **1a** was converted into two singlets that each integrated to 9 hydrogens indicating the desired product had formed. The splitting of the singlet could be noted in Figure 4.3 where the two new TMS resonances

now appeared at δ 0.50 ppm and δ 0.19 ppm and there does not appear to be any other

residual TMS resonances indicating the reaction produced the intended chiral germanium

species exclusively.
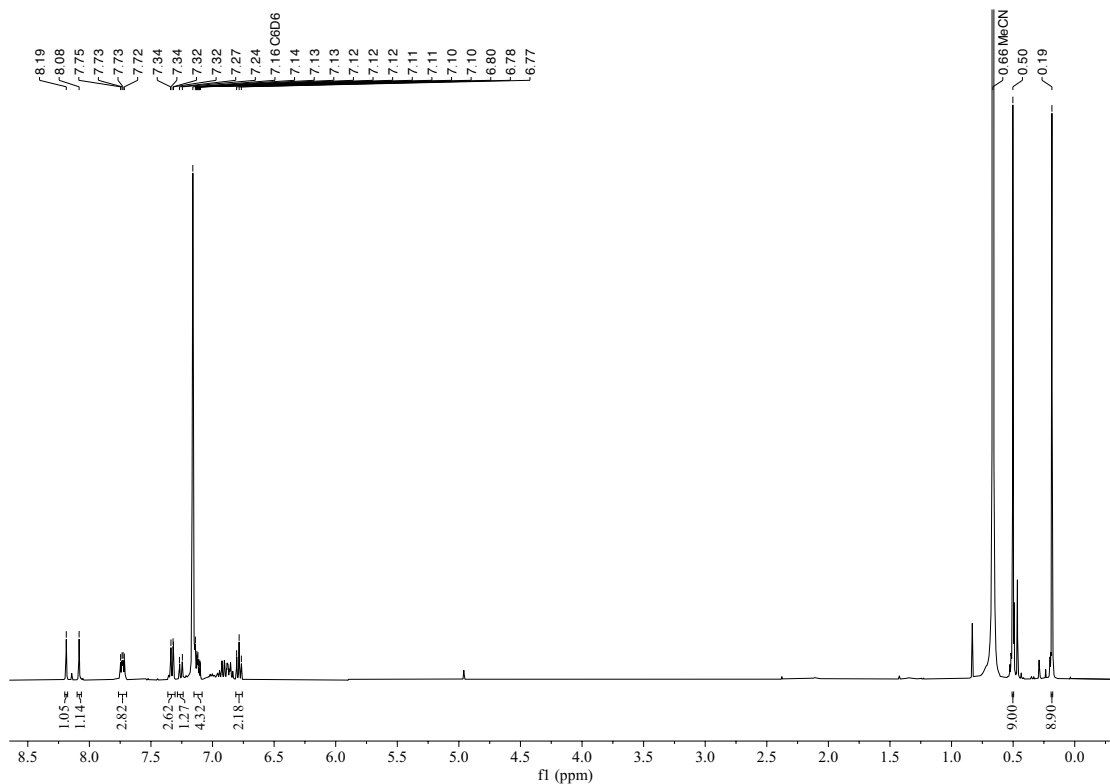
Figure 4.3: ^{1}H NMR spectra of compound **1a**.

Based on the ^{1}H NMR spectra indicating compound **1a** had formed successfully, the solid

was dissolved in a 1:1 mixture of acetonitrile and hexane in an effort to obtain suitable

crystals for X-ray crystallography analysis. Suitable crystals were obtained after one week

of slow evaporation, and a crystal structure was acquired confirming compound **1a** was

synthesized successfully and is shown in Figure 4.4 as an ORTEP diagram with relevant

bond distances (Å) and bond angles (°) in Table 4.5.
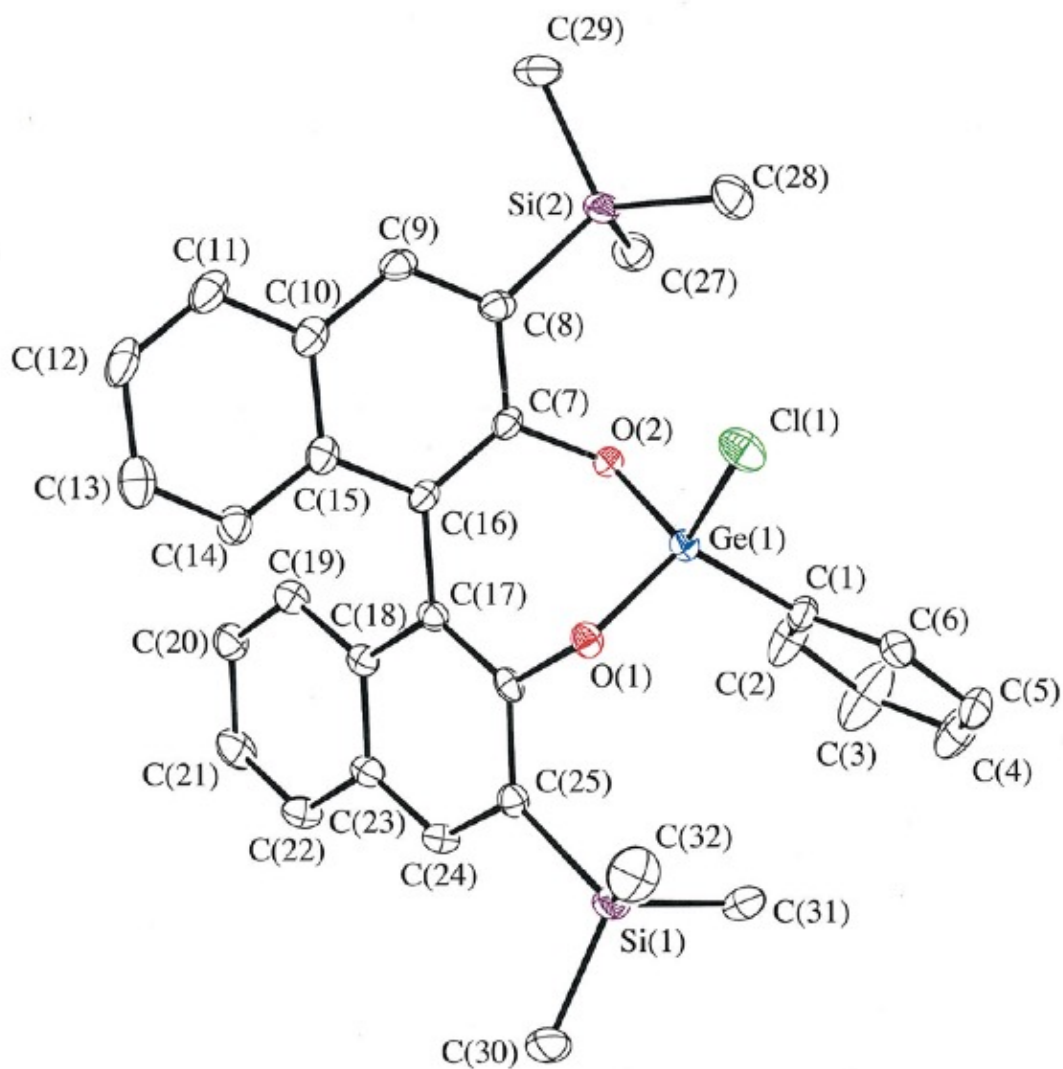
Figure 4.4: ORTEP crystal structure of compound **1a**.

Bond Lengths	(Å)	Bond Angles	(deg)
Ge(1)-Cl(1)	2.1354(9)	O(1)-Ge(1)-Cl(1)	101.40(7)
Ge(1)-O(1)	1.779(2)	O(1)-Ge(1)-C(1)	114.78(12)
Ge(1)-O(2)	1.773(2)	O(2)-Ge(1)-Cl(1)	111.12(7)
Ge(1)-C(1)	1.902(3)	O(2)-Ge(1)-O(1)	106.48(9)
O(1)-C(26)	1.399(3)	O(2)-Ge(1)-C(1)	110.95(12)

O(2)-C(7)	1.404(4)	C(1)-Ge(1)-Cl(1)	111.68(10)
		C(26)-O(1)-Ge(1)	116.41(18)
		C(7)-O(2)-Ge(1)	115.49(19)
		C(2)-C(1)-Ge(1)	119.7(2)
		C(6)-C(1)-Ge(1)	119.7(3)
		O(2)-C(7)-C(8)	116.1(3)
		C(16)-C(7)-O(2)	119.5(3)
		C(17)-C(26)-O(1)	119.0(3)

Table 4.5 Selected bond distances (Å) and angles (deg) for compound **1a**.

The average Ge-O bond distance in compound **1a** is 1.776 Å which is consistent with that expected for germanium(IV)-oxygen single bonds since they range between 1.8 to 2.0 Å. The germanium-carbon bonds are also consistent with other reported structures, as well as the germanium-chloride bond length.[10,145–150] Further analysis of the crystal structure of compound **1a** reveals that the geometry around the germanium atoms reflects a distorted tetrahedral structure with the angles between the C(1)-Ge(1)-O(1), and O(2)-Ge(1)-Cl(1) being larger than 109° (114° and 111° respectively). These angles are larger than normal due to the steric bulk of the phenyl ring causing angles O(1)-Ge(1)-Cl(1) and O(2)-Ge(1)-O(1) to accommodate the steric bulk and be significantly smaller (101° and 106° respectively). Due to the sterics, this increases the angles between the aromatic carbons C(7), C(16), C(17), and C(26) of the seven membered ring to average 117° giving the ring a slight distortion.

With the now complete characterization of compound **1a**, the next step in the synthetic process was to reduce the germanium-chloride species to a germanium-hydride species so it could be used as a hydrogermylation agent. This was first done by reacting

compound **1a** or **1b** with a solution of lithium aluminum hydride (LiAlH₄) in THF at 0°C.

This reaction is typically used for the formation of germanium hydrides; however, when

analyzed via ^{1}H NMR spectroscopy the spectra revealed the presence of only one resonance

belonging to the residual protio solvent present in the deuterated solvent (C_6D_6). The lack

of resonances in the spectra suggested that the product was not soluble in nonpolar organic

solvents and as such did not produce the intended product. The predicted product formation

following the reduction of compound **1a** and **1b** with LiAlH₄ was assumed to be a salt of

the binaphthol compound and is shown in Scheme 4.9.
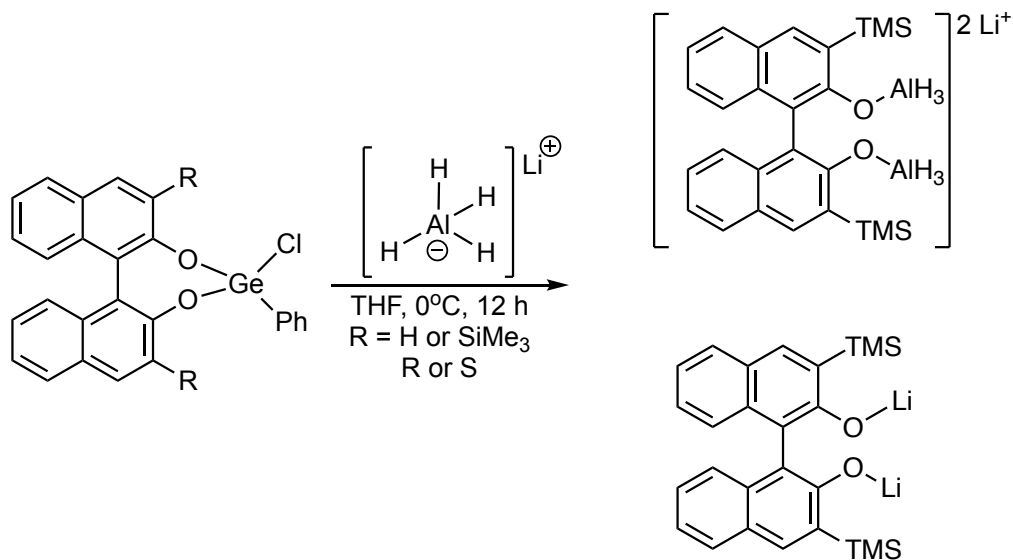
Scheme 4.9: Possible product formation following the reaction of compound **1a** with LiAlH₄.

Due to the high reactivity of LiAlH₄ it appeared that LiAlH₄ was reducing both the

germanium-chloride bond as well as cleaving the germanium-oxygen bond due to the

oxophilicity of the aluminum. This was consistent with the absence of signals in the ^{1}H

NMR spectrum when using an organic deuterated solvent, and when the polar solvent,

($D_3C)_2SO$, was used there were no visible hydride resonances in the NMR spectra.

Due to the results obtained from using LiAlH₄, it was decided to use a slightly less reactive reducing agent such as lithium borohydride (LiBH₄). Under the same reaction conditions LiBH₄ was added to a solution of compound **1a** or compound **1b** in THF at 0° C. Upon analysis of the reaction via NMR spectroscopy, it was revealed that there was no reaction, and the product was only the starting material compound **1a** or **1b**. The reaction scheme for this reaction is shown in Scheme 4.10. Due to these failed experiments, a series of reducing agents with varying reactivities were tested to find the best potential reagent to form the chiral germanium hydride species.
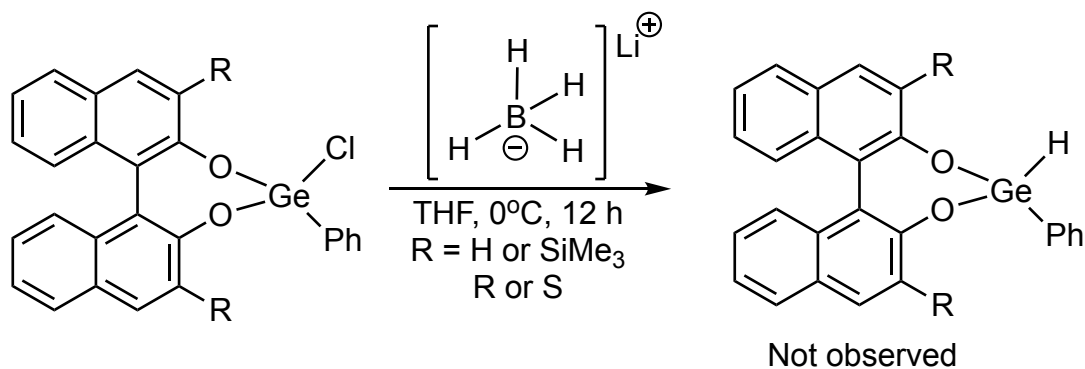
Scheme 4.10: Attempted synthesis of the chiral germanium hydride using LiBH₄.

The next reducing agent that was used was $Bu_3{}^nSnH$ under two different conditions, in an effort to form the chiral germanium hydride species. Due to the steric nature of $Bu_3{}^nSnH$ and its ability to undergo radical chain reduction reactions, it was perceived that it would be reactive enough to only reduce the germanium-halide bond and not interact with the germanium-oxygen bond. One reaction was done with a radical initiator while another was left to react for 5 days and upon NMR analysis it was revealed that both conditions failed to produce the chiral germanium hydride species and only showed the unreacted starting material compound **1a** or **1b**. The reaction scheme for this reaction is shown in Scheme 4.11.
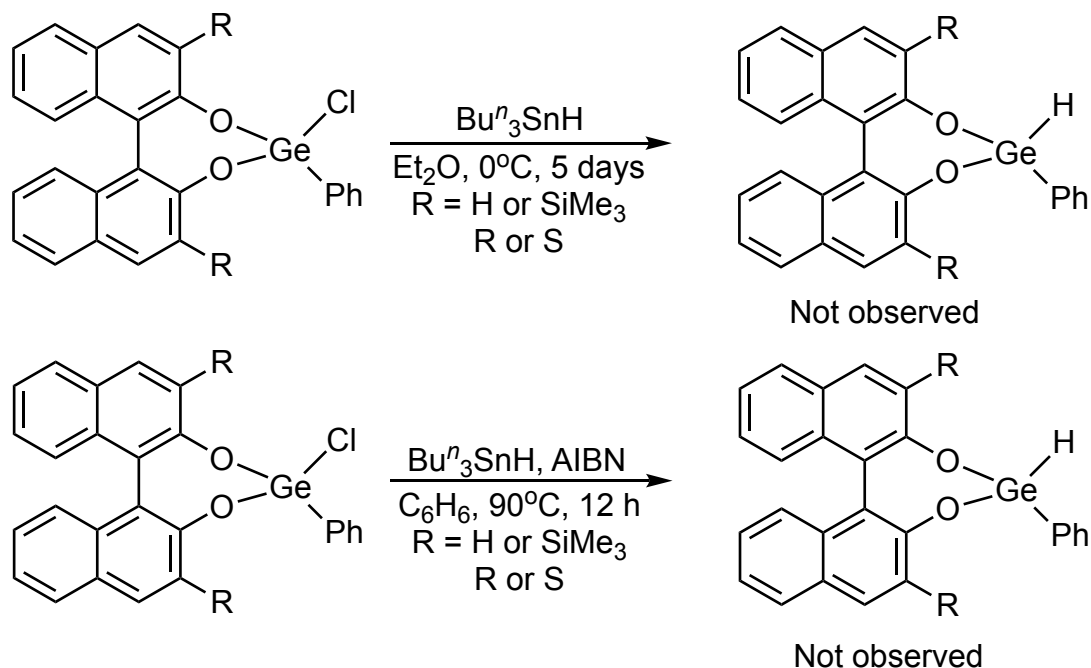
Scheme 4.11: Attempted synthesis of the chiral germanium hydride species under different reaction conditions with Bu_3^nSnH.

Diisobutylaluminum hydride (DIBAL-H) was then used in an effort to synthesize the desired chiral germanium hydride species. Compound **1a** or **1b** was dissolved in dry benzene, and to a solution of DIBAL-H was added dropwise and left to react overnight. After a low pressure kugelrohr distillation (0.001 torr) a white solid remained, which was the analyzed via NMR spectroscopy. The results of this reaction revealed that DIBAL-H had cleaved the germanium-oxygen bond similar to $LiAlH_4$ to yield a binaphthol species with an oxygen-aluminum bond. It was then surmised that any aluminum containing reducing agent will cleave the germanium-oxygen bond while also reducing the germanium-chloride bond. It can be deduced that the oxophilicity of the aluminum, coupled with the ring strain brought upon the binaphthol compound, will consistently cleave the germanium-oxygen bond no matter how sterically hindered the reducing agent is. The overall scheme of this reaction is shown in Scheme 4.12.
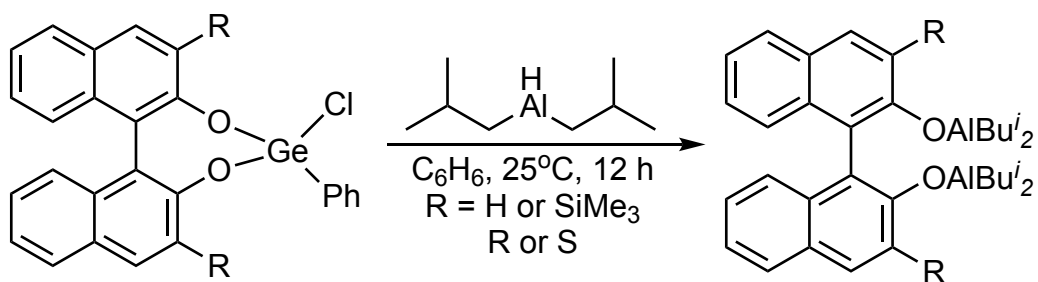
Scheme 4.12: The attempted synthesis of the desired chiral germanium hydride species using DIBAL-H as a reducing agent.

The final reducing agent that was used in an attempt to synthesize the desired chiral germanium hydride was potassium hydride (KH). KH was added slowly to a stirring solution of compound **1a** in THF at 25°C, and while initially the reaction appeared to be producing the intended hydride species, it was realized quickly that upon formation of the hydride species it was quickly being reduced by the unreacted KH in the solution to a form a green germanium anionic salt species (compound **4a**). The reaction lasted one hour, and it was noted that H_2 gas was being released until the reaction was complete, and the green color persisted. It was then confirmed that all of the germanium hydride species had been consumed by KH when a ^1H NMR spectra revealed no visible hydride species. However, due to the unexpected formation of compound **4a** that can now act as a strong nucleophile, it was postulated that compound **4a** can do a nucleophilic attack on a proton source to form the desired chiral hydride species (compound **5**). Therefore, compound **4a** was then reacted with ammonium chloride in THF at 70° C for 12 hours. Upon completion of the reaction and analysis via ^1H NMR spectroscopy, a hydride resonance was observed at δ 5.35 ppm along with a hydroxy resonance at δ 4.85 ppm. This mixture of resonance signals suggested that upon introduction of a proton source, the reaction was competitive between protonating the germanium-oxygen bond to reform the binaphthol compound as well as protonation of germanium to form compound **5**. This mixture of compounds again proved

93

to be impossible to purify due to the similarities of both compounds as well as its high sensitivity to air and moisture. The overall reaction scheme for these reactions is shown in Scheme 4.13.
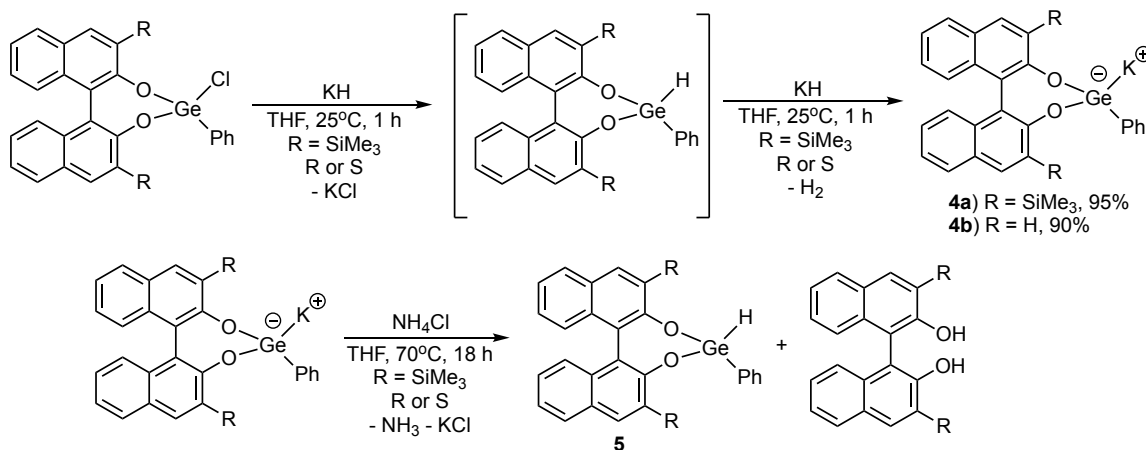
Scheme 4.13: Compound **1a** reacting with KH to produce compound **4a**, followed by a competitive reaction with NH$_4$Cl that produces compound **5** and the binaphthol compound.

Due to the number of failed reduction attempts, a new synthetic pathway was postulated where phenylgermaniumtrichloride was reduced to yield phenylgermaniumtrihydride (PhGeH$_3$), then using by using CuCl$_2$ the compound can selectively be rechlorinated to produce phenylgermaniumdichloro hydride (PhGe(H)Cl$_2$).[151] Upon complete formation of PhGe(H)Cl$_2$, the compound can then be reacted with the chiral binaphthol species to yield compound **5** without the use of reducing agents that can cleave the germanium-oxygen bond. This reaction scheme is shown in Scheme 4.14.
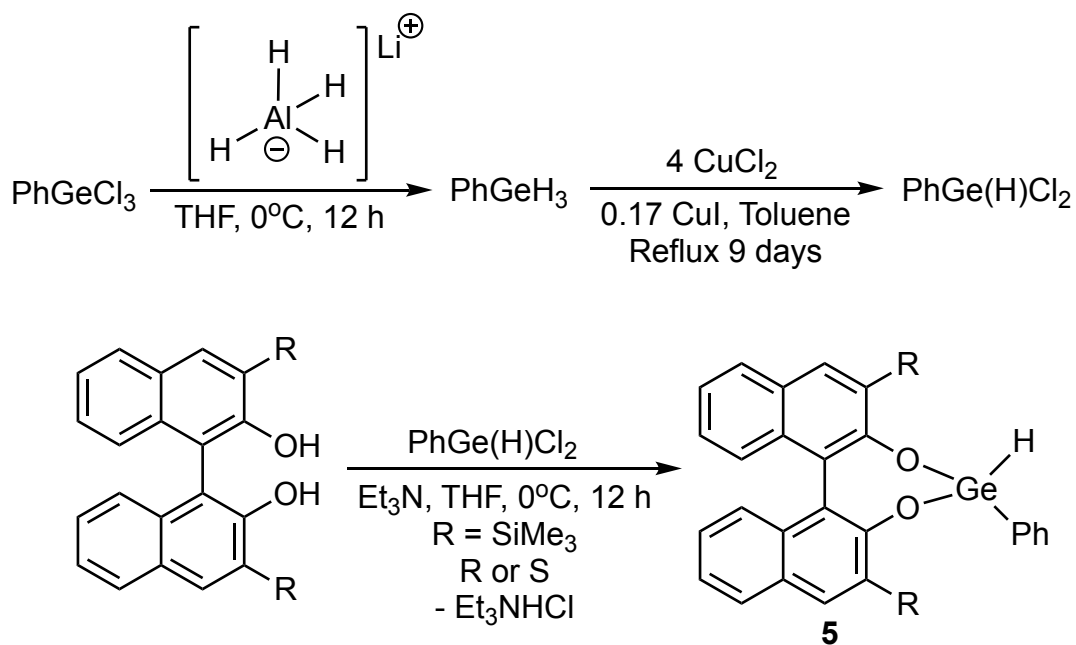
Scheme 4.14: A proposed reaction scheme for the synthesis of PhGe(H)Cl$_2$ that can then be reacted with the binaphthol species to form compound **5**.[151]

However, due to PhGe(H)Cl$_2$ having two chlorides bonded to the germanium(IV) center, the pKa of the hydride could be low enough due to the chlorides and may potentially be deprotonated by Et$_3$N and undergo a competitive reaction between the hydroxy groups and PhGe(H)Cl$_2$. To test this theory, PhGe(H)Cl was synthesized under the same conditions as PhGe(H)Cl$_2$ and then was reacted with Et$_3$N to determine if this could occur. Using a method developed by Kunai,[151] PhGe(H)Cl was reacted with Et$_3$N in THF at 25°C, and upon addition of Et$_3$N a white precipitate was immediately formed that was then confirmed to be Et$_3$NHCl. The overall scheme for this reaction is shown in Scheme 4.15. Due to the results of the previous reaction, it was surmised that the compound PhGe(H)Cl$_2$ would undergo a competitive reaction with binaphthol to form compound **5** with this method.

$$\text{Ph}_2\text{GeCl}_2 \xrightarrow[\text{THF, 0°C, 12 h}]{\left[\begin{array}{c}\text{H} \\ \text{H}-\text{Al}^{\ominus}-\text{H} \\ \text{H}\end{array}\right]\text{Li}^{\oplus}} \text{Ph}_2\text{GeH}_2 \xrightarrow[\substack{\text{Toluene} \\ \text{Reflux 31 h}}]{2 \text{ CuCl}_2} \text{Ph}_2\text{Ge(H)Cl} \xrightarrow[\text{THF, 0°C, 1 h}]{\text{Et}_3\text{N}} [\text{Ph}_2\text{Ge:}]_n + \text{Et}_3\text{NHCl}$$
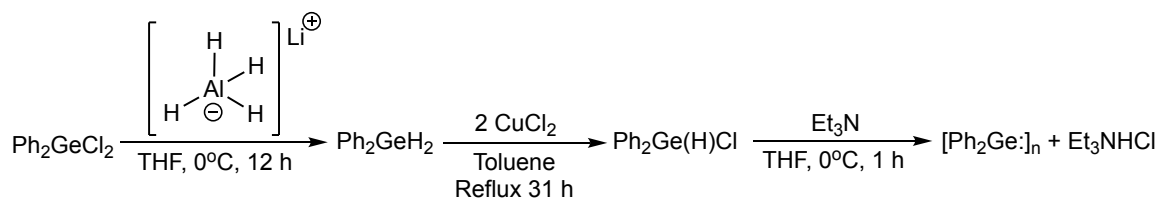
Scheme 4.15. Formation of Ph$_2$Ge(H)Cl followed by a reaction with Et$_3$N to yield a germylene and Et$_3$NHCl.[151]

Nonetheless, the results of the reaction between PhGe(H)Cl and Et$_3$N to form a germylene and Et$_3$NHCl did reveal a unique property that gave further insight to the mechanism followed when forming compound **1a**. It was determined that the germanium-chloride species will readily dechlorinate to form a germylium ion before quickly polymerizing via a germylene formation. The proposed mechanism for this reaction is shown in Scheme 4.16. This information allowed for another proposed mechanism to be developed for the formation of compound **1a** which is shown in Scheme 4.17. What was initially thought to be a S$_N$2 nucleophilic type attack brought upon by the deprotonation of the binaphthol species has now been suggested to be more of a S$_N$1 type reaction. While Et$_3$N does deprotonate the hydroxy group to form Et$_3$NH$^+$, the germanium(IV) species will readily dechlorinate to provide the chloride counter anion for Et$_3$NH and form a germylium ion before being attacked by the deprotonated hydroxy group. This process repeats once more and is then completed to yield compound **1a**.
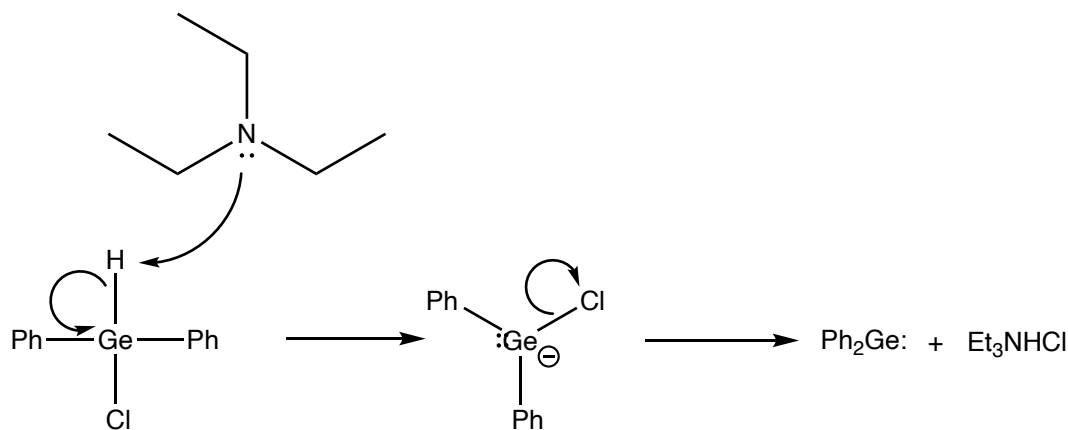
Scheme 4.16: Proposed mechanism for the reaction between PhGe(H)Cl and Et$_3$N.
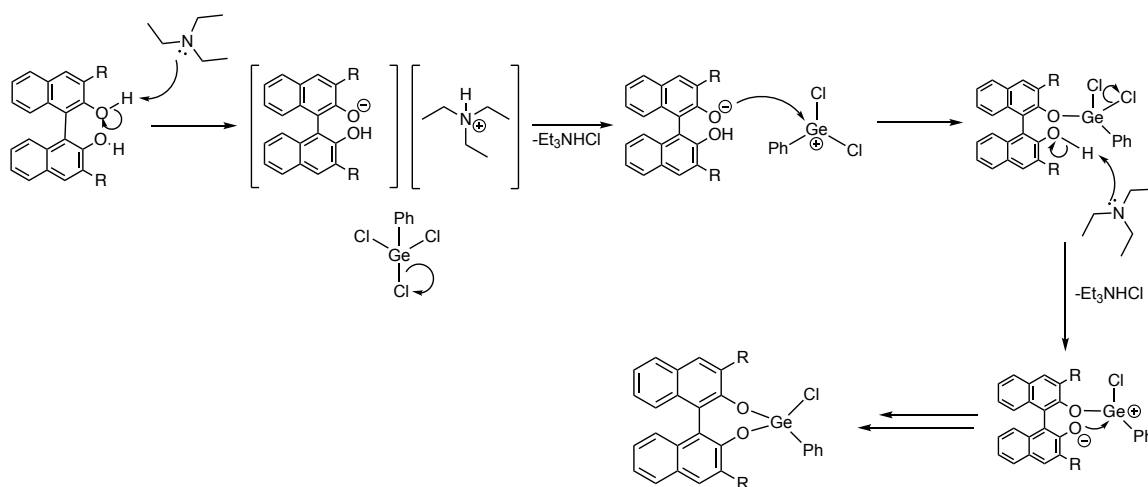
Scheme 4.17: Proposed mechanism for the formation of compound **1a** undergoing a S$_N$1 type reaction.

The ability of a germanium compound to readily dechlorinate itself and form a germylium ion under ideal conditions proposed a new projected avenue for the synthesis of compound **5** as well as new functionality studies. With this newly discovered property, compound **1a** was reacted with the Lewis acid AlCl$_3$, in an effort to observe if the chloride will readily occupy the empty p-orbital on AlCl$_3$ and form a chiral germylium ion Lewis acid-base adduct. Upon addition of AlCl$_3$ the color of the reaction immediately changed from colorless to dark brown, indicating that the chloride had occupied the p-orbital of

AlCl₃ and a germylium ion had formed. While we are unaware of other possible characterization techniques other than X-ray crystallography that can definitively show a germylium ion has formed, we have attempted to obtain a crystal structure of the compounds through slow evaporation in toluene. After one week the vessel revealed large yellow crystals unfortunately, these crystals were revealed to only be the starting material compound **1a**. It was postulated that the dechlorination reaction of compound **1a** underwent an equilibrium reaction between dechlorination and rechlorination where the starting material was heavily favored due to its stable uncharged state. This reaction is shown in Scheme 4.18.
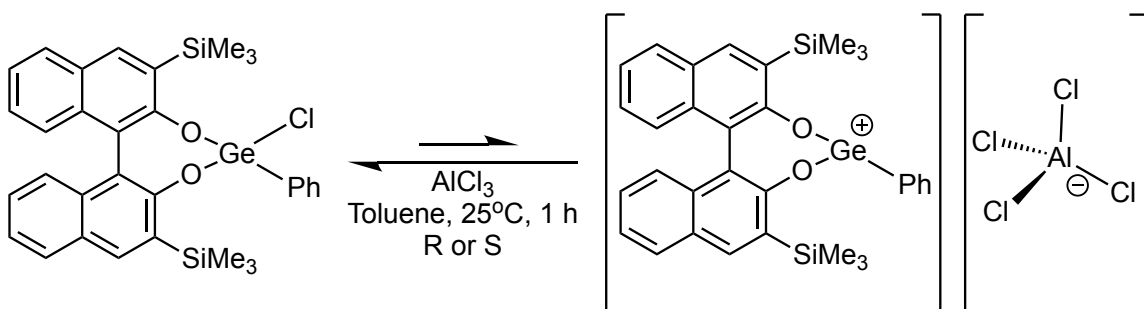
Scheme 4.18: Proposed equilibrium reaction occurring when compound **1a** reacts with AlCl₃.

Our current attempts to obtain suitable crystals have taken this into account and we are attempting to isolate the chiral germylium Lewis acid-base adduct as a single crystal. The theory is that due to the ring being so structurally rigid it should allow for the formation of a chiral Lewis acid that resists racemization, even upon formation of the germylium ion. After a thorough literature search, we were unable to find any compounds similar to the one presented involving germanium atoms. We believe this new compound could present a novel avenue for germylium ion small molecule activation or catalysis. Our goal with this newly formed adduct is to explore the functionality of the germylium ion by attempting to do anionic exchange reactions, to form compound **5** with potentially milder reducing

agents such as LiBH$_4$ or sodium borohydride (NaBH$_4$) that are more susceptible to react with germylium ions, and to perform mechanistic studies with Friedel-Crafts reactions to selectively replace the chloride on the germanium with other organic compounds. The outline for these reactions is shown in Scheme 4.19.
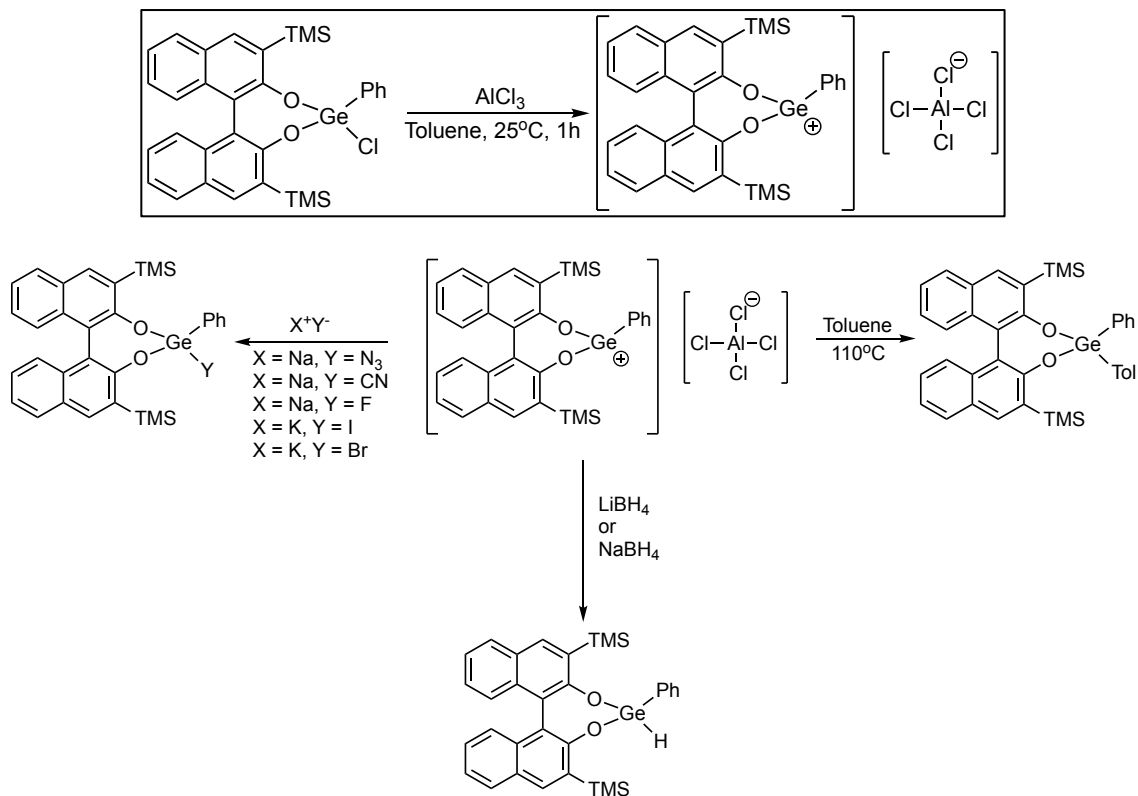
Scheme 4.19. Proposed experiments that can be performed on a germylium ion species to explore its functionality.

4.3 Conclusion

The synthesis of multiple chiral germanium species for use as potential hydrogermylation agents have shown that reaction conditions rely on the steric bulk of the germanium(IV) center as well as the chiral auxiliary. The use of smaller substituents such as methyl groups on a germanium(IV) center allows for di- and tri-substitution to occur at the germanium atom resulting in a mixture of products. Other substituents such as benzyl and phenyl seem to be large or bulky enough to prevent tri-substitution from occurring and

result in only di-substitution. While full characterization of compound **3a** and **3b** could not be achieved, compound **1a** was successfully characterized and is an example of a new chiral germanium compound.

Attempted reduction of the germanium-chloride bond to a germanium-hydride bond in compound **1a** proved to be unsuccessful after multiple attempts with different reducing agents of varying reactivity. It was found that the combination of a distorted tetrahedral geometry on the germanium, oxophilic reducing agents, and ring strain all played a role in the decomposition of compound **1a**. The reducing agents screened were either too reactive, not reactive enough, or produced inseparable mixtures of the intended product and starting materials. Alternative synthetic pathways were attempted with the goal of synthesizing compound **5**; however, due to the reaction conditions these alternative routes were not feasable. Although, it was through trial and error that further insight into a second proposed mechanism and several unique properties were discovered with regard to germanium-chloride bonds.

The proposed formation of a chiral germylium ion Lewis acid-base adduct has yet to be reported, and is in the process of being fully characterized. Proposed functionality studies performed on this compound indicate the potential for the formation of compound **5** for hydrogermylation with milder reducing agents such as $NaBH_4$, Friedel-Crafts mechanistic studies, as well as anionic exchange reactions. Overall, the possibility of isolating a chiral germylium ion represents a rare example of the ability of germanium compounds to undergo unique transformations and potentially exhibit small molecule activation reactions or catalytic reactions.

4.4 Experimental Section

General Remarks

Handling and manipulation of air and moisture sensitive compounds were carried out under a nitrogen atmosphere using standard Schlenk, syringe, and glovebox techniques. Solvents were dried using a Glass Contour solvent purification system and were further dried with molecular sieves. Compounds that are not sensitive to air or moisture were done on a benchtop using standard glassware. The compound 1,1`-bi-2-naphthol for both the *R* and *S* conformations were purchased enantiopure from Gelest and were used without further purification. NMR spectra were acquired using a Bruker Avance III spectrometer operating at 400.0 MHz (^{1}H) or 100.57 MHz (^{13}C).

Table 4.6 Crystallographic data for compound **1a**

Empirical formula	$C_{32}H_{33}ClGeO_2Si_2$
Formula weight	613.80
Temperature	100.0K
Wavelength	0.71073 Å
Crystal system	Orthorhombic
Space group	$P2_12_12_1$
Unit cell dimensions	a = 8.3282(14) Å, α= 90°.
	b = 10.3916(17) Å, β= 90°.
	c = 35.481(6) Å, γ = 90°.
Volume	3070.6(9) Å^3
Density	1.328 Mg/m^3
Absorption coefficient	1.190 mm^{-1}
F(000)	1272
Crystal Ssize	0.31 x 0.29 x 0.18 mm^3
Theta range for data collection	2.042 to 28.278°
Index ranges	-11<=h<=10, -13<=k<=13, -44<=l<=47

Reflections collected	26087
Independent reflections	7581 [R(int) = 0.0573]
Completeness to theta = 25.242°	99.9 %
Absorption correction	Semi-empirical from equivalents
Max. and min. transmission	0.7457 and 0.6530
Refinement method	Full-matrix least-squares on F^2
Data / restraints / parameters	7581 / 0 / 349
Goodness-of-fit on F^2	1.023
Final R indices [I>2sigma(I)]	R1 = 0.0347 wR2 = 0.0725
R indices (all data)	R1 = 0.0399 wR2 = 0.0741
Absolute structure parameter	0.016(5)
Largest diff. peak and hole	0.631 and -0.326 e.Å^{-3}

Synthesis of 2,2'-bis((trimethylsilyl)oxy)-1,1'-binaphthalene (R or S)

1,1`-Bi-2-naphthol (2.00 g, 6.98 mmol) was charged to an oven-dried Schlenk flask along with 15 mL of dry THF and a magnetic stir-bar. In a separate oven-dried Schlenk flask equipped with a stir bar, chlorotrimethylsilane (2.15 eq, 1.91 mL, 15.02 mmol) was charged along with 15 mL of THF and then cannulated slowly into the solution of 1,1`-bi-2-naphthol and cooled to 0° C with stirring. To the solution was added Et_3N (4 eq, 3.89 mL, 27.92 mmol) dropwise and the reaction was left to react overnight. Upon completion, the reaction was filtered through a double-sided frit with celite to remove Et_3NHCl and the volatiles were removed *in vacuo* to yield 2,2'-bis((trimethylsilyl)oxy)-1,1'-binaphthalene as a yellow oil for the *S* conformation and as a clear oil for the *R* conformation. (2.85 g, 94%). ^{1}H NMR (C_6D_6, 25 °C): *δ* 7.72 (dt, *J* = 7.6 Hz, 4H, *aryl*), 7.39 (dt, *J* = 8.4, 1.0 Hz, 2 H, *aryl*), 7.22 – 7.12 (m, 4H, *aryl*), 7.09 – 6.99 (m, 2 H, *aryl*), -0.11 (s, 18H, *-SiMe₃*).

Synthesis of 3,3'-bis(dilithio)-2,2'-bis((trimethylsilyl)oxy)-1,1'-binaphthalene (R or S)

2,2'-Bis((trimethylsilyl)oxy)-1,1'-binaphthalene (2.85 g, 6.62 mmol) was charged to an oven-dried Schlenk flask equipped with a stir bar along with 15 mL of dry diethyl ether (Et$_2$O) and the solution was cooled to 0°C. In a separate oven-dried Schlenk flask equipped with a stir bar, ^{n}BuLi (2.5 M, 4 eq, 10.6 mL) was charged and left to stir. After 5 minutes, the ^{n}BuLi solution was cannulated dropwise to the solution of 2,2'-bis((trimethylsilyl)oxy)-1,1'-binaphthalene with vigorous stirring and left to react overnight. Upon completion of the reaction, the solution was filtered through a double-sided fritz, washed with hexane, and the volatiles were removed *in vacuo*. The final product yield was 1.95 g (66%) as a brown crystalline solid for both the *R* and *S* conformation that was only slightly soluble in deuterated benzene. As such the ^{1}H NMR could not be accurately taken.

Synthesis of 3,3'-bis(trimethylsilyl)-[1,1'-binaphthalene]-2,2'-diol (R or S)

3,3'-Bis(dilithio)-2,2'-bis((trimethylsilyl)oxy)-1,1'-binaphthalene (2.05 g, 4.63 mmol) was charged to an oven-dried Schlenk flask equipped with stir bar along with 15 mL of dry Et$_2$O and left to dissolve for 5 minutes. To an addition funnel was added chlorotrimethylsilane (1.08 g, 9.96 mmol) under an inert atmosphere and this was fitted to the top of the Schlenk flask containing 3,3'-bis(dilithio)-2,2'-bis((trimethylsilyl)oxy)-1,1'-binaphthalene solution. Trimethylchlorosilane was added dropwise to the solution and the reaction was left to react for 2 hours where upon completion was quenched with 25 mL of 6M HCl in an ice bath. The solution as then filtered and extracted 3 times with 20 mL

quantities of Et$_2$O, dried with MgSO$_4$, filtered through a cotton plug, and then filtered again through a silica plug. The volatiles were removed *in vacuo* to yield a white fluffy solid for the *R* conformation and a light-yellow fluffy solid for the *S* conformer (1.97 g, 98%). ^{1}H NMR (C$_6$D$_6$, 25 °C): δ 8.14 (s, 2H, *aryl*), 7.72 (d, *J* = 7.9 Hz, 2H, *aryl*), 7.13 (dd, *J* = 9.9, 1.2 Hz, 3H, *aryl*), 7.00 (ddd, *J* = 8.4, 7.0, 1.4 Hz, 3H, *aryl*), 4.85 (s, 2H, *-OH*), 0.47 (s, 18H, *-SiMe$_3$*). ^{13}C NMR (C$_6$D$_6$, 25 °C): δ 157.67 (C), 146.72 (CH), 138.29 (C), 135.06 (C), 129.93 (C), 128.94 (CH), 124.41 (CH), 124.06 (CH) 120.98 (CH), 110.16 (C), -0.73 (-CH$_3$).

Synthesis of compounds 1a (R or S)

3,3'-Bis(trimethylsilyl)-[1,1'-binaphthalene]-2,2'-diol (1.00 g, 2.32 mmol) was charged to an oven dried Schlenk flask along with a stir bar, 15 mL of dry THF, and left to dissolve for 5 minutes. In a separate oven dried Schlenk flask was charged phenylgermaniumtrichloride (0.6 g, 2.35 mmol) along with 15 mL of dry THF, and a stir bar. The solution of phenylgermaniumtrichloride was cannulated into the solution of 3,3'-bis(trimethylsilyl)-[1,1'-binaphthalene]-2,2'-diol, and Et$_3$N (1.25 mL, 9.29 mmol) was added dropwise to the solution causing an immediate precipitation of Et$_3$NHCl. The reaction was left to react overnight and upon completion was filtered and the volatiles were removed *in vacuo* to yield a white solid for both the *R* and *S* conformations (1.39 g, 97%). ^{1}H NMR (C$_6$D$_6$, 25 °C): δ 8.19 (s, 1H, *aryl*), 8.08 (s, 1H, *aryl*), 7.73(dd, *J* = 7.8, 4.5 Hz, 3H, *aryl*), 7.33 (dd, *J* = 8.2, 1.3 Hz, 3H, *aryl*), 7.26 (d, *J* = 9.5 Hz, 1H, *aryl*), 7.19 – 7.08 (m, 4H, *aryl*), 6.78 (t, *J* = 7.7 Hz, 2H, *aryl*), 0.50 (s, 9H, *-SiMe$_3$*), 0.19 (s, 9H, *-SiMe$_3$*).

Synthesis of 1b

[1,1'-Binaphthalene]-2,2'-diol (477 mg, 1.67 mmol) was charged to an oven dried Schlenk flask equipped with a stir bar, 15 mL of dry THF was added and the mixture was left to dissolve for 5 minutes. In a separate oven-dried Schlenk flask was charged phenylgermaniumtrichloride (0.4 g, 1.67 mmol) along with 15 mL of dry THF, and a stir bar. The solution of phenylgermaniumtrichloride was cannulated into the solution of [1,1'-binaphthalene]-2,2'-diol, and Et$_3$N (0.46 mL, 6.66 mmol) was added dropwise to the solution causing an immediate precipitation of Et$_3$NHCl. The reaction was left to react overnight and upon completion was filtered and the volatiles were removed *in vacuo* to yield a white solid for both the *R* and *S* conformations (730 mg, 93%). ^{1}H NMR (C$_6$D$_6$, 25 °C): δ 7.77 – 7.63 (m, 1H, *aryl*), 7.61 (t, J = 4.5 Hz, 3H, *aryl*), 7.54 – 7.41 (m, 3H, *aryl*), 7.40 – 7.31 (m, 1H, *aryl*), 7.16 (s, 1H, *aryl*), 7.10 (ddd, J = 8.2, 6.7, 1.2 Hz, 2H, *aryl*), 6.94 (dddt, J = 12.9, 10.8, 9.2, 4.2, Hz, 4H, *aryl*), 6.85 – 6.70 (m, 1H, *aryl*), 6.29 (t, J = 7.7 Hz, 1H).

Attempted synthesis of **2a**

3,3'-Bis(trimethylsilyl)-[1,1'-binaphthalene]-2,2'-diol (444 mg, 1.03 mmol) was charged to an oven dried Schlenk flask along with a stir bar, 15 mL of dry THF, and left to dissolve for 5 minutes. In a separate oven dried Schlenk flask was charged methylgermaniumtrichloride (200 mg, 1.03 mmol) along with 15 mL of dry THF, and a stir bar. The solution of methylgermaniumtrichloride was cannulated into the solution of 3,3'-bis(trimethylsilyl)-[1,1'-binaphthalene]-2,2'-diol, and Et$_3$N (0.57 mL, 4.12 mmol) was added dropwise to the solution causing an immediate precipitation of Et$_3$NHCl. The

reaction was left to react overnight and upon completion was filtered and the volatiles were

removed *in vacuo* to yield a brown solid for both the *R* and *S* conformations (0.49 g, 87%).

Attempted synthesis of 2b

[1,1'-binaphthalene]-2,2'-diol (368 mg, 1.29 mmol) was charged to an oven dried

Schlenk flask along with a stir bar, 15 mL of dry THF, and left to dissolve for 5 minutes.

In a separate oven dried Schlenk flask was charged methylgermaniumtrichloride (250 mg,

1.29 mmol) along with 15 mL of dry THF, and a stir bar. The solution of

methylgermaniumtrichloride was cannulated into the solution of [1,1'-binaphthalene]-2,2'-

diol, and Et$_3$N (0.72 mL, 5.14 mmol) was added dropwise to the solution causing an

immediate precipitation of Et$_3$NHCl. The reaction was left to react overnight and upon

completion was filtered and the volatiles were removed *in vacuo* to yield a white solid for

both the *R* and *S* conformations (440 mg, 84%).

Attempted synthesis of 3a

3,3'-bis(trimethylsilyl)-[1,1'-binaphthalene]-2,2'-diol (500 mg, 1.16 mmol) was

charged to an oven dried Schlenk flask along with a stir bar, 15 mL of dry THF, and left to

dissolve for 5 minutes. In a separate oven dried Schlenk flask was charged

benzylgermaniumtrichloride (313 mg, 1.16 mmol) along with 15 mL of dry THF, and a stir

bar. The solution of benzylgermaniumtrichloride was cannulated into the solution of 3,3'-

bis(trimethylsilyl)-[1,1'-binaphthalene]-2,2'-diol, and Et$_3$N (0.65 mL, 4.64 mmol) was

added dropwise to the solution causing an immediate precipitation of Et$_3$NHCl. The

reaction was left to react overnight and upon completion was filtered and the volatiles were

removed *in vacuo* to yield a white sticky solid for both the *R* and *S* conformations (660 mg, 91%).

*Attempted synthesis of **3b***

[1,1'-binaphthalene]-2,2'-diol (519 mg, 1.81 mmol) was charged to an oven dried Schlenk flask along with a stir bar, 15 mL of dry THF, and left to dissolve for 5 minutes. In a separate oven dried Schlenk flask was charged benzylgermaniumtrichloride (490 mg, 1,81 mmol) along with 15 mL of dry THF, and a stir bar. The solution of benzylgermaniumtrichloride was cannulated into the solution of [1,1'-binaphthalene]-2,2'-diol, and Et$_3$N (1.01 mL, 7.25 mmol) was added dropwise to the solution causing an immediate precipitation of Et$_3$NHCl. The reaction was left to react overnight and upon completion was filtered and the volatiles were removed *in vacuo* to yield a white solid for both the *R* and *S* conformations (810 mg, 93%).

*Synthesis of compound **4a***

To an oven-dried Schlenk flask was charged compound **1a** (220 mg, 0.35 mmol) along with 15 mL of dry THF and a stir bar. In a separate Schlenk flask was charged with KH (30 wt %, 240 mg, 5.98 mmol) and washed with excess amounts of hexane to remove unwanted mineral oil. Once the mineral oil was removed, the excess hexane was removed *in vacuo* and to the Schlenk flask was charged 20 mL of dry THF and a stir bar. With flowing nitrogen and a needle vent, compound **1a** was cannulated dropwise into the solution of KH and left to react for 1 hour. As the reaction proceeded, visible bubbles could be seen coming out of the solution and the color of the solution began to turn green. Upon

completion, the solution was filtered through a double-sided frit and the volatiles were removed *in vacuo* to yield a green solid for both the *R* and *S* conformation (190 mg, 95%). ^{1}H NMR (C$_6$D$_6$, 25 °C): δ 8.35 (s, 1H, *aryl*), 7.99 – 6.79, 6.62 (t, J = 7.5 Hz, 1H) 0.50 (s, 9H, -*SiMe$_3$*), -0.17 (s, 9H, -*SiMe$_3$*).

Synthesis of compound 4b

To an oven-dried Schlenk flask was charged compound **1b** (220 mg, 0.46 mmol) along with 15 mL of dry THF and a stir bar. In a separate Schlenk flask was charged with KH (30 wt %, 300 mg, 7.48 mmol) and washed with excess amounts of hexane to remove unwanted mineral oil. Once the mineral oil was removed, the excess hexane was removed *in vacuo* and to the Schlenk flask was charged 20 mL of dry THF and a stir bar. With blowing nitrogen and a needle vent, compound **1b** was cannulated dropwise into the solution of KH and left to react for 1 hour. As the reaction proceeded, visible bubbles could be seen coming out of the solution and the color of the solution began to turn orange. Upon completion, the solution was filtered through a double-sided fritz and the volatiles were removed *in vacuo* to yield an orange solid for both the *R* and *S* conformation (180 mg, 90%). ^{1}H NMR (C$_6$D$_6$, 25 °C): δ 7.74 – 6.75.

Attempted synthesis of compound 5

To an oven-dried Schlenk tube was charged compound **4a** (190 mg, 0.30 mmol) along with a stir bar, ammonium chloride (240 mg, 0.457 mmol) and 20 mL of dry THF. The solution was placed in an oil bath at 70°C for 18 hours and left to react. Upon completion the reaction was filtered, and the volatiles were removed *in vacuo* to yield a white solid for both the R and S conformations. This was attempted with both the TMS substituted and non-substituted binaphthol chiral auxiliary.

Synthesis of Ph$_2$Ge:and Et$_3$NHCl

In an oven-dried flask was placed PhGe(H)Cl (100 mg, 0.38 mmol), 5 mL of dry THF, and a stir bar. Et$_3$N (1.0 mL, 7.17 mmol) was added dropwise and upon addition Et$_3$NHCl immediately began to precipitate out of solution indicating the reaction was forming Ph$_2$Ge: as well.

REFERENCES

(1)   Winkler, C. *Berichte der Dtsch. Chem. Gesellschaft* **1886**, *19* (210).

(2)   Winkler, C. *Jouran fur Prakt. Chemie* **1886**, *142* (177).

(3)   Edwards, P. P.; Egdell, R. G.; Fenske, D.; Yao, B. The Periodic Law of the Chemical Elements: The New System of Atomic Weights Which Renders Evident the Analogies Which Exist between Bodies *Philisophical Trans. R. Soc. A* **2020**, *378* (2180), 1–11.

(4)   Winkler, C. Die Chemie Ist Schwierig : Winkler. **2020**, *45* (1), 8–15.

(5)   Hayashi, T.; Uchimaru, Y.; Reddy, N. P.; Tanaka, M. *Chem. Lett.* **1992**, *647.*

(6)   Satge, J. Some Applications of Germanium and Its Derivatives. *Main Gr. Met. Chem.* **2004**, *27* (301).

(7)   Amadoruge, M. L.; Weinert, C. S. Singly Bonded Catenated Germanes: Eighty Years of Progress. *Chem. Rev.* **2008**, *108* (10), 4253–4294. https://doi.org/10.1021/cr800197r.

(8)   Balaji, V.; Michl, J. *Polyhedron* **1991**, *10* (11), 1265–1284.

(9)   Weinert, C. S. 3.13 Germanium Organometallics. **2007**, 699–808.

(10)   Weinert, C. S. Syntheses, Structures and Properties of Linear and Branched Oligogermanes. *Dalt. Trans.* **2009**, No. 10, 1691–1699. https://doi.org/10.1039/B816067H.

(11)   Zeigler, J. M. Polysilanes-Prototypical σ-Conjugated Polymers. *Synth. Met.* **1989**, *28* (1–2), 581–591.

(12)   Kimata, Y.; Suzuki, H.; Satoh, S.; Kuriyama, A. Synthesis of Oligosilanes by Electrolysis of Hydrosilanes. *Chem. Lett.* **1994**, *23* (7), 1163–1164.

(13)   Zuev, V.; Skvortsov, N. Synthesis and Characterization of Poly [Phenyl (Fluoroalkyloxaalkane) Silanediyl] *J. Polym. Sci. Part A* **2003**, *41* (23), 3861–3767.

(14)   Matsumoto, H.; Tanaka, R.; Kyushin, S. Syntheses, Structures, and Properties of Ladder Oligosilanes. *Phosphorus, Sulfur Silicon Relat. Elem.* **2001**, *168–169*, 89–92. https://doi.org/10.1080/10426500108546535.

(15)   Sita, L. Heavy-Metal Organic Chemistry: Building with Tin. *Acc. Chem. Res.* **1994**, *27* (7), 191–197.

(16)   Sita, L. Sandorfy Huckel Molecular Orbital Approximation for Modeling the Electronic Structures of Long-Chain Polystannanes. *J. Am. Chem. Soc.* **1995**, *117* (30), 8049–8050.

(17)   Sita, L. A New Strategy for the Synthesis of Homologously Pure Linear Polystannane Oligomers. *Organometallics* **1992**, *11* (4), 1442–1444.

(18)   Imori, T.; Tilley, T. D. High Molecular Mass Polystannanes via Dehydropolymerization of Di (n-Butyl) Stannane. *J. Am. Chem. Soc. Chem. Commun.* **1993**, *21* (1607).

(19)   Babcock, J. R.; Sita, L. Highly Branched, High Molecular Weight Polystannane from Dibutylstannane via a Novel Dehydropolymerization/Rearrangement Process. *J. Am. Chem. Soc.* **1996**, *118* (49), 12481–12482.

(20)   Mochida, K.; Hayakawa, M.; Tsuchikawa, T.; Yasuo, Y.; Masanobu, W.; Hisaharu, H. Synthesis and Photochemical Reactions of Polystannanes. *Chem. Lett.* **1998**, *27* (1), 91–92.

(21)   Morgan, G. T.; Drew, H. D. K. Aromatic Derivatives of Germanium. *J. Am. Chem. Soc.* **1925**, *127* (0), 1760–1768.

(22)   Neumann, W. P.; Niermann, H. Organozinnverbindungen, II. Darstellung von Organozinn-mono-,-di-und-tri-hydriden. *Justus Liebigs Ann. Chem.* **1965**, *683* (1), 1–11.

(23)   Riviere, P.; Satgé, J. Germylgermylènes: Nouveaux Intermediaires Organiques Du Germanium Divalent. *J. Organomet. Chem.* **1973**, *63,* 167–174.

(24)   Gilamn, H.; Gerow, C. The Reactions of Triphenylgermane with Some Organometallic Compounds. A New Method for the Preparation of Triphenylgermyllithium. *J. Am. Chem. Soc.* **1956**, *78* (20), 5435–5438.

(25)   Neumann, W. P.; Kühlein, K. Über Cyclische Phenylgermanium-Verbindungen [(C$_6$H$_5$) 2Ge]. *Tetrahedron Lett.* **1963**, *4* (23), 1541–1545.

(26)   Riviere, P.; Riviere-Baudet, M.; Satge, J. *Compr. Organometallic Chemistry II; Elsevier* **1995**, 137–216.

(27)   Kipping, F. S.; Sands, J. E. *J. Chem. Soc. Trans.* **1921**, *119*, 830–847.

(28)   Baumgartner, T.; Jäkle, F. *Main Group Strategies towards Functional Hybrid Materials*; John Wiley & Sons: Chichester, UK, 2018.

(29)   Brown, M. P.; Fowles, G. W. A. *J. Am. Chem. Soc.* **1958**, 2811.

(30)   Triplett, K.; Curtis, M. D. *J. Organomet. Chem.* **1976**, *107* (1), 23–32.

(31)   Seyferth, D. Vinyl Derivatives of the Metals. IV. The Preparation of Vinylgermanium Compounds by the Grignard Method. *J. Am. Chem. Soc.* **1957**, *79* (11), 2738–2740.

(32)   Glocking, F.; Hooton, K. A. *J. Chem. Soc.* **1962**, 3509.

(33)   Roller, S.; Simon, D.; Dräger, M. Über Polygermane: XIV. Polygermane Als Nebenprodukte Der Grignard-Reaktion von PhMgBr Mit GeCl₄. *J. Organomet. Chem.* **1986**, *301* (11), 27–40.

(34)   Cross, R. J.; Glocking, F. Infrared Spectra of Organogermanes. *J. Organomet. Chem.* **1965**, *3* (2), 146–155.

(35)   Castel, A.; Riviere, P.; Saint-Rock, B.; Satgé, J. Synthesis and UV Spectral Study of Polymetallic Chains (Ge, Si) - Theoretical - Analysis of Substitution Effects *J. Organomet. Chem.* **1983**, *247* (2), 149–160.

(36)   Tamborski, C.; Ford, F. E.; Lehn, W. L.; Moore, G. J.; Soloski, E. J. Synthesis of Organolithium Compounds of Some Group IV and V Elements. *J. Org. Chem.* **1962**, *27* (2), 619–621.

(37)   Bulten, E. J.; Noltes, J. G. Trialkylgermyl Alkali Metal Derivatives. *Tetrahedron Lett.* **1966**, *7* (36), 4389–4392.

(38)   Azemi, T.; Yokoyama, Y.; Mochida, K. Development of Novel and Efficient Synthesis of Group 14 Element (Ge and Sn) Catenates by Use of Samarium (II) Diiodide. *J. Organomet. Chem.* **2005**, *690* (6), 1588–1593.

(39)   Yokoyama, Y.; Hayakawa, M.; Azemi, T.; Mochida, K. The First Application of Samarium(II) Diiodide for the Formation of Group 14 Element Catenates: Synthesis of Tri- or Poly-Germanes and Polystannanes. *J. Chem. Soc. Chem. Comm.* **1995**, No. 22, 2275.

(40)   Lide, D. R. *CRC Handbook of Chemistry and Physics*, 87th ed.; CRC Press: Boca Raton, FL, 2006.

(41)   Sita, L. Structure/Property Relationships of Polystannanes. *Adv. Organomet. Chem.* **1995**, No. 38, 189.

(42)   Shibata, K.; Weinert, C. S.; Sita, L. R. Deconvoluting Steric and Electronic Substituent Effects on the Properties of Linear Oligostannanes: Synthesis and Characterization of a New Series Incorporating the Bu$^t_2$Sn Group. *Organometallics* **1998**, *No.* 17, 2241.

(43)   Bochkarev, M. N.; Vyazankin, N. S.; Bochkarev, L. N.; Razuvaev, G. A. Reactivity of the Germanium-Germanium Bond in 1, 1, 1-Triethyl-2, 2, 2-Tris (Pentafluorophenyl) Digermane. *J. Organomet. Chem.* **1976**, *110* (2), 149–157.

(44)   Zaitsev, K. V; Kapranov, A. A.; Churakov, A. V; Poleshchuk, O. K.; Oprunenko, Y. F.; Tarasevich, B. N.; Zaitseva, G. S.; Karlov, S. S. " Donor − Acceptor " Oligogermanes: Synthesis, Structure, and Electronic Properties. *Organometallics* **2013**, *32* (21), 6500–6510.

(45)   Baines, K. M.; Cooke, J. A.; Dixon, C. E.; Liu, H. W.; Netherton, M. R. Thermolysis of Hexamesitylsiladigermirane or Hexamesitylcyclotrigermane in the Presence of 2, 3-Dimethylbutadiene or Water. *Organometallics* **1994**, *13* (2), 631–634.

(46)   Subashi, E.; Rheingold, A. L.; Weinert, C. S. Preparation of Oligogermanes via the Hydrogermolysis Reaction. *Organometallics* **2006**, *25* (13), 3211–3219. https://doi.org/10.1021/om060115x.

(47)   Amadoruge, M. L.; DiPasquale, A. G.; Rheingold, A. L.; Weinert, C. S. Hydrogermolysis Reactions Involving the α-Germylated Nitriles R_3GeCH_2CN (R = Ph, Pr^i, Bu^t) and Germanium Amides R_3GeNMe_2 (R = Pr^i, Bu^t) with Ph_3GeH: Substituent-Dependent Reactivity and Crystal Structures of $Pr^i_3GeGePh_3$ and $Bu^t_3Ge[NHC(CH_3)CHCN]$. *J. Organomet. Chem.* **2008**, *693* (10), 1771–1778. https://doi.org/10.1016/j.jorganchem.2008.01.045.

(48)   Schrick, E. K.; Forget, T. J.; Roewe, K. D.; Schrick, A. C.; Moore, C. E.; Golen, J. A.; Rheingold, A. L.; Materer, N. F.; Weinert, C. S. Substituent Effects in Digermanes: Electrochemical, Theoretical, and Structural Investigations. *Organometallics* **2013**, *32* (7), 2245–2256.

(49)   Amadoruge, M. L.; Yoder, C. H.; Conneywerdy, J. H.; Heroux, K.; Rheingold, A. L.; Weinert, C. S. ^{73}Ge NMR Spectral Investigations of Singly Bonded Oligogermanes. *Organometallics* **2009**, *28*, 3067.

(50)   Roewe, K. D.; Golen, J. A.; Rheingold, A. L.; Weinert, C. S. Synthesis, Structure, and Properties of the Hexagermane $Pr^i_3Ge(GePh_2)_4GePr^i_3$. *Can. J. Chem.* **2014**, *92* (6), 533–541.

(51)   Samanamu, C. R.; Amadoruge, M. L.; Schrick, A. C.; Chen, C.; Golen, J. A.; Rheingold, A. L.; Materer, N. F.; Weinert, C. S. Synthetic, Structural, and Physical Investigations of the Large Linear and Branched Oligogermanes $Ph_3GeGePh_2GePh_2GePh_2H$, Ge_5Ph_{12}, and $(Ph_3Ge)_4Ge$. *Organometallics* **2012**, *31*, 4374.

(52)   Amadoruge, M. L.; Golen, J. A.; Rheingold, A. L.; Weinert, C. S. Preparation, Structure, and Reactivity of Discrete Branched Oligogermanes. *Organometallics* **2009**, *28* (15), 4628. https://doi.org/10.1021/om900565g.

(53)   Samanamu, C. R.; Amadoruge, M. L.; Yoder, C. H.; Golen, J. A.; Moore, C. E.; Rheingold, A. L.; Materer, N. F.; Weinert, C. S. Syntheses, Structures, and Electronic Properties of the Branched Oligogermanes $(Ph_3Ge)_3GeH$ and $(Ph_3Ge)_3GeX$ (X = Cl, Br, I). *Organometallics* **2011**, *30* (5), 1046–1058. https://doi.org/10.1021/om101091c.

(54) Hayatifar, A.; Shumaker, F. A.; Komanduri, S. P.; Hallenbeck, S. A.; Rheingold, A. L.; Weinert, C. S. Synthesis of the Elusive Branched Fluoro-Oligogermane (Ph$_3$Ge)$_3$GeF: A Structural, Spectroscopic, Electrochemical, and Computational Study. *Organometallics* **2018**, *37* (12), 1852–1859. https://doi.org/10.1021/acs.organomet.8b00095.

(55) Komanduri, S. P.; Shumaker, F. A.; Hallenbeck, S. A.; Knight, C. J.; Yoder, C. H.; Buckwalter, B. A.; Dufresne, C. P.; Fernandez, E. J.; Kaffel, C. A.; Nazareno, R. E.; Neu, M.; Reeves, G.; Rivard, J. T.; Shackelford, L. J.; Weinert, C. S. Structure/Property Relationships in Branched Oligogermanes. Preparation of (Me$_3$Ge)$_3$GePh, (Me$_2$Bu^{t}Ge)$_3$GePh, and (Me$_2$PhGe)$_3$GePh and Investigation of Their Properties by Spectroscopic, Spectrometric and Electrochemical Methods. *J. Organomet. Chem.* **2017**, *848*, 104–113. https://doi.org/10.1016/j.jorganchem.2017.07.021.

(56) Miller, R. D.; Michl, J. Polysilane High Polymers. *Chem. Rev.* **1989**, *89* (6), 1359–1410. https://doi.org/10.1021/cr00096a006.

(57) Balaji, V.; Michl, J. Singlet Excitation in Polysilanes: Ab Initio Calculations on Oligosilane Models. *Polyhedron* **1991**, *10* (11), 1265–1284. https://doi.org/10.1016/S0277-5387(00)86103-3.

(58) West, R. The Polysilane High Polymers. *J. Organomet. Chem.* **1986**, *300* (1–2), 327–346. https://doi.org/10.1016/0022-328X(86)84068-2.

(59) Sita, L. R. A New Strategy for the Synthesis of Homologously Pure Linear Polystannane Oligomers. *Organometallics* **1992**, *11* (4), 1442–1444. https://doi.org/10.1021/om00040a007.

(60) Sita, L. R. Heavy-Metal Organic Chemistry: Building with Tin. *Acc. Chem. Res.* **1994**, *27* (7), 191–197. https://doi.org/10.1021/ar00043a002.

(61) Su, T. A.; Li, H.; Zhang, V.; Neupane, M.; Batra, A.; Klausen, R. S.; Kumar, B.; Steigerwald, M. L.; Venkataraman, L.; Nuckolls, C. Single-Molecule Conductance in Atomically Precise Germanium Wires. *J. Am. Chem. Soc.* **2015**, *137* (38), 12400–12405. https://doi.org/10.1021/jacs.5b08155.

(62) Zaitsev, K. V.; Kapranov, A. A.; Churakov, A. V.; Poleshchuk, O. K.; Oprunenko, Y. F.; Tarasevich, B. N.; Zaitseva, G. S.; Karlov, S. S. "Donor-Acceptor" Oligogermanes: Synthesis, Structure, and Electronic Properties. *Organometallics* **2013**, *32* (21), 6500–6510. https://doi.org/10.1021/om4008218.

(63) Zaitsev, K. V.; Lermontova, E. K.; Churakov, A. V.; Tafeenko, V. A.; Tarasevich, B. N.; Poleshchuk, O. K.; Kharcheva, A. V.; Magdesieva, T. V.; Nikitin, O. M.; Zaitseva, G. S.; Karlov, S. S. Compounds of Group 14 Elements with an Element-Element (E = Si, Ge, Sn) Bond: Effect of the Nature of the Element Atom. *Organometallics* **2015**, *34* (12), 2765–2774. https://doi.org/10.1021/om501293t.

(64) Zaitsev, K. V.; Tafeenko, V. A.; Oprunenko, Y. F.; Kharcheva, A. V.; Zhanabil, Z.; Suleimen, Y.; Lam, K.; Zaitsev, V. B.; Zaitseva, A. V.; Zaitseva, G. S.; Karlov, S. S. Molecular Oligogermanes and Related Compounds: Structure, Optical and Semiconductor Properties. *Chem. - An Asian J.* **2017**, *12* (11), 1240–1249. https://doi.org/10.1002/asia.201700151.

(65) Roewe, K. D.; Rheingold, A. L.; Weinert, C. S. A Luminescent and Dichroic Hexagermane. *Chem. Commun.* **2013**, *49* (75), 8380–8382. https://doi.org/10.1039/c3cc45450a.

(66) Weinert, C. S. Synthetic, Structural, and Physical Aspects of Organo-Oligogermanes. *Comments Inorg. Chem.* **2011**, *32* (2), 55–87. https://doi.org/10.1080/02603594.2011.618854.

(67) Drew, K. CCXXXIV.-Aromatic Derivatives of Germanium. *J. Chem Soc. Trans*. **1925**. 127. 1760-1768.

(68) Mochida, K.; Hodota, C.; Hata, R.; Fukuzumi, S. Charge-Transfer Spectra of Permethylated Polygermanes—TCNE To Afford 1:1 Adducts. *Organometallics* **1993**, *12* (2), 586–588. https://doi.org/10.1021/om00026a052.

(69) Arbor, A. Synthesis and Reactivity of Some t-Butyl-Disilanes and Digermanes. *J. Organomet. Chem.* **1976**, *107*, 23–32.

(70) A, E. S. S.; Castel, A.; Riviere, P.; Satgi, J. Synthese Et Etude Spectrale De Chaines Polymetallees '(Ge, Si); Analyse Theorique Des Effets De Substitution. *J. Organomet. Chem.* **1983**, *247*, 149–160.

(71) Neumann, W. P.; Kühlein, K. Uber Cyclische Phenylgermanium-Verbindungen [(C6H5)2Ge]N. *Tetrahedron Lett.* **1963**, *4* (23), 1541–1545. https://doi.org/10.1016/S0040-4039(01)90868-8.

(72) Mochida, K.; Maeyama, S.; Wakasa, M.; Hayashi, H. Synthesis, Photochemical and Conducting Properties of Oligo(Digermanylene-Phenylene)s and Related Compounds. *Polyhedron* **1999**, *17* (22), 3963–3967. https://doi.org/10.1016/S0277-5387(98)00194-6.

(73) Roller, S.; Simon, D.; Dräger, M. Über Polygermane. XIV. Polygermane Als Nebenprodukte Der Grignard-Reaktion von PhMgBr Mit GeCl4. *J. Organomet. Chem.* **1986**, *301* (1), 27–40. https://doi.org/10.1016/0022-328X(86)82053-8.

(74) Azemi, T.; Yokoyama, Y.; Mochida, K. Development of Novel and Efficient Synthesis of Group 14 Element (Ge and Sn) Catenates by Use of Samarium (II) Diiodide. *J. Organomet. Chem.* **2005**, *690* (6), 1588–1593. https://doi.org/10.1016/j.jorganchem.2004.12.032.

(75) The First Application of Bromine. *Sci. Am.* **1892**, *34*, 14027. https://doi.org/10.1038/scientificamerican10291892-14027asupp.

(76)   Amadoruge, M. L.; Short, E. K.; Moore, C.; Rheingold, A. L.; Weinert, C. S. Structural, Spectral, and Electrochemical Investigations of Para-Tolyl-Substituted Oligogermanes. *J. Organomet. Chem.* **2010**, *695* (14), 1813–1823. https://doi.org/10.1016/j.jorganchem.2010.04.015.

(77)   Komanduri, S. P.; Shumaker, F. A.; Roewe, K. D.; Wolf, M.; Uhlig, F.; Moore, C. E.; Rheingold, A. L.; Weinert, C. S. A Series of Isopropyl-Substituted Oligogermanes $Pr^i_3Ge(GePh_2)NGePr^i_3$ (n = 0-3) Featuring a Luminescent and Dichroic Pentagermane $Pr^i_3Ge(GePh_2)_3GePr^i_3$. *Organometallics* **2016**, *35* (18), 3240–3247. https://doi.org/10.1021/acs.organomet.6b00596.

(78)   Samanamu, C. R.; Amadoruge, M. L.; Schrick, A. C.; Chen, C.; Golen, J. A.; Rheingold, A. L.; Materer, N. F.; Weinert, C. S. Synthetic, Structural, and Physical Investigations of the Large Linear and Branched Oligogermanes $Ph_3GeGePh_2GePh_2GePh_2H$, Ge_5Ph_{12}, and $(Ph_3Ge)_4Ge$. *Organometallics* **2012**, *31* (11), 4374–4385. https://doi.org/10.1021/om300385n.

(79)   Schrick, E. K.; Forget, T. J.; Roewe, K. D.; Schrick, A. C.; Moore, C. E.; Golen, J. A.; Rheingold, A. L.; Materer, N. F.; Weinert, C. S. Substituent Effects in Digermanes: Electrochemical, Theoretical, and Structural Investigations. *Organometallics* **2013**, *32* (7), 2245–2256. https://doi.org/10.1021/om400132z.

(80)   Komanduri, S. P.; Schrick, A. C.; Feasley, C. L.; Dufresne, C. P.; Weinert, C. S. Photodecompostion of the Oligogermanes $^nBu_3GeGePh_2Ge^nBu_3$ and $^nBu_3GeGePh_3$: Identification of the Photoproducts by Spectroscopic and Spectrometric Methods. *Eur. J. Inorg. Chem.* **2016**, *2016* (19), 3196–3203. https://doi.org/10.1002/ejic.201600421.

(81)   Schrick, A. C.; Weinert, C. S. Oligogermanes as Molecular Precursors for Germanium(0) Nanoparticles: Size Control and Size-Dependent Fluorescence. *Mater. Res. Bull.* **2013**, *48* (10), 4390–4394. https://doi.org/10.1016/j.materresbull.2013.05.113.

(82)   Léal, M. A.; Begic, K.; Campbell, J.; Kirkman, N.; Myers, D.; Schrick, A. C.; Rheingold, A. L.; Weinert, C. S. Preparation, Absorption Spectra, and Electrochemsitry of the Trigermanes $R_3GeGePh_2GeR_3$(R_3 = Bu^tMe_2, $PhMe_2$, Bu^n_3) and Tetragermanes $R_3Ge(GePh_2)_2GeR_3$ (R_3 = Et_3, Bu^n_3). *J. Organomet. Chem.* **2020**, *925*. https://doi.org/10.1016/j.jorganchem.2020.121467.

(83)   Hanson, P. Properties in Terms of Group Connectivity. *J. Chem. Soc. Perkin. Trans. 2.* **1984**, 101–108.

(84)   Anslyn, D. V.; Dougherty, D. A. *Modern Physical Organic Chemistry*; University Science Books: Sausolito, California, **2006**.

(85)   Taft, J. R. W. *Steric Effects in Organic Chemistry*; John Wiley and Sons: New York, N.Y., **1956**.

(86)   Okano, M.; Mochida, K. Electrochemical Properties and UV Spectra of Permethylpolygermanes. *Chemistry Letters*. **1990**, 701–704. https://doi.org/10.1246/cl.1990.701.

(87)   Zaitsev, K. V.; Lam, K.; Zhanabil, Z.; Suleimen, Y.; Kharcheva, A. V.; Tafeenko, V. A.; Oprunenko, Y. F.; Poleshchuk, O. K.; Lermontova, E. K.; Churakov, A. V. Oligogermanes Containing Only Electron-Withdrawing Substituents: Synthesis and Properties. *Organometallics* **2017**, *36* (2), 298–309. https://doi.org/10.1021/acs.organomet.6b00767.

(88)   McMurry, J. *Fundamentals of Organic Chemistry*, 3rd Edition.; Wadsworth Inc.: Belmont, California, 1994.

(89)   Schrick, A. C. Structural and Physical Investigations of Novel Germanium Compounds: Aryloxides, Nanomaterials, and Photolysis of Oligoermanes. Oklahoma State University, 2009.

(90)   Amadoruge, M. L.; Yoder, C. H.; Conneywerdy, J. H.; Heroux, K.; Rheingold, A. L.; Weinert, C. S. ^{73}Ge NMR Spectral Investigations of Singly Bonded Oligogermanes. *Organometallics* **2009**, *28* (10), 3067–3073. https://doi.org/10.1021/om900035r.

(91)   Dolomanov, O. V.; Bourhis, L. J.; Gildea, R. J.; Howard, J. A. K.; Puschmann, H. OLEX2: A Complete Structure Solution, Refinement and Analysis Program. *J. Appl. Crystallogr.* **2009**, *42* (2), 339–341. https://doi.org/10.1107/S0021889808042726.

(92)   Sheldrick, G. M. A Short History of SHELX. *Acta Crystallogr. Sect. A Found. Crystallogr.* **2008**, *64* (1), 112–122. https://doi.org/10.1107/S0108767307043930.

(93)   Bourissou, D.; Guerret, O.; Gabbaï, F. P.; Bertrand, G. Stable Carbenes. *Chem. Rev.* **2000**, *100* (1), 39–91. https://doi.org/10.1021/cr940472u.

(94)   Mizuhata, Y.; Sasamori, T.; Tokitoh, N. Stable Heavier Carbene Analogues. *Chem. Rev.* **2009**, *109* (8), 3479–3511. https://doi.org/10.1021/cr900093s.

(95)   Lappert, M. F.; Rowe, R. S. The Role of Group 14 Element Carbene Analogues in Transition Metal Chemistry. *Coord. Chem. Rev.* **1990**, *100* (C), 267–292. https://doi.org/10.1016/0010-8545(90)85012-H.

(96)   Neumann, W. P. Germylenes and Stannylenes. *Chem. Rev.* **1991**, *91* (3), 311–334. https://doi.org/10.1021/cr00003a002.

(97)   Cotton, B. J. D.; Davidson, P. J.; Lappert, M. F.; Sciences, M. Subvalent Group 4B Metal Alkyls and Amides. Part 112 The Chemistry and Properties of Bis[Bis(Trimethylsilyl)Methyl]Tin (11) and Its Lead Analogue. *J. Chem. Soc. Dalton. Trans.* **1976**. 2275-2286.

(98)   Chorley, R. W.; Hitchcock, P. B.; Lappert, M. F.; Leung, W. P.; Power, P. P.; Olmstead, M. M. Subvalent Group 14 Metal Compounds. XIV. The X-Ray Crystal Structures of Two Monomeric Group 14 Metal Bisamides, Ge[N(SiMe$_3$)$_2$]$_2$ and Sn[NC(Me)$_2$ (CH$_2$)$_3$CMe$_2$]$_2$. *Inorganica Chim. Acta* **1992**, *198–200* (C), 203–209. https://doi.org/10.1016/S0020-1693(00)92362-4.

(99)   Davidson, P. J.; Harris, D. H.; Lappert, M. F. 2268 Subvalent Group 4B Metal Alkyls and Amides . Part I. *J. Chem. Soc. Dalt. Trans.* **1976**, *21* (2268), 2268–2274.

(100)   Goldberg, D. E.; Hitchcock, P. B.; Lappert, M. F.; Markthomas, K.; Thorne, A. J.; Haaland, A.; Schilling, B. E. R. Subvalent Group 4B Metal Alkyls and Amides. Part 9. Germanium and Tin Alkene Analogues, the Dimetallenes M$_2$R$_4$ [M = Ge or Sn, R = CH(SiMe$_3$)$_2$]: X-Ray Structures, Molecular Orbital Calculations for M$_2$H$_4$, and Trends in the Series M$_2$R$'_4$ [M = C, Si, Ge, Or Sn; R' = R, Ph, C$_6$H$_2$Me$_3$-2,4,6, or C$_6$H$_3$Et$_2$-2,6.] *J. Chem. Soc. Trans.* **1986**, 2387-2394.

(101)   Miller, K. A.; Bartolin, J. M.; O'Neill, R. M.; Sweeder, R. D.; Owens, T. M.; Kampf, J. W.; Banaszak Holl, M. M.; Wells, N. J. C-H Activation of Ethers and Alkanes by Germylene-Aryl Halide Complexes. *J. Am. Chem. Soc.* **2003**, *125* (30), 8986–8987. https://doi.org/10.1021/ja0357285.

(102)   Miller, K. A.; Watson, T. W.; Bender IV, J. E.; Banaszak Holl, M. M.; Kampf, J. W. Intermolecular C-H Insertions and Cyclization Reactions Involving a Stable Germylene. *J. Am. Chem. Soc.* **2001**, *123* (5), 982–983. https://doi.org/10.1021/ja0026408.

(103)   Walker, R. H.; Miller, K. A.; Scott, S. L.; Cygan, Z. T.; Bartolin, J. M.; Kampf, J. W.; Holl, M. M. B. Silylene- and Germylene-Mediated C-H Activation: Reaction with Alkanes, Ethers, and Amines. *Organometallics* **2009**, *28* (9), 2744–2755. https://doi.org/10.1021/om900182z.

(104)   Sweeder, R. D.; Miller, K. A.; Edwards, F. A.; Wang, J.; Banaszak Holl, M. M.; Kampf, J. W. Exploring Two Reactions of Ketones with Ge[CH(SiMe$_3$)$_2$]$_2$: CH and OH Insertion. *Organometallics* **2003**, *22* (24), 5054–5062. https://doi.org/10.1021/om030308+.

(105)   Harris, D. H.; Lappert, M. F. Monomeric, Volatile Bivalent Amides of Group IV$_B$ Elements, M(NR$^1_2$)$_2$ and M(NR^{1}R$_2$)$_2$ (M=Ge, Sn, or Pb; R^1 =Me$_3$Si, R^2=Me$_3$C). *J. Chem. Soc. Chem. Commun.* **1974**, No. 21, 895–896. https://doi.org/10.1039/C39740000895.

(106)   Al-Ktaifani, M. M.; Hitchcock, P. B.; Lappert, M. F.; Nixon, J. F.; Uiterweerd, P. Specific Insertion Reactions of a Germylene, Stannylene and Plumbylene into the Unique P-P Bond of the Hexaphospha-Pentaprismane Cage, P$_6$C$_4$^{t}Bu$_4$: Crystal and Molecular Structures of P$_6$C$_4$^{t}Bu$_4$ER$_2$ (E = Ge, Sn, R = N(SiMe$_3$)$_2$; E = Pb, R = (C$_6$H$_3$(NMe$_2$)$_2$-2,6). *Dalt. Trans.* **2008**, *2* (21), 2825–2831. https://doi.org/10.1039/b800458g.

(107)   Ellis, D.; Hitchcock, P. B.; Lappert, M. F. Preparation and X-Ray Structure of [Ge{N(SiMe$_3$)$_2$}$_2$(μ-O)]$_2$, A Rare 1,3-Cyclodigermoxane. *J. Chem. Soc. Dalt. Trans.* **1992**, No. 23, 3397–3398. https://doi.org/10.1039/DT9920003397.

(108) Lappert, M. F.; Misra, M. C.; Onyszchuk, M.; Rowe, R. S.; Power, P. P.; Slade, M. J. Subvalent Group 14 Metal Compounds XI. Oxidative Addition Reactions of Organic Halides or Acid Anhydrides (Including CH_4- NCl_n, PhBr, $BrN(SiMe_3)_2$, $Bu^t COCl$, or $(CF_3CO)_2O$) to Some Bivalent Group 14 Metal Amides or Alkyls. *J. Organomet. Chem.* **1987**, *330* (1–2), 31–46. https://doi.org/10.1016/0022-328X(87)80276-0.

(109) Lappert, M. F.; Power, P. P. Subvalent Group 4B Metal Alkyls and Amides. Part 7. Transition-metal Chemistry of Metal (II) Bis(trimethylsily1)amides M' $(NR_2)_2$ (R = $SiMe_3$; M' = Ge, Sn, or Pb). *J. Chem. Soc., Dalton Trans.* **1985**, 51–57.

(110) Zhu, Q.; Ford L., K.; Roskamp J., E. Synthesis of Triphenylphosphonium Trichlorogermanate and Analogs. Preparation of Germylenes from Triphenylphosphonium Trichlorogermanate. *Herteroatom Chem.* **1992**, *3* (5/6), 647–649.

(111) York, J. T.; Young, V. G.; Tolman, W. B. Heterobimetallic Activation of Dioxygen: Characterization and Reactivity of Novel Cu(I)-Ge(II) Complexes. *Inorg. Chem.* **2006**, *45* (10), 4191–4198. https://doi.org/10.1021/ic060050q.

(112) Cabeza, J. A.; García-Álvarez, P.; Polo, D. Reactivity of Diaminogermylenes with Ruthenium Carbonyl: Ru_3Ge_3 and $RuGe_2$ Derivatives. *Inorg. Chem.* **2011**, *50* (13), 6195–6199. https://doi.org/10.1021/ic2009682.

(113) Litz, E. K.; Bender IV, E. J.; Kampf, W. J.; Holl Banaszak, M. M. Transition Metal Germylene Complexes as Hydrogenation Catalystst: The Synthesis of a Rare Bis(Amino)Germane. *Angew. Chem. Int. Ed. Engl.* **1997**, *36* (5), 496–498.

(114) Gehrhus, B.; Hitchcock, P. B.; Lappert, M. F. New Reactions of Silyene: Insertion into M-N Bonds of $M[N(SiMe_3)_2]_2$ (M = Ge, Sn, or Pb). *Angew. Chem. Int. Ed. Engl.* **1997**, *36* (22), 2514–2516.

(115) Dickie, D. A.; Macintosh, I. S.; Ino, D. D.; He, Q.; Labeodan, O. A.; Jennings, M. C.; Schatte, G.; Walsby, C. J.; Clyburne, J. A. C. Synthesis of the Bulky M-Terphenyl Phenol Ar*OH (Ar* = C_6H_3-2,6-Mes_2, Mes = 2,4,6-Trimethylphenyl) and the Preparation and Structural Characterization of Several of Its Metal Complexes. *Can. J. Chem.* **2008**, *86* (1), 20–31. https://doi.org/10.1139/V07-131.

(116) Glidewell, C.; Lloyd, D.; Lumbard, K. W. Formation of Germanium-Nitrogen Double Bonds in Reactions of the Electron-Rich Germylene Bis[Bis(Trimethylsilyl)amido]Germanium(II) with a Range of Diazo-Compounds. *J. Chem. Soc. Dalt. Trans.* **1987**, No. 3, 501–508. https://doi.org/10.1039/DT9870000501.

(117) Hitchcock, P. B.; Jasim, H. A.; Lappert, M. F.; Leung, W. P.; Rai, A. K.; Taylor, R. E. Subvalent Group 14 Metal Compounds-XIII. Oxidative Addition Reactions of Germanium and Tin Amides $M(NR_2)_2$ (R = $SiMe_3$, M = Ge or Sn) with Sulphur, Selenium, Tellurium or MeOOCCCCOOMe; X-Ray Structures of $[Ge(NR_2)_2(\mu$-Te)]_2$ and $Sn(NR_2)_2CC(OMe)OSn(NR_2)_2CC(OMe)O$. *Polyhedron* **1991**, *10* (11), 1203–1213. https://doi.org/10.1016/S0277-5387(00)86096-9.

(118) Weinert, C. S.; Fenwick, A. E.; Fanwick, P. E.; Rothwell, I. P. Synthesis, Structures and Reactivity of Novel Germanium(II) Aryloxide and Arylsulfide Complexes. *J. Chem. Soc. Dalt. Trans.* **2003**, *3* (4), 532–539. https://doi.org/10.1039/b211077f.

(119) Townsend, E. M.; Kilyanek, S. M.; Schrock, R. R.; Müller, P.; Smith, S. J.; Hoveyda, A. H. High Oxidation State Molybdenum Imido Heteroatom-Substituted Alkylidene Complexes. *Organometallics* **2013**, *32* (16), 4612–4617. https://doi.org/10.1021/om400584f.

(120) Yates, P.; Hyee, J. E. The Tetraphenylphenols. *J. Org. Chem.* **1962**, *27* (11), 4101–4103. https://doi.org/10.1021/jo01058a533.

(121) Dakternieks, D.; Schiesser, C. H. Current Chemistry: The Quest for Single-Enantiomer Outcomes in Free-Radical Chemistry. *Aust. J. Chem.* **2001**, *54* (2), 89–91.

(122) Schiesser, C. H.; Skidmore, M. A.; White, J. M. Stannanes from Cholic Acid as Enantioselective Free-Radical Reducing Agents. *Aust. J. Chem.* **2001**, *54* (3), 199–204.

(123) Curran, D. P.; Porter, N. A.; Bernd, G. *Stereochemistry of Radcal Reactions*; VCH Publishers, Inc.: New York, N.Y., 1996.

(124) Carland, M. W.; Schiesser, C. H. *The Chemistry of Organic Germanium, Tin, and Lead Compounds*, Volume 2.; Wiley: Chichester, 2002.

(125) Bernd, G. *Radicals in Organic Synthesis: Formation of Carbon-Carbon Bonds*; Pergamon, Oxford, 1986.

(126) Renaud, P.; Sibi, M. P. *Radicals in Organic Synthesis*; Wiley, 2008.

(127) Nanni, D.; Curran, D. P. Synthesis and Some Reactions of the First Chiral Tin Hydride Containing a C2-Symmetric Binaphthyl Substituent. *Tetrahedron Asymmetry* **1996**, *7* (8), 2417–2422. https://doi.org/10.1016/0957-4166(96)00300-X.

(128) Dakternieks, D.; Perchyonok, V. T.; Schiesser, C. H. Single Enantiomer Free-Radical Chemistry - Lewis Acid-Mediated Reductions of Racemic Halides Using Chiral Non-Racemic Stannanes. *Tetrahedron Asymmetry* **2003**, *14* (19), 3057–3068. https://doi.org/10.1016/j.tetasy.2003.07.012.

(129) Schwarzkopf, K.; Blumenstein, M.; Hayen, A.; Metzger, J. O. Enantioselectivity of the Transfer of Hydrogen Atoms to Acyclic Prochiral Carbon-Centred Radicals Using Chiral Tin Hydrides. *European J. Org. Chem.* **1998**, *9* (1), 177–181.

(130) Murakata, M.; Tsutsui, H.; Takeuchi, N.; Hoshino, O. Enantioselective Radical-Mediated Reduction of α-Alkyl-α- Iododihydrocoumarins in the Presence of a Chiral Magnesium Iodide. *Tetrahedron* **1999**, *55* (34), 10295–10304. https://doi.org/10.1016/S0040-4020(99)00584-0.

(131) Zeng, L.; Dakternieks, D.; Duthie, A.; Perchyonok, T.; Schiesser, C. Synthesis, Characterization and Enantioselective Free Radical Reductions of (1*R*,2*S*,5*R*)-Menthyldiphenylgermane and Its Enantiomer. *Tetrahedron Asymmetry* **2004**, *15* (16), 2547–2554. https://doi.org/10.1016/j.tetasy.2004.06.020.

(132) Chatgilialoglu, C.; Griller, D.; Lesage, M. Tris(Trimethylsilyl)Silane. A New Reducing Agent. *J. Org. Chem.* **1988**, *53* (15), 3641–3642.

(133) Crich, D.; Sun, S. A Practical Method for the Removal of Organotin Residues from Reaction Mixtures. *J. Org. Chem.* **1996**, *61* (20), 7200–7201. https://doi.org/10.1021/jo960751c.

(134) Lusztyk, J.; Maillard, B.; Ingold, K. U. Pentamethyldisilyl Radical: Absolute Rate Constants for Its Formation and SOme Halogen Abstraction and Addition Reactions. *J. Org. Chem.* **1986**, *51* (13), 2457–2460.

(135) Chatgilialoglu, C.; Ingold, K. U.; Scaiano, J. C. Absolute Rate Constants for the Addition of Triethylsilyl Radicals to the Carbonyl Group. *J. Am. Chem. Soc.* **1982**, *104* (19), 5119–5123. https://doi.org/10.1021/ja00383a021.

(136) Gilman, H.; Atwell, W. H.; Sen, P. K.; Smith, C. L. Branched-Chain Organic Polysilanes Containing the Silicon-Hydrogen Group. *J. Organomet. Chem.* **1965**, *4* (2), 163–167. https://doi.org/10.1016/S0022-328X(00)84384-3.

(137) Chatgilialoglu, C. Organosilanes as Radical-Based Reducing Agents in Synthesis. *Acc. Chem. Res.* **1992**, *25* (4), 188–194. https://doi.org/10.1021/ar00016a003.

(138) Ballestri, M.; Chatgilialoglu, C.; Clark, K. B.; Griller, D.; Giese, B.; Kopping, B. Tris(Trimethylsilyl)Silane as a Radical-Based Reducing Agent in Synthesis. *J. Org. Chem.* **1991**, *56*, 678–683.

(139) Barton, D. H. R.; Doo, O. J.; Jaszberenyi, J. C. An Improved Radical Chain Procedure for the Deoxygenation of Secondary and Primary Alcohols Using Diphenylsilane as Hydrogen Atom Donor and Triethylborane-Air as Initiator. *Tetrahedron Lett.* **1990**, *31* (33), 4681–4684. https://doi.org/10.1016/S0040-4039(00)97705-0.

(140) Schummer, D.; Höfle, G. Tris(Trimethylsilyl)Silane as a Reagent for the Radical Deoxygenation of Alchols. *Synlett* **1990**, *11*, 705–706.

(141) Arya, P.; Samson, C.; Lesage, M.; Griller, D. Tris(Trimethylsilyl)Silane (TTMSS): Formation of Carbon-Centered Radicals from 1,3-Dithiolanes and 1,3-Dithianes. *J. Org. Chem.* **1990**, *55*, 6248–6250.

(142) Arya, P.; Lesage, M.; Wayner, D. D. M. Tris(Trimethylsilyl)Silane (TTMSS) Oxathiolane : Formation of and Thiazolidine Carbon-Centered Derivatives. *Tetrahedron Lett.* **1991**, *32* (25), 2853–2856.

(143) Gualtieri, G.; Geib, S. J.; Curran, D. P. A New Class of Chiral Organogermanes Derived from C2-Symmetric Dithiols: Synthesis, Characterization and Stereoselective Free Radical Reactions. *J. Org. Chem.* **2003**, *68* (13), 5013–5019. https://doi.org/10.1021/jo026625s.

(144) Kauch, M.; Snieckus, V.; Hoppe, D. Substitution of Hydroxybiaryls via Directed Ortho-Lithiation of *N*-Silylated *O*-Aryl *N*-Isopropylcarbamates. *J. Org. Chem.* **2005**, *70* (18), 7149–7158. https://doi.org/10.1021/jo0506938.

(145) Boyle, T. J.; Tribby, L. J.; Ottley, L. A. M.; Han, S. M. Synthesis and Characterization of Germanium Corrdination Compounds for Production of Germanium Nanomaterial. *Eur. J. Inorg. Chem.* **2009**, *36*, 5550–5560.

(146) Weinert, C. S.; Fanwick, P. E.; Rothwell, I. P. Novel Germanium(II) Binaphthoxide Complexes: Synthesis and Crystal Structure of (R,R)-[Ge{OC$_{20}$H$_{10}$(OSiMe$_3$)-2′-(SiMe$_3$)$_2$-3,3′}$_2$] and (R)-[Ge{O$_2$C$_{20}$H$_{10}$(SiMe$_2$Ph)$_2$-3,3′}{NH$_3$}]; Catalytic Function of Ge[N(SiMe$_3$)$_2$]$_2$ for the Mono-Silylation of 3,3′-Disubstituted-1,1′-bi-2,2′-naphthols. *J. Chem. Soc. Dalt. Trans.* **2002**, 15, 2948–2950.

(147) Wetherby, A. E.; Goeller, L. R.; DiPasquale, A. G.; Rheingold, A. L.; Weinert, C. S. Synthesis and Structures of an Unusual Germanium(II) Calix[4]Arene Complex and the First Germanium(II) Calix[8]Arene Complex and Their Reactivity with Diiron Nonacarbonyl. *Inorg. Chem.* **2007**, *46* (18), 7579–7586.

(148) Wetherby, A. E.; Goeller, L. R.; DiPasquale, A. G.; Rheingold, A. L.; Weinert, C. S. Metal-Dependent Reactions of Bulky Metal(II) Amides M[N(SiMe$_3$)$_2$]$_2$ with 3,3′-Disubstituted Binaphthols (HO)$_2$C$_{20}$H$_{10}$(SiR$_3$)$_2$-3,3′: Selective Conversion of One Equivalent −OH Group to a Silyl Ether −OSiMe$_3$. *Inorg. Chem.* **2008**, *47* (6), 2162–2170.

(149) Wetherby, A. E.; Rheingold, A. L.; Feasley, C. L.; Weinert, C. S. Synthesis and Crystal Structure of a Germanium(II) Calix[6]Arene Containing Unusual Diamidosilyl Ether Groups. *Polyhedron.* **2008**, *27* (7), 1841–1847.

(150) Weinert, C. S. An NMR (^{1}H and [77]Se) Investigation of the Reaction of Ge[N(SiMe$_3$)$_2$]$_2$ with Mesitylselenol: Formation of (MesSe)$_4$Ge. *Main Gr. Met. Chem.* **2007**, *30* (2–3), 93–100.

(151) Joji, O.; Yutaka, T.; Arihiro, I.; Heqing, T.; Atsutaka, K. Selective Synthesis of Chlorohydrogermanes from Mono-, Di-, and Trihydrogermanes. *Chem. Lett.* **2001**, *30* (9), 886–887.

VITA

Miguel Angel Leal Junior

Candidate for the Degree of

Doctor of Philosophy

Thesis: SYNTHESIS AND CHARACTERIZATION OF CHIRAL GERMANIUM
COMPOUNDS FOR ASYMMETRIC HYDROGERMYLATION OF
ORGANIC COMPOUNDS

Major Field: Chemistry

Biographical:

Education:

Completed the requirements for the Doctor of Philosophy in Chemistry at
Oklahoma State University, Stillwater, Oklahoma in May, 2021.

Completed the requirements for the Bachelor of Science in Chemistry at
University of Texas Rio Grande Valley, Brownsville, Texas in 2016.

Publications:
[1] M. Jasim Uddin*, Glenn Grissom, Miguel Leal, Veronica Galvez, Tarek
Trad, Ahmed Touhami, Nazmul Islam, Jason Parson, H. Justin Moore,
ASME 2016 *International Mechanical Engineering Congress
Exposition*, **2017**.
[2] Miguel A. Leal, Kevin Begic, John Campbell, Nolan Kirkman, Dawson
Myers, Aaron C. Schrick, Arnold L. Rheingold, and Charles S.
Weinert*. *Journal of Organometallic Chemistry*, 925, **2020**, 121467.
[3] Glenn Grissom, Brishty Deb Chourdhury, Miguel Leal, Sk. Md. Ali
Zaker Shawon, Ahmed Touhami, Okenwa Okoli, M. Jasim Uddin*.
Advanced Material Interfaces, **2020**, *Submitted*.

Professional Memberships:
- American Chemical Society